EVOLUTION, DEVELOPMENT, AND HOMOLOGY OF THE AMNIOTE DERMAL SKELETON AND PECTORAL APPARATUS

by

Matthew K. Vickaryous

Submitted in partial fulfillment of the requirements
for the degree of Doctor of Philosophy

at

Dalhousie University
Halifax, Nova Scotia
October 2006

Your file Votre référence
ISBN: 978-0-494-27186-5
Our file Notre référence
ISBN: 978-0-494-27186-5

DALHOUSIE UNIVERSITY

To comply with the Canadian Privacy Act the National Library of Canada has requested that the following pages be removed from this copy of the thesis:

Preliminary Pages

Examiners Signature Page (pii)

Dalhousie Library Copyright Agreement (piii)

Appendices

Copyright Releases (if applicable)

DEDICATION

For Jalene.

TABLE OF CONTENTS

LIST OF FIGURES

LIST OF TABLES

ABSTRACT

The dermal skeleton and pectoral apparatus have long been recognized as major determinants of vertebrate morphology. Until recently however, details of tissue development and diversity, particularly among amniotes, have been lacking. Furthermore, the homology of various elements remains uncertain. This research is broadly divided into two sections. First I investigated the development of the pectoral apparatus and determined that the long held interpretation of coracoid homology is incorrect. I find that the reptilian coracoid is homologous with the coracoid process of therian mammals and not, as previously suggested, the procoracoid of monotreme mammals. Using this information, I devised a new scenario for the evolution of the coracoid involving changes in the aggregation, proliferation, and differentiation of pre-skeletal cell condensations. I also re-explored the historic subject of furcula (wishbone) homology. Employing Colin Patterson's three tests of homology, I find that each of the interclavicle and the furcula pass the observational tests of similarity (similar topographic position, and pattern and mode of development) and conjunction (neither co-exists with the other). My test of congruence examined several competing hypotheses, and determined that each of the neomorphic origin and furcula as the homologue of the interclavicle to be equally parsimonious, although the results only differ by a single evolutionary step from the predominant furcula-equals-clavicles hypothesis. Hence, I find the homology of the furcula to be ambiguous.

Second, I investigated dermal skeleton development in *Alligator mississippiensis*. I document the first report of chondroid bone in a non-avian reptile. I also find that *A. mississippiensis* lacks secondary cartilage. My study further demonstrates that the rugose pattern of bony ornamentation across the skull (and osteoderms) of this taxon develops from the localized concentrations of bone deposition by osteoblasts; osteoclasts, while present, are restricted to deep bone surfaces. Similar to many amniotes, *A. mississippiensis* develops osteoderms, bony inclusions of the dermis. I compared the development of osteoderms in *A. mississippiensis* with the mammal *Dasypus novemcinctus* and observed that all osteoderms shared a relatively late onset and asynchronous pattern of development. For *D. novemcinctus*, I find that osteoderms begin as condensations of osteoblasts secreting osteoid. This mode of development is consistent with intramembranous ossification. For *A. mississippiensis*, I find that osteoderms develop in the absence of osteoblastic cells and osteoid; bone develops via the direct transformation of preexisting dense irregular connective tissue. I have identified this mode of bone formation as metaplasia. My studies clearly demonstrate that osteoderms are not histologically uniform but may involve a range of tissues including uncalcified and calcified dense connective tissues. Between taxa, not all osteoderms develop by homologous processes. However, I conclude that osteoderms may share a deep homology, connected by the structural and skeletogenic properties of the dermis.

ACKNOWLEDGEMENTS

Many individuals made large contributions to this research and all deserve special recognition, although none moreso than my supervisor Dr. Brian K. Hall. His support inside and outside the laboratory has been exceptional, and I could not have asked for more. Many thanks Brian. Also, the members of my admission to candidacy, preliminary exam, and thesis defence committees have all done a tremendous job of providing me with excellent advice and direction, and I am indebted to their careful scrutiny of my work. Thanks to Drs. Alan Pinder, Boris Kablar, and Ian Mobbs of Dalhousie University, Dr. David Cone of St. Mary's University, and a special thanks to my external examiner Dr. Kathleen Smith of Duke University. None of the work involving *Alligator mississippiensis* could have been done without the extraordinary assistance of Dr. Ruth Elsey and the staff of the Rockefeller Wildlife Refuge, Grand Chenier, Louisiana. Her role in this and virtually all other research involving *A. mississippiensis* cannot be overstated. Many thanks Ruth. During my visits to the Rockefeller I also benefited from interactions with Jimmy (James) Hartobey, Jeb Linscombe, Megan Pearson, Scooter Trosclair, and John Turner. Special thanks to Dr. Val Lance (San Diego Zoo), who provided me with great insight into crocodylian behaviour. I would also like to thank Dr. Gerd Müller (University of Vienna) for kindly donating several embryonic specimens to get me started, and Prof. Mark W. J. Ferguson (University of Manchester), for putting his vast collection at my disposal. The Texas Cooperative Wildlife Collection (Department of Wildlife and Fisheries Sciences, Texas A&M University, College Station, Texas) and the University of Kansas Natural History Museum (Lawrence, Kansas; specifically Dr. R. Timm) generously provided the *Dasypus novemcinctus* specimens used in this study. I am also indebted to Dr. Tim J. Gaudin (Department of Biological and Environmental Sciences, University of Tennessee at Chattanooga) for supplying me with an advanced copy of his phylogenetic study of armadillos. Dr. Stuart S. Sumida (California State University, San Bernardino), Tim Fedak (www.figs.ca and Dalhousie University), Dr. Anthony P. Russell (University of

Calgary) and an anonymous reviewer provided very useful comments on the coracoid study - their input is greatly appreciated. Tim Fedak also rendered my original drafts into presentable figures. Two anonymous reviewers and Dr. Frederick Harrison (Journal of Morphology) provided excellent comments on the armadillo osteoderm study. Ms. Donna Krailo and Ms. Alma Cameron (Dalhousie University) provided unparalleled technical and logistical support underpinning virtually every aspect of this research. Many thanks Donna and Alma. Another debt of gratitude is owed to Ms. Jessica Arbour (Dalhousie University), who as part of a summer undergraduate internship serially sectioned dozens of blocks and stained hundreds of slides. Excellent work Jessica. The sum total of my histological knowledge was carefully gleaned from the expertise of Drs. Brian K. Hall, P.Eckhard Witten (AKVAFORSK Institute of Aquaculture Research), Alison Cole, and Tamara Franz-Odendaal (formerly of Dalhousie University, currently of Mount Saint Vincent University, both in Halifax), and Ms. Alma Cameron. Dr. Ping Li and Mr. Carey Isenor (Dalhousie University) assisted with the scanning electron microscopy. My stay in Halifax was made all the better by numerous outstanding friends and colleagues including Tim Fedak, Maximus Westhead, Alison Cole, Jon Stone, Brian and June Hall, Eckhard Witten, Tamara Franz-Odendaal, Francois Odendaal, Alma Cameron, Donna Krailo, Rebecca MacEachern, Brad Tucker, Marie Tounissoux, Aine Humble, Arthur Macalla, Michelle Connolly, Wendy Olson, Greg Handrigan, Tara Edwards, Will MacDonald, Jen Legere, Neely Vincent, and Lisa Budney. Saving the best for last, I am proud to thank Jalene Lumb for all her support, encouragement, and willingness to go back and forth across the country. This work was funded by a Jurassic Foundation Grant and two Lett awards to M.K.V. and an NSERC operating grant to B.K.H.

CHAPTER 1. INTRODUCTION

OVERVIEW

The vertebrate skeleton is a complex and dynamic organ system consisting of a broad spectrum of cell types, tissues, and morphologically disparate components. As a matter of convenience, it is routine (and frequently necessary) to conceptually partition the vertebrate skeleton (hereafter, the skeleton) into more discretely defined components for the purpose of study (Vickaryous et al., 2003). Such considerations may be based on histology (e.g., cartilage versus bone), topographic position (axial versus appendicular), or mode of development (intramembranous versus endochondral ossification), although none are mutually exclusive. From the perspective of evolutionary developmental biology, it is practical to consider the complete skeleton as composed primarily of two phylogenetically and developmentally distinct systems. The focus of the current study, the dermal skeleton (= exoskeleton, dermoskeleton, desmoskeleton), does not preform in cartilage, and either develops in association with the basement membrane of the ectoderm, or is homologous with such elements in the ancestor (Patterson, 1977). Although definitive evidence is, as yet, lacking for postcranial bones (although see McGonnell and Graham, 2002), as currently understood, all elements of the dermal skeleton are derived from the neural crest germ layer (Smith and Hall, 1990, 1993). In contrast, the endoskeleton does preform in cartilage and may remain cartilaginous throughout ontogeny or later become replaced by bone tissue (Patterson, 1977). Elements of the endoskeleton may be derived from either the neural crest or from mesoderm (Smith and Hall, 1990, 1993). Supplementing these two systems are a variety of small, poorly known, and difficult to categorise elements, including sesamoids, mineralized tendons, and bones and cartilages of the genitalia (e.g., baculum). While some of these skeletal outliers initiated development in cartilage (e.g., sesamoids), others undergo metaplasia, the direct transformation from one fully differentiated tissue into another (e.g., mineralized tendons form as regular dense connective tissue is transformed into bone; see Vickaryous and Olson, in press). Adding to the confusion, metaplasia is commonly considered a pathological process (Beresford, 1981).

Ancestrally, the dermal skeleton can be traced back more than 500 million years as the once all-encasing superficial mosaic of mineralized tissues that characterized many early stem gnathostomes (viz. structural-grade ostracoderms; Smith and Hall, 1990, 1993; Zylberberg et al., 1992; Donoghue and Sansom, 2002; Sire and Huysseune, 2003). Among extant taxa, the legacy of this pervasive external skeleton is best observed among aquatic non-tetrapods ("fish"), particularly basal members of Actinopterygii and Sarcopterygii. A recent review by Sire and Huysseune (2003) demonstrated that the dermal skeleton of modern aquatic non-tetrapods consists of the dermatocranium, teeth, postcranial dermal bones, fin rays, and various elements associated with the integument, including odontodes, dermal denticles, mineralized scales, and scutes. Interestingly, while all these elements demonstrate differences in morphology and/or topographic position, comparative development studies (including the tissue environment in which they develop [mesenchyme versus well-structured dermis], the presence or absence of papillae, and the relationship of the element with the epidermis), provide much needed structural data to inform about skeletal and skeletal tissue evolution (see review by Sire and Huysseune, 2003 and references therein). For example, isolated postcranial teleost odontodes are now understood to be extra-oral teeth (Sire, 2001; Sire and Huysseune, 2003). However despite the impressive progress, many important questions pertaining to the determination of homology at the level of the tissue and organ remain unanswered (e.g., are elasmoid scales of sarcopteryians and actinopterygians homologous?).

For amniotes, far less is known. It is commonly observed that the amniote dermal skeleton has undergone widespread reduction and, with the exception of turtles, what remains is largely confined to the skull as the dermatocranium and teeth. Although less obvious, and thus frequently overlooked, other dermal skeleton remnants are manifest within most groups. For example, various taxa develop elements that reinforce the integument (viz. osteoderms; Moss, 1969; Zylberberg and Castanet, 1985; Levrat-Calviac and Zylberberg, 1986; Chapters 4 and 5), as well as bones that brace the abdomen (viz. gastralia; Romer, 1956; Claessens, 2004; Chapter 5). In addition, one or more dermal bones typically contribute to the amniote pectoral girdle (Chapters 2 and 3). As will be demonstrated, the homology of these pectoral elements requires revision.

Excluding the dentition (and possibly osteoderms; see below), early dermal skeletal development is often summarized as intramembranous ossification—the formation of bone without a cartilage precursor from specialized (and phenotypically distinct) cells (osteoblasts)—giving rise to woven bone. However, mounting evidence demonstrates that this process also gives rise to chondroid bone, a skeletal tissue where chondrocyte-like cells reside within a bony (or osteoid) matrix (Beresford, 1993). At present, dermatocranial chondroid bone has been observed in various teleosts (Huysseune and Verraes, 1986; Huysseune and Sire, 1990; Huysseune, 2000; Witten and Hall, 2003; Gillis et al., 2006), mammals (Beresford, 1981, 1993; Vinkka, 1982), and birds (Lengelé et al., 1996a, b), but not in lissamphibians or non-avian reptiles. Curiously, many taxa reported with chondroid bone also develop secondary cartilage. Secondary (adventitious) cartilage forms in association with dermal bones only after osteogenesis has been initiated. As of yet, this tissue is also unknown for lissamphibians and non-avian reptiles (Hall, 1984).

One particularly enigmatic element of the amniote dermal skeleton is the osteoderm. Osteoderms are skeletal organs that form within the integument. Osteoderms have a broad and yet inconsistent taxonomically distribution (e.g., one group of mammals, all crocodylians, and some structural-grade lizards). As a result, it has been proposed that osteoderms are non-homologous (Hill, 2005; see also Sire and Huysseune, 2003). To date, the mode of skeletogenesis giving rise to osteoderms is poorly understood, although it has been suggested that metaplasia may play a role (e.g., Zylberberg and Castanet, 1985; Main et al., 2005). In addition, individual osteoderms reportedly consist of a spectrum of tissues, including bone and calcified connective tissue (Moss, 1969). As a result, it may be questioned whether osteoderms are components of the dermal skeleton *per se*, or if they in fact belong to the skeletal outlier assemblage.

The purpose of this study is to investigate and document the development of the (non-dental) dermal skeleton in amniotes. Developmental data will then be employed to address several outstanding questions, including: is our current understanding of pectoral apparatus homology correct? How does the dermal skeleton develop in non-avian reptiles, and does it involve chondroid bone and/or secondary cartilage? How do osteoderms develop, and does metaplasia play a role? In the thesis, this work is arranged

sequentially as four independent but interrelated and partially overlapping studies. For the sake of discussion here, I have broadly divided this research into two sections: (i) evolution and development of the amniote pectoral apparatus; and (ii) amniote osteoderm development.

EVOLUTION AND DEVELOPMENT OF THE AMNIOTE PECTORAL APPARATUS

Prior to the evolution of digit-bearing limbs, the dermatocranium and pectoral apparatus articulated across the gill chamber. Although long since disconnected in tetrapods, the dermatocranium and pectoral apparatus share an otherwise exceptional skeletal feature: they are both composed of multiple elements from the dermal and endoskeletal systems. In amniotes, the pectoral apparatus includes, at least ancestrally, an unpaired, midventrally positioned dermal element: the interclavicle (monotremes, non-ophidian lepidosaurs, and crocodylians), entoplastron (turtles), or furcula (avians). Whereas the entoplastron is widely regarded as the turtle homologue of the interclavicle, the furcula has historically been considered unique to avians. In recent years however, the furcula has been recognized from the skeletal remains of numerous fossil non-avian (and non-volant) theropods; accordingly, it is now effectively regarded as a theropod synapomorphy. What remains unclear however, is the identity of the equivalent element(s) (if any) among theropod outgroups. Although invariably accepted as the fused clavicles (collar bones), two alternative proposals—the furcula as a neomorph or the homologue of an element previously considered lost—have yet to be rigorously explored (Bryant and Russell, 1993). The purpose of this study was to reevaluate the homology of the furcula using Colin Patteron's (1982) three tests (of homology). Using embryos of *Gallus gallus* (the domestic fowl) and *Alligator mississippiensis* (the American alligator), the following questions were considered: do the furcula and interclavicle share a similar topology, and pattern and mode of development (test of similarity)?; do the furcula and interclavicle co-exist in the same organism (test of conjunction)?; and do the furcula and interclavicle share a common pattern of descent, or is it more parsimonious to consider the furcula as equivalent to the fused clavicles, or as a neomorph (test of congruence)?

During the course of my investigation of the development of dermal elements contributing to the pectoral apparatus (see above; Chapter 3), an important opportunity arose to reexamine the evolution, development, and homology of endoskeletal components (Chapter 2). Among limbed amniotes, the pectoral endoskeleton includes a pair of scapulae, an unpaired sternum, and one or two pairs of coracoids. For extant forms, only monotreme mammals retain two separate coracoid elements; each of therian mammals (marsupials + placentals) and reptiles (including birds) demonstrate only a single pair. It has long been understood that the coracoid bone of mammals and reptiles were not directly comparable; i.e., non-homologous (e.g., Romer, 1922). For mammals, the combination of fossil and developmental data has augmented what is known about pectoral evolution in this clade. Among reptiles, the situation has been largely overlooked. Drawing upon data gleaned from experimental embryology, the fossil record, and recent phylogenetic hypotheses, this study seeks to: analyse the development of the pectoral apparatus in amniotes; readdress the homology of the reptilian coracoid (viz. is the reptilian coracoid homologous or non-homologous with the mammalian coracoid/coracoid process?); and revise the scenario of coracoid evolution.

AMNIOTE OSTEODERM DEVELOPMENT

The presence of skeletal inclusions within the integument is widespread among representative members of most major tetrapod lineages. For the majority of taxa, including anurans, cingulatan mammals (e.g., structural-grade armadillos; Chapter 4), and reptiles (e.g, crocodylians; Chapter 5), these elements are osteoderms, bony investments localized within the dermis. Based on structure and position, it has been hypothesized that all tetrapod osteoderms are homologous and all develop via homologous processes (Moss, 1969).

Previous work on the squamate *Heloderma horridum*, the Gila monster, reported that during osteoderm development, parts of the pre-existing dermis directly transform into a range of skeletal tissues including, calcified connective tissue and bone, without an accompanying change in (embedded) cell morphology (Moss, 1969). Such a tissue transformation is consistent with metaplasia (Beresford, 1981). A similar mode of skeletogenesis has also been suggested for the osteoderms of anurans (Ruibal and

Shoemaker, 1984). In part, these conclusions draw support from two observations: osteoderms appear to require a well-structured and fully differentiated dermis in which to develop; and there are no recognizable differences between the organic extracellular matrix of the dermis and unmineralized osteoderm. For most taxa however, the specific developmental events leading to the formation of the skeletally mature osteoderm remain unexplored.

The purpose of this study was to investigate how osteoderms develop at the tissue structure level in two representative amniotes: the mammal *Dasypus novemcinctus*, and the reptile *Alligator mississippiensis*. More specifically, this study is concerned with documenting the pattern and mode of osteoderm formation throughout ontogeny in each of these evolutionarily disparate taxa. Following this, several key questions will be addressed: do all osteoderms demonstrate a similar pattern of skeletogenesis; do all osteoderms arise via homologous developmental processes; are osteoderms homologous at the organ level?

In order to compare the development of osteoderms with other components of the dermal skeleton, a complementary study was undertaken using the crocodylian *Alligator mississippiensis*. Unlike most modern amniotes, crocodylians develop a wide variety of dermal skeletal elements (in addition to the obvious presence of the dermatocranium), including an interclavicle, gastralia (abdominal ribs), and palpebrals (eyelid bones). The purpose of this study was to document and analyze the pattern and mode of dermal skeletogenesis and then address the follow questions: what is the pattern of skeletogenesis for elements of the dermal skeleton; do elements of the dermal skeleton arise via homologous developmental processes; do elements of the dermal skeleton develop chondroid bone and/or secondary cartilage; and finally, are osteoderms components of the dermal skeleton, or should they be clustered in amongst skeletal outliers such as mineralized tendons?

CHAPTER 2. HOMOLOGY OF THE REPTILIAN CORACOID AND A REAPPRAISAL OF THE EVOLUTION AND DEVELOPMENT OF THE AMNIOTE PECTORAL APPARATUS

The following chapter is published as: Vickaryous MK and Hall BK. 2006. Homology of the reptilian coracoid and a reappraisal of the evolution and development of the amniote pectoral apparatus. Journal of Anatomy 208; 263-285.

INTRODUCTION

Among limbed (and many limbless) amniotes, elements of the shoulder girdle and sternum partially encircle the ribcage to form a structural yoke that indirectly connects the forelimbs to the axial skeleton. Herein referred to as the pectoral apparatus, this skeletogenous nexus demonstrates enormous taxonomic variation and multiple (independent) instances of elements appearing to have been lost and/or insensibly combined. Furthermore, the pectoral apparatus includes both dermal and replacement bones. These features underscore the difficulty of determining homology for various pectoral components.

Historic observations from both the fossil record and ontogenetic studies initially provided a well-structured scenario of the morphological transformation of mammals from the earliest stem synapsids. However, subtle yet important evolutionary details are only now being understood through the use of experimental methods and detailed developmental analyses at the level of the cell.

Among reptiles, sister group to synapsids, the situation has been less clear. Despite an increased knowledge of embryology and phylogenetics, and an abundance of new palaeontological data, the prevalent hypothesis regarding the homology of the reptilian coracoid has remained largely unchanged for more than 80 years. Unlike mammals, there has been little consideration given to the development of the reptilian pectoral apparatus as a whole. This paper has three main objectives: (1) to review the morphology and development of the pectoral apparatus in both extinct and extant amniotes; (2) to re-address homology of the reptilian coracoid; and (3) to re-evaluate the scenario of coracoid evolution in amniotes.

EARLY EVOLUTION OF THE PECTORAL APPARATUS – A BRIEF REVIEW

Except for the sternum, most pectoral elements were present in osteichthyians well before the appearance of limbs. Among non-digit bearing members (Fig. 1A) this region is dominated by elements of the dermal skeleton, including the cleithrum, clavicle and unpaired interclavicle. These components are linked to the caudalmost portion of the head skeleton overlying the gill chamber. Articulation with the humerus occurs at the relatively small and laterally obscured endoskeletal component of the pectoral apparatus, the primary girdle[1]. The primary girdle of non-digit bearing osteichthyians is the undivided scapulocoracoid.

With the evolution of digit-bearing limbs (Fig. 1B) elements linking the head skeleton with the pectoral apparatus were lost, resulting in a decoupling of the dermal girdle from the skull (Clack, 2002). Furthermore, the once modest scapulocoracoid adopted a more prominent and laterally facing profile. Further reduction of the dermal girdle (in particular the cleithrum) and enlargement of the primary girdle characterizes more deeply nested non-amniote tetrapods (Fig. 1C). Among these and more derived tetrapods, the singular scapulocoracoid is partitioned into two elements, a dorsal scapula and a ventral coracoid.

Among basal amniotes (Figs 1D, E) the lone coracoid is replaced by two discrete components, a cranial *procoracoid* and a caudal *metacoracoid* (see Table 1 for a listing of coracoid synonyms). For modern taxa, the scapula is the most widely conserved element of the pectoral apparatus, absent only in some lepidosauromorphs (e.g., ophidians). Monotremes are unique in retaining both the procoracoid and metacoracoid, whereas therian mammals (marsupials and eutherians) and reptiles (including birds) each maintain only one of the two elements; in therians the procoracoid no longer forms a discrete entity and the metacoracoid is a rudiment that fuses with the scapula, giving rise to the coracoid process. Conversely, in reptiles it has long been assumed that the metacoracoid has disappeared and only the procoracoid remains. The procoracoid is understood to be equivalent to the coracoid of non-amniote tetrapods. Consequently,

[1] The primary girdle includes those elements pre-forming in cartilage that develop before the dermal pectoral contributions. This includes the scapulocoracoid and all derivatives thereof.

modern authors typically refer to this element in reptiles as simply *the coracoid* (e.g., McGonnell, 2001), a designation adopted hereafter to avoid unnecessary confusion.

In comparison with the rest of the pectoral apparatus, the sternum is often poorly preserved or entirely absent from fossil taxa. This observation is usually explained in the context of histology; unlike other pectoral components that ossify, the sternum often remains cartilaginous. Notwithstanding its poor palaeontological representation, the sternum is considered characteristic of virtually all tetrapods (including lissamphibians and most amniotes, with the exception of turtles [although see below] and ophidians), with preserved material dating back to at least the Late Permian (256-248 million years ago; Vaughn, 1955).

A QUESTION OF HOMOLOGY - THE CORACOID CONUNDRUM

Questions concerning the homology of various pectoral elements rank as some of the oldest in comparative anatomy. In a celebrated series of woodcuts, Belon (1555) compared the skeletons of a man and a bird. Using a series of labels, Belon accurately identified the majority of the homologous elements between the two specimens. One of his few misinterpretations was to pair the avian coracoid with the human clavicle. Although this particular hypothesis has long since become abandoned, the homology of the coracoid element(s) remained as a topic of considerable debate for early anatomists.

Prior to the late 1800's, it was commonly held that of the two coracoid elements present in basal amniotes and monotremes, only the caudalmost element, the metacoracoid, was retained by modern reptiles and therians (e.g., Parker, 1868; Flower, 1876; Fig. 2A). The cranialmost element, the procoracoid, was assumed to be lost. Soon however, new developmental and palaeontological evidence began to confuse the issue. Howes (1887, 1893) observed that the developing scapula of a generic rabbit consisted of three discrete centres—one giving rise to the blade and scapular spine, one forming the coracoid process and one contributing to the glenoid. He interpreted these centres as corresponding to the scapula, procoracoid and metacoracoid of monotremes, therefore suggesting that the procoracoid was not lost (Fig. 2B).

An alternative opinion was expressed by Lydekker (1893), who compared the development of the coracoid process of a sloth with the dual coracoid elements of what

was then considered a basal reptile (viz., *Dicynodon* sp., now considered to be a basal synapsid). He concluded that the procoracoid was homologous with the therian coracoid process of the scapula, and that the caudalmost element, what he named the metacoracoid, was the only coracoid element of reptiles (Fig. 2C). This was later rebutted by Broom (1899), who returned to the notion that modern amniotes, with the exception of monotremes, had lost the procoracoid.

While aspects of the debate continued—e.g., Gregory and Camp (1918; see also Hanson 1920) argued that basal amniotes originally had three coracoid elements: the epicoracoid, coracoid and metacoracoid—the work of Williston (1911, 1925) is often cited as the basis for our modern interpretation of reptilian coracoid homology (Broom, 1912; Case and Williston, 1913; Hanson, 1920; Romer, 1922, 1956). Williston examined a variety of what were then considered to be fossil 'reptilian' taxa (most of which have since been recollected as Amniota outgroups) and noted that whereas the scapula and procoracoid were generally fused, the metacoracoid, if present at all, was often poorly sutured or completely unattached. Williston and others (e.g., Broom, 1912; Case and Williston, 1913) interpreted this as evidence for the anagenetic disappearance of the metacoracoid amongst modern reptiles.

Adopting the interpretation of Williston, Romer (1956; see also 1922) expanded the argument. Observing that non-amniote tetrapods (e.g., *Seymouria* spp., lissamphibians), therians and modern reptiles have only one coracoid element, whereas some basal amniotes (e.g., *Dimetrodon* spp.; see below) had two, Romer formulated an evolutionary scenario (Fig. 3), whereby the procoracoid was the primitive element. This procoracoid was retained by reptiles and some synapsids (e.g., monotremes). Among basal synapsids a second more caudal element, the metacoracoid, developed. In therians the procoracoid disappears whereas the metacoracoid is retained, albeit in a reduced form as the coracoid process of the scapula. Among those fossil reptiles that demonstrated both coracoid elements, Romer suggested that for some taxa this reflected a proximate genealogy with synapsids. For others he stated "[w]e must assume either that the general reptile stem early acquired a second coracoid element which survived only in synapsids, other reptiles rapidly losing it again, or that parallelism occurred, with the development of a second coracoid in two or more lines. The second assumption is the more

reasonable, but the situation is far from clear." (1956, p. 309). Indeed the situation remains uncertain, for as alluded to above, revised phylogenetic hypotheses of Amniota (Fig. 4) have weakened some of the fundamental underpinnings to the modern theory of reptilian coracoid homology as established by Williston (1911, 1925).

CELL CONDENSATIONS

Elucidating the evolution and development of a morphological complex such as the pectoral apparatus is a daunting task. Variation in the embryological origin, adult phenotype and overall number of constituent elements often leads to confusion regarding each component's anatomical and phylogenetic identity. Atchley and Hall (1991) created a model for understanding complex structures that begins with the identification of fundamental developmental units. At the cellular level, these fundamental developmental units are cell condensations characterized as "...the raw material of morphology..."(Hall and Miyake 1992, p. 108). All organs, bones included, begin as aggregations of cells (Atchley and Hall, 1991; Eames et al., 2003), with those condensations presaging the skeleton referred to (collectively) as the membranous skeleton (Grüneberg, 1963; Hall and Miyake, 1992). Unlike adult skeletal elements, which may fail to form or become insensibly assimilated into other bones and cartilages, cell condensations are present (at least briefly) as discretely recognizable units. During both development and evolution, cell condensations may experience variation as a result of changes in mitosis (cell proliferation), identity (differentiation), the size of the aggregation, and/or localized heterochrony (Atchley and Hall, 1991; Hall and Miyake, 1992; Dollé et al., 1993). Consequently, cell condensations provide a useful means for establishing homology of elements in a multipartite structure (Hall and Miyake, 1992; see also Klima, 1973, 1987), and are critical for the study of the evolution and development of the pectoral apparatus.

THE SYNAPSID PECTORAL APPARATUS

EXTANT DEVELOPMENT AND MORPHOLOGY

In order to effectively address the question of reptilian coracoid homology it is first necessary to review the pectoral apparatus of mammals. As will be demonstrated, in

mammals the transformation of the pectoral apparatus from a multipartite complex (characteristic of basal forms and monotremes) to one of relatively few elements (such as therians) is achieved by a reorganization of cell condensations. Elements are not lost *per se*, but have become insensibly integrated and thus are no longer discretely identifiable. Lessons drawn from the mammalian case study are subsequently used to underpin the revised scenario of coracoid homology in reptiles and illustrate the overall trend among amniotes towards morphological evolution of the pectoral apparatus.

Unique among modern amniotes, adult monotremes retain each of the scapula, procoracoid, metacoracoid, clavicle, interclavicle, and sternum (Fig. 5A, B). Despite the rarity of available material, morphogenesis of the monotreme pectoral apparatus has been well documented (Klima, 1973; 1985). During development, each ipsilateral scapula, procoracoid and metacoracoid arise from a common homogeneous endochondral condensation—the coracoid-scapular plate (Fig. 5C; Klima, 1973). The glenoid (for articulation with the humerus) develops at the intersection of the scapula and metacoracoid, to the exclusion of the procoracoid. Midventrally, these elements are bridged by a midline T-shaped interclavicle.

Developmentally the interclavicle is exceptional, receiving contributions from two skeletogenetic sources: an unpaired endochondral condensation (the *pars chondralis interclaviculae*) that combines with paired intramembranous condensations (the *pars desmalis interclaviculae*) to form a composite anlagen (Fig. 5C; Klima, 1973, 1987). A pair of slender clavicles forms along the cranial margin of the interclavicle, each derived from a single intramembranous condensation. The skeletally mature sternum includes a cranialmost manubrium sterni, followed by a series of variably co-ossified block-like sternebrae (and in tachyglossids, but not *Ornithorhynchus anatinus*, a terminal xiphisternum), all of which develop from a longitudinal pair of condensations, the sternal bands (Klima, 1973).

In contrast to adult monotremes, the pectoral apparatus of therians is composed of fewer osteological components, with only the scapula and sternum present in all forms. Adult therians lack a discrete interclavicle (although see below), the clavicles may be reduced or completely absent (e.g., ungulates, peramelid marsupials; Flower, 1876; see

also Hall, 2001), and the coracoid elements are either rudimentary or vestigial (Klima, 1973, 1985, 1987).

The scapula is the only therian pectoral apparatus element to articulate with the forelimbs. Although morphologically variable in profile (Fig. 6A-C), virtually all therian scapulae have a coracoid process adjacent to the glenoid and at least one conspicuous scapular spine that divides the lateral surface into two relatively large, shallow fossae (Sánchez-Villagra and Maier, 2002). The distal terminus of the scapular spine gives rise to a second process—the acromion—that comes into close proximity or articulates with the clavicle, when present.

Similar to monotremes, therians develop a coracoid-scapular plate early during morphogenesis that becomes dominated by the presumptive scapula. However while the procoracoid precursor is initially present, it does not develop beyond a rudiment, merging with the sternal bands and a median (unpaired) endochondral condensation (Fig. 6D; discussed below), or a vestige nested between the clavicle and manubrium sterni. Among various marsupial lineages (e.g., dasyurids) these vestiges—the praeclavia (Klima, 1987)—are relatively common, and may remain cartilaginous or ossify with age. For eutherians such vestiges (termed suprasternals; Hanson, 1919; Klima, 1968; 1972; 1987) are rare and considered to be atavisms.

Similar to the procoracoid, the metacoracoid primordium develops only as a rudiment. Initially it joins the procoracoid in contacting the manubrium sterni. This connection is transient, however, and eventually disappears, with the metacoracoid remaining firmly affixed to the scapular condensation (Fig. 6A). Ultimately, the metacoracoid gives rise to the coracoid process. In some taxa (e.g., the marsupial *Monodelphis domestica*, the insectivores *Crocidura russula* and *Suncus etruscus*) the metacoracoid condensation also contributes to the glenoid (Sánchez-Villagra and Maier, 2002; Groβmann et al., 2002).

The acromion develops prior to the scapular spine, arising from a cartilaginous primordium that splits off the scapula (Sánchez-Villagra and Maier, 2002, 2003; Groβmann et al., 2002). In most taxa, the scapular spine subsequently forms by appositional ossification of the scapular perichondrium (e.g., *M. domestica*, *C. russula*; Sánchez-Villagra and Maier, 2002; Groβmann et al., 2002). However, in the rodent

Mesocricetus auratus, the spine reportedly develops from a cartilage precursor stemming from the acromion (Groβmann et al., 2002).

Experimental work on the laboratory rodent, *Mus musculus*, illustrates that normal development of the mature scapula is dependent on expression of *Pax1*, *Hoxc6* and *Emx2* genes. The acromion is greatly affected in mutants deficient for *Pax1* (*undulated mutants*), and may be completely absent, present and grossly deformed, or present and fused with the clavicle (compare Fig. 6E-F; Timmons et al., 1994; Dietrich and Gruss, 1995). In contrast, defects of the rest of the scapula including the scapular spine involve a relatively minor reduction in size. Similarly, the scapular blade remains virtually unchanged in mice with a mutation in the platelet-derived growth factor α gene receptor (*PDGFαR*; required for normal patterning of the somites) or *Hoxc6*, whereas the acromion (*PDGFαR*; Soriano, 1997), or acromion and glenoid (*Hoxc6*; Pellegrini et al., 2001) are altered. In another dramatic deviation, the scapular blade fails to form in *Emx2* homozygous knockout mutants, with only the coracoid process, acromion and glenoid of the scapula developing (Pellegrini et al., 2001). Data from the mouse mutants is consistent with the individuation of pectoral elements, which is consistent with an independent evolutionary origin.

The bulk of the sternum is derived exclusively from condensations of lateral plate mesoderm—the sternal bands. As noted earlier, the cranial end of the sternum, the manubrium sterni, receives contributions from three distinct sources: the procoracoid rudiments, the sternal bands, and an unpaired cartilaginous condensation (Fig. 6D). Based on location, morphology and histology of the unpaired condensation, Klima (1987) identified this unmatched rudiment as the homologue of the pars chondralis interclaviculae of monotremes. As for the scapula, mutations in *Pax1* lead to defects of the sternum (Timmons et al., 1994)

Unique to mysticete (toothless) cetaceans, the sternal bands fail to form during embryogenesis. Among adults however, the sternum is present, derived exclusively from the procoracoid rudiments and the pars chondralis interclaviculae (Klima, 1978, 1985, 1987, 1990).

FOSSIL EVIDENCE

Among outgroups to modern mammals (Monotremata + Theria) the pectoral apparatus includes both the procoracoid and the metacoracoid (Fig. 7; Luo et al., 2002). Whereas the glenoid is restricted to the metacoracoid and scapula among monotremes and various closely related lineages (e.g., *Morganucodon* spp., *Sinoconodon rigneyi*; Jenkins and Parrington, 1976; Luo et al., 2002), it receives a minor contribution from the procoracoid in more basal synapsids (see Romer, 1956; Jenkins and Parrington, 1976). In the basalmost forms, the paraphyletic "pelycosaurian-grade synapsids" or "pelycosaurs" (e.g., *Dimetrodon* spp.), each of the procoracoid and metacoracoid gain prominence as broad, plate-like elements. Among "pelycosaurs" it has frequently been observed that the scapula and procoracoid are co-ossified (or at least tightly sutured), whereas the junction between the metacoracoid and the other elements is rarely fused or well sutured (e.g., Williston, 1911; Case and Williston, 1913; Romer and Price, 1940).

DISCUSSION

Developmental and palaeontological evidence clearly demonstrates that whereas the modern adult therian pectoral apparatus is composed of few elements, ontogenetically and historically it is quantitatively more complex. Embryological data suggest that the majority of the membranous skeleton initiating the multipartite pectoral pattern of monotremes (Fig. 5C) is retained by virtually all therians, regardless of the adult phenotype (Fig. 6D). Hence, the sequential nonappearance of discrete pectoral ossifications amongst modern adult therians (both developmentally and phylogenetically) may be correlated with reorganization of skeletogenetic condensations. The presence of a discrete procoracoid and metacoracoid is primitive for mammals but lost in therians. The therian procoracoid unites with the pars chondralis interclaviculae and sternal bands to form the manubrium sterni, although in some taxa a discrete portion may be retained as a separate element (the praeclavium or suprasternal). Uniquely therian features of the pectoral apparatus include derivatives of the metacoracoid (the coracoid process and, at least among some eutherians, the acromion and multipartite glenoid) and the combined procoracoid and interclavicle (the composite manubrium sterni).

THE REPTILIAN PECTORAL APPARATUS

Among reptiles the morphological diversity of the pectoral apparatus is immense. In the interest of clarity, this review recognizes three structurally similar groups: ornithodirans (birds and their ancestors), non-avian diapsids (a paraphyletic group consisting of lepidosauromorphs, crocodylians and their fossil relatives) and Testudines (turtles).

REPTILIA → DIAPSIDA → ORNITHODIRA

EXTANT DEVELOPMENT AND MORPHOLOGY

The avian pectoral apparatus consists of a narrow blade-like scapula, tubular/strut-like coracoid, and a large unsegmented (and usually keeled) sternum (Fig. 8). Most (but not all) modern avians also demonstrate a single chevron-shaped furcula (Parker, 1868; Hall, 2001; Chapter 2). As in mammals the scapula and coracoid develop from a unified homogeneous condensation at the base of the limb bud (Romanoff, 1960; Hamilton, 1965). During chondrogenesis, the prospective elements detach from one another, and typically remain separated prior to and following ossification (Fig. 8; Romanoff, 1960), although in some large flightless birds the scapula and coracoid may secondarily rejoin post-hatching (Glutz von Blotzheim, 1958; see also Elzanowski, 1988). In many taxa the coracoid develops a bony medial projection, the procoracoid process.

Using the domestic fowl *Gallus gallus*, it has been established experimentally that the scapula is derived, at least in part, from an embryological source distinct from the rest of the pectoral apparatus. Whereas the coracoid and sternum are derivatives of lateral plate mesoderm, chick-quail transplantation experiments by Chevallier (1975, 1977; see also Beresford, 1983) have shown that most of the scapula arises from somites. More recently Huang et al. (2000) demonstrated that the proximal-most portion of the scapula (the area around the glenoid), like the coracoid, is derived from lateral plate mesoderm. Other experimental observations further reinforce this idea. While *Talpid*[3] chick mutants demonstrate several primary girdle defects, the deviant scapula morphology (resembling an open chevron with tooth-like projections) is considerably more severe than the modestly foreshortened coracoid (Fig 9; Ede and Kelly, 1964). Work examining the role of *Pax1* found that repression of this gene by application of BMP-2 and –4 soaked beads

resulted in defects of the proximal part of the scapula and (in some instances) the coracoid, including coracoid aplasia (Hofmann et al., 1998). Localized application of retinoic acid (via bead implants) or tissue grafts of the polarizing region of an exogenous limb bud to the developing wing buds of *G. gallus* enlarges the *Hoxc6* (formerly *Xlhbox 1*) gradient and may result in fusion of the scapula with the coracoid, as well as duplication or foreshortening of the coracoid and absence of the procoracoid process (Oliver et al., 1990; see also Williams, 2003). Thus patterning of the procoracoid process appears to be at least partially independent from the rest of the coracoid.

Whereas modern researchers have largely overlooked the development of the procoracoid process, early anatomists recorded that it developed independent of the rest of the avian coracoid (Fig. 10A; Newton and Gadow, 1893-1896; Parker, 1868). Indeed Parker remarked "[t]he præ-coracoid (procoracoid) is always segmented from the head of the coracoid" (p. 143), and noted that it may become mineralized independent of the latter. Lindsay (1885) and Broom (1906b) later examined the development of the procoracoid process in *Struthio camelus* (the ostrich; Fig. 10B) but arrived at conflicting interpretations. Whereas Lindsay argued that the procoracoid process developed independent of the coracoid, according to Broom the procoracoid process represents a "descending process of the scapula" (p. 357). Broom further argued that the procoracoid process could not be homologous with the procoracoid of basal amniotes as such a bone was not present in any immediate ancestors of modern avians (although see below).

FOSSIL EVIDENCE

The morphology of the pectoral apparatus in most fossil avians is similar to that of modern birds including the 'U' or 'Y'-shaped furcula, although the procoracoid process often appears to be absent (Chiappe et al., 1999). In the basalmost avian taxon (*Archaeopteryx lithographica*) the coracoid no longer exhibits the strut-like morphology of modern forms, but instead is almost rectangular when viewed cranially (Fig. 11; Ostrom, 1976; Elzanowski, 2002). The morphology of the coracoid among non-avian dinosaurs (e.g., non-avian theropods, sauropodomorphs, ornithischians) is structurally conserved as a broad and plate-like element.

REPTILIA → DIAPSIDA → NON-AVIAN DIAPSIDS

EXTANT DEVELOPMENT AND MORPHOLOGY

With the exception of ophidians (among which the forelimbs and pectoral apparatus are always absent, even as rudiments; Cohn and Tickle, 1999), modern pseudosuchians (crocodylians) and lepidosauromorphs (sphenodontids + squamates), including virtually all limbless 'lizards' and some amphisbaenians, develop a scapula and coracoid (Fig. 12; Parker, 1868; Cope 1892; Camp, 1923; Zangerl, 1945; Stokely, 1947; Montero et al., 1999; Kearney, 2002;). Each element is capped distal to the glenoid by a cartilaginous extension (the suprascapular and epicoracoidal cartilages). The morphology of the lepidosauromorph scapula and coracoid (including cartilaginous extensions) is highly variable and frequently includes multiple deep emarginations, fenestrations or both along the cranioventral borders (Fig. 12B; Romer, 1956; Lécuru, 1968b). Among various authors it has been suggested that there is an additional pectoral element—the pre- or procoracoid—that either remains cartilaginous (and has been suggested as part of the epicoracoidal cartilage; Broom, 1906a; Romer, 1956; Skinner, 1959) or forms an ossified strut-like process between two emarginations/fenestrations (e.g., Parker, 1868; Cope, 1892). Conrad (2006) observed an independent ossification (his precoracoid) separated from the coracoid by a suture in subadult specimens of *Shinisaurus crocodilurus* (Fig 12C). Regrettably, the situation for most taxa remains unresolved. A comparable procoracoid element has not been reported for crocodylians.

FOSSIL EVIDENCE

The pectoral apparatus of fossil non-avian diapsids such as pseudosuchians, lepidosauromorphs and basal archosauromorphs falls within the morphological range revealed by modern forms. As in extant (skeletally mature) taxa there is only one discrete coracoid ossification, although numerous specimens preserve evidence of the cartilaginous epicoracoidal and suprascapular cartilages (Osborn, 1899; Müller, 2001). Notwithstanding their absence among non-avian diapsids, both the procoracoid and metacoracoid are present among immature and some adult specimens of the diapsid outgroup Captorhinidae (Fig. 13). Conspicuously, in larger (adult-sized) material all elements of the captorhinid primary girdle are fused, often with the sutures obliterated.

As in synapsids (and proganosaurs; see below), the scapula and procoracoid are the first primary girdle elements to coalesce (Holmes, 1977; Sumida, 1989).

REPTILIA → ? PROGANOSAURIA/?DIAPSIDA → TESTUDINES

EXTANT DEVELOPMENT AND MORPHOLOGY

The phylogenetic position of Testudines remains contested, oscillating between the traditional assignment as a proganosaur (e.g., Romer, 1956; Lee, 1996, 1997; proganosaurs include all members of the group formerly identified as Anapsida [Modesto and Anderson, 2004]), and the more recent inclusion as a member of Diapsida (e.g., Rieppel and deBraga, 1996; deBraga and Rieppel, 1997). Irrespective of the genealogical scenario, the morphology of the pectoral apparatus of turtles is unique among amniotes, and (at least amongst adults) bears little resemblance to that of other taxa. Of particular note is the radical emplacement of the replacement bones of the pectoral apparatus within the rib cage, integration of clavicular and interclavicular homologues (the paired epiplastra and median entoplastron respectively; e.g., Parker, 1868; Romer, 1956; Rieppel, 1993; Gilbert et al., 2001) into the plastron, and the apparent absence of a sternum (although see below). Whereas developmental studies have not specifically targeted the turtle pectoral apparatus, a variety of incidental observations have been made during investigations of gross embryology and ontogeny of the carapace/plastron.

In adults, the primary girdle forms a triradiate structure with slender dorsal, caudal and ventromedial processes (Fig. 14A, B). The glenoid is positioned at the crux. Whereas the column-like dorsal ramus is widely accepted as the scapula, the identity of the remaining processes has been the subject of debate. The ventromedial or acromial process has been identified as the homologue of the procoracoid (e.g., Parker, 1868; Korringa, 1938; Gaffney, 1990; deBraga and Rieppel, 1997) or alternatively, as an outgrowth of the scapula (e.g., Romer, 1956; Walker, 1947, 1973; Lee, 1997). The caudal ramus (the coracoid) has been presumed to represent either the metacoracoid (e.g., Parker, 1868; Gaffney, 1990; deBraga and Rieppel, 1997; Lee, 1997) or the procoracoid (Walker, 1947, 1973).

During the earliest stages of chondrogenesis, the presumptive scapula, acromial process and coracoid of each side develop from either a unified trifurcate condensation or

a trifurcate condensation in which the caudal ramus is initially isolated (Fig. 14C; Walker, 1947; Rieppel, 1993c; Sheil, 2003, 2005). In at least one taxon (*Chrysemys picta marginata*), a supracoracoid foramen transmitting a neurovascular bundle, is present early during development, nested between the presumptive scapula and coracoid (Walker, 1947). As the scapula and coracoid continue to differentiate, the neurovascular bundle is liberated from the now cartilaginous complex and the foramen disappears. In all taxa studied thus far (e.g., *Apalone spinifera*, *Chelydra serpentina*) each ramus begins to ossify from a separate centre within the condensation. The notion of the scapula developing independent of the other replacement bones is supported by the extirpation experiments of Burke (1991b). The majority of *C. serpentina* embryos that had cervical somites 8-12 removed demonstrated scapular aplasia or incomplete scapula development, whereas the acromial process, coracoid and elements of the limb appear to have been minimally affected.

FOSSIL EVIDENCE AND DISCUSSION, HYPOTHESIS 1 – TESTUDINES AS PROGANOSAURIA

The remarkable osteology of turtles dates back over 200 millions years (Gaffney, 1990). Similar to modern forms, the oldest well-preserved fossil taxon, *Proganochelys quenstedti*, has a bony shell (plastron/carapace) and an internalized primary girdle. Although lacking a strictly tripodal morphology, the primary girdle does consist of a scapula with a prominent acromial process and a coracoid (14E, F). A supracoracoid foramen is present nested in the suture between the two elements, similar to the aforementioned (albeit transient) aperture of modern turtle embryos.

In view of their unusual morphology, the genealogical relationship of turtles to other amniotes is difficult to unequivocally resolve. Historically however, they have long been considered members of Proganosauria (demonstrating the anapsid condition, a skull without temporal fenestrations; Fig. 15A). Among the most deeply nested non-turtle fossil proganosaurs (e.g., pareiasaurs and procolophonids), the pectoral apparatus closely resembles the morphology previously noted for basal synapsids (viz., "pelycosaurian grade synapsids"), with a robust, plate-like procoracoid and metacoracoid (Lee, 1996, 1997; deBraga, 2003). As in basal synapsids, the glenoid may receive contributions from

the metacoracoid and scapula alone, or include minor involvement of the procoracoid. Among basal proganosaurs (e.g., mesosaurids, millerettids), the scapula and coracoid element(s) are typically fused together into a single element (Gow, 1972; Modesto, 1999). Unfortunately, few data are available on the ontogeny of fossil proganosaurs and it remains unclear if both coracoids are present and fuse together during early skeletogenesis or if one element fails to form.

Corresponding to the burgeoning interest in testudine evolution, several efforts have been made to resolve the identification of the acromial process. At present, two competing views are held: the acromial process as an outgrowth of the scapula or as the homologue of the procoracoid (see below). Assuming Testudines as proganosaurs, it has recently been proposed that the evolution of the acromial process may be traced phylogenetically from procolophonids—which lack any conspicuous scapular processes—to pareiasaurs—that demonstrate an incipient ridge-like projection—to modern turtles and allies (Fig. 15A; Lee, 1996, 1997; although see Rieppel [1996] for an contradictory interpretation of the same data). According to this hypothesis, the advent of the acromial process (in pareiasaurs) precedes loss of the procoracoid.

FOSSIL EVIDENCE AND DISCUSSION, HYPOTHESIS 2 – TESTUDINES AS DIAPSIDS

Recently, a number of studies have suggested Testudines represent derived diapsids more closely related to lepidosauromorphs than archosauromorphs (Fig. 15B; Rieppel and deBraga, 1996; deBraga and Rieppel, 1997; Rieppel and Reisz, 1999; see also Wilkinson et al., 1997). While it is widely acknowledged that this relationship seems counterintuitive (conventional diapsid skulls are fenestrated, turtle skulls are not), the hypothesis gleans support from its global or broad-based perspective (Rieppel and Reisz, 1999); the removal of certain groups not normally considered in turtle phylogenetics (viz., sauropterygians, a sister group to lepidosauromorphs not discussed here) repositions Testudines within Proganosauria. Among the anatomical details used to underscore the diapsid theory is a reappraisal of the acromial process of the scapula. Various authors (Gaffney, 1990; Rieppel, 1996; de Braga and Rieppel, 1997) have rejected the homology of the acromial process as an outgrowth of the scapula and

alternatively suggested that it is homologous with the procoracoid (Fig. 15B). Indeed the acromial process shares with the procoracoid a similar topology and is likewise connected with the interclavicle/clavicle homologues. Accordingly, Gaffney (1990) has used this evidence to hypothesize that the coracoid element of Testudines represents the metacoracoid and not the procoracoid (see discussion below).

REPTILIA DISCUSSION - EVOLUTION OF THE AMNIOTE CORACOID(S)

Previous work suggested that the procoracoid is maintained by modern reptiles whereas the metacoracoid was either independently derived (homoplasious) and lost in some basal members, or was only transiently present. This investigation finds the procoracoid-equals-coracoid proposal to be inconsistent with current data, and indicates (following the work of Gaffney, 1990) that the reptilian coracoid is the homologue of the metacoracoid. For the sake of convenience this evidence may be summarized in three main categories, although none are mutually exclusive.

(1) Palaeontology and genealogy: Regardless of genealogical scenario, a three-element primary girdle is plesiomorphic for all amniotes. Within each of Synapsida and Reptilia one coracoid element appears to be independently lost. However fossil material representing various ontogenetic stages of both basal synapsids (e.g., specimens of *Dimetrodon*; Romer and Price, 1940) and reptiles (*Captorhinus* sp.; Holmes, 1977) demonstrates that this apparent loss is an example of two skeletal centres coalescing to form a single mature morphology. Thus while the procoracoid is present and discrete among subadults, it generally fuses with the scapula (and the sutures disappear) in larger 'adult-sized' individuals (see Fig. 13). Consequently the scapula element of skeletally mature specimens in effect represents the scapula + procoracoid. In contrast, the metacoracoid frequently remains independent and discrete (Williston, 1925; Romer and Price, 1940; see also Gaffney, 1990).

(2) Topography and connectivity: Several arguments can be made on the basis of the position and association of the various elements. Among basal amniotes the glenoid is

dominated by the metacoracoid, with a decreasing contribution from the scapula and (when apparent) the procoracoid. According to the theory of Williston (1925) and Romer (1956), the glenoid of modern reptiles is taken over by the formerly minimally contributing procoracoid. In contrast, the revised hypothesis presented herein proposes that the glenoid of extant reptiles, similar to basal forms, remains dominated by the metacoracoid.

Of the two coracoid elements of basal amniotes, only the procoracoid contacts both the clavicle and interclavicle. In Testudines (including *Proganochelys quenstedti*), the acromial process shares a common topology with the procoracoid of basal amniotes and retains a comparable contact with the clavicle-interclavicle homologues (viz., the epiplastron and entoplastron; Gaffney, 1990; Fig. 14A). Among avians, the procoracoid process also demonstrates a similar connection with the intramembranously derived furcula. In both these representative amniotes, the process contacting the dermal element(s) is held to be the procoracoid, secondarily joined with either the scapula (Testudines) or coracoid (Aves). Gaffney (1990) also observed that the interpreted position of supracoracoideus muscle attachment on the procoracoid of basal amniotes (*sensu* Romer, 1922; Holmes, 1977) corresponds to the same muscle origin on the acromial process of the turtle coracoid.

(3) Development and experimental embryology: Among therians, the sternum and primary girdle elements receive contributions from multiple embryonic condensations. For instance, the skeletally mature scapula element minimally represents a coalescence of the metacoracoid rudiment with the scapular condensation, and the manubrium sterni integrates components of the procoracoid, pars chondralis interclaviculae rudiment and sternal band. These developmental data are supplemented by evidence gleaned from the study of mutant mouse strains. In *Emx2* mutants, the coracoid process, acromion and glenoid develop, whereas the blade of the scapula fails to form (Pellegrini et al., 2001). This indicates that *Emx2* plays a role in patterning the scapular condensation but not the metacoracoid rudiment. In contrast, normal development for derivatives of the metacoracoid (e.g., coracoid process, glenoid and acromion) is dependent on *Pax1*, *PDGFαR* and *Hoxc6* (Timmons et al., 1994; Soriano, 1997; Pellegrini et al., 2001; Fig.

6E, F). At the present time however the embryological source of the mammalian scapula (somites and/or lateral plate mesoderm) remains to be determined.

Among lepidosauromorphs the presence of a discrete procoracoid has been reported (Fig. 12C; Conrad, 2005), although in most instances it is unclear if the element in question is different from the coracoid element proper or the epicoracoidal cartilage. In the reptilian lineage Pseudosuchia there is (presently) no evidence for the development of more than one coracoid element, even transiently. However, neither group has been explored experimentally so future efforts will undoubtedly yield important data.

Among avians, the procoracoid process of the coracoid, as noted above, occupies a comparable position and set of articulations with the procoracoid of basal amniotes. Furthermore, it develops independent of the coracoid, and fuses with the latter at some later point of skeletogenesis (Fig. 10A; Parker, 1868). Experiments on the avian *Gallus gallus* that enlarge the *Hoxc6* gradient result in a reduction or complete absence of the procoracoid process (a derivative of the procoracoid), along with defects of the glenoid region of the scapula (possible procoracoid or metacoracoid origin) and (meta)coracoid malformations (Oliver et al., 1990). Other experimental work (including somite extirpation, chick-quail grafting and gene expression labeling), also demonstrates that the avian scapula receives contributions from more than one embryological source, viz. somites and lateral plate mesoderm (see Chevallier, 1977; Timmons, et al., 1994; Hofmann et al., 1998; Huang et al., 2000; Pellegrini et al., 2001). In contrast, the (meta)coracoid is exclusively lateral plate. Huang et al. (2000) suggested that the non-somitic source of the scapula was homologous with the metacoracoid. It should be noted however the procoracoid is a comparable candidate. Similar to scapula development in mice, the gene *Pax1* has been observed to play a role in patterning of the normal avian scapula element (Hofmann, et al., 1998; Huang et al., 2000), whereas *Hoxc6* is involved in regulation of the procoracoid and metacoracoid derivatives. Indeed mutations of *Pax1* and *Hoxc6* in *G. gallus* embryos results in primary girdle defects, minimally including the proximal part of the scapula, and in more extreme cases, the coracoid (Oliver et al., 1990; Hofmann et al., 1998). This indicates that similar to mice, *Pax1* and *Hoxc6* play a role in specifically patterning derivatives of the metacoracoid and (at least in avians) the procoracoid.

As with the avian procoracoid process, the acromial process of Testudines is topographically, connectively and developmentally comparable with the procoracoid. During skeletogenesis each of the turtle scapula, acromial process and coracoid arises from separate centres of ossification (Parker, 1868; Rieppel, 1993c, Sheil, 2003). Removal (extirpation) of cervical-thoracic somites results in aplasia of the scapular blade but has little effect on the development of the acromial process, glenoid region or coracoid, (Burke, 1991b). The data clearly imply a separate origin for each of the acromial process and scapula blade, one that may readily be explained by integration of the procoracoid rudiment into the scapula. This parallels the fusion/integration of the procoracoid and scapula in basal diapsids and synapsids.

REMAINING ISSUES

Two remaining issues deserving mention necessitate a brief departure before assembling a new scenario of coracoid evolution. The first concerns the position of the supracoracoid foramen. Among basal amniotes the procoracoid is pierced by a neurovascular passage, the supracoracoid foramen, proximal to the procoracoid-metacoracoid contact. Acceptance of the procoracoid equals coracoid hypothesis for non-basal reptiles requires that the supracoracoid foramen relocate within the metacoracoid. As observed by Gaffney (1990), in the basal testudine *Proganochelys quenstedti*, and Walker (1947), in developing *Chrysemys picta marginata*, this aperture has shifted position to be found within the suture connecting the remaining coracoid with the scapula (Fig. 14F). Among extant reptiles (exclusive of Testudines) the supracoracoid opening for the neurovascular bundle only pierces the coracoid, the modern homologue of the basal amniote metacoracoid. It is the contention here that, following the condition of *P. quenstedti* and embryonic *C. p. marginata* the supracoracoid foramen has further migrated to become bounded by the metacoracoid proper.

The second topic relates to the apparent absence of the sternum in turtles. The view that turtles lack this pectoral element is widely held (e.g., Parker, 1868; Romer, 1956) inasmuch as the ventrally positioned plastron develops entirely via intramembranous ossification (Parker, 1868; Gilbert et al., 2001). Nevertheless, Walker

(1947) suggested that a connective tissue band (the acromialcoracoid ligament; Wyneken, 2001) linking each ipsilateral acromial process and coracoid might be homologous with the sternum. Walker offered four observations to support his hypothesis: (1) ligaments may represent vestiges of cartilage (e.g., in *undulated* mutant mice a ligament may replace the acromion [Timmons et al., 1994]; see also Hall [1970] for a discussion of the relationship between fibroblasts [producing ligaments] and chondroblasts [producing cartilage]); (2) the acromialcoracoid ligament and sternum are both fundamentally paired structures; (3) the acromialcoracoid ligament and sternum arise in association with the coracoid; and (4) the acromialcoracoid ligament and sternum share a general topography with the rest of the pectoral apparatus. However unlike the sternum, acromialcoracoid ligaments do not contact the ribs and do not extend cranially to the clavicular homologues (the epiplastra) or caudally past the coracoids. Walker countered these differences by remarking that acromialcoracoid ligaments represent vestiges (and therefore are not developed to the same extent as a sternum) and that turtle ribs are fully integrated into the carapace (having become ensnared by the carapacial ridge; see Ruckes, 1929; Burke, 1991a; Gilbert et al., 2001). Moreover, as has been demonstrated for other parts of the pectoral apparatus (see above), the mere absence of a skeletal counterpart does not necessarily speak to definitive nonexistence. This notion arguably receives indirect support from a study conducted on the marine reptile clade Plesiosauria.

Similar to Testudines, among plesiosaurs a discrete sternum is both unreported and architecturally problematic. Whereas turtles demonstrate a well-ossified plastron, in plesiosaurs the presence of sternum seems to be precluded by the enlarged and ventrally displaced coracoids. However unlike turtles, in which the ribs are integrated into the carapace, in plesiosaurs the ribs make no obvious connections with any preserved skeletal elements. Nicholls and Russell (1991) reviewed the issue of the sternum in plesiosaurs and, based on data gleaned from sternal development, function and phylogeny, found that the suggestion of such an element was anatomically justified and functionally required. Without a sternum, the pleisosaur girdle would likely be unable to withstand tensile forces associated with cranially directed movements of the forelimbs (Nicholls and Russell, 1991). Nicholls and Russell postulated that the position of the unmineralized (and thus unpreserved) sternum was dorsal (visceral) to the coracoid. Whereas these data

do not speak directly to the presence or existence of a sternum in Testudines (indeed the architecture of the turtle pectoral apparatus fundamentally differs from that of plesiosaurs in the internalization of these elements with respect to the ribcage), they suggest that connective tissues in this region (e.g., the acromialcoracoid ligament) might represent a latent homologue (*sensu* Stone and Hall, 2004). Finally, it is worth observing that regardless of genealogical affinity (proganosaur or diapsid), the ancestors of modern turtles did demonstrate ossified rib cages requiring a sternal underpinning.

A NEW SCENARIO

A revised scenario for the evolution of the amniote primary girdle is offered (Fig. 16), drawing on a global review of available data (documented above) and taking into consideration the role of cell condensations in skeletogenesis. It is argued that disruptions in pre-skeletogenic cell aggregation, proliferation and differentiation, and the acceleration (or retardation) of osteogenesis play vital roles in the evolution of the amniote primary girdle. Plesiomorphically, basal tetrapods have a unified scapulocoracoid (e.g., *Acanthostega gunnari*) or a scapula and a single coracoid (e.g., *Seymouria* spp.). Among basal amniotes, the primary girdle consists of a scapula, procoracoid and metacoracoid. This transformation may be achieved as the normal osteogenic pattern of the condensation forming the membrane skeleton of the primary girdle elements (the coracoid-scapular plate, *sensu* Klima, 1973, 1987) is delayed and/or the failure (and delay) of pre-skeletogenic cells to differentiate, resulting in the formation of sutural contacts. The metacoracoid is more strongly influenced by osteogenic retardation, and unlike the procoracoid will often appear discrete even late in ontogeny.

Within Synapsida, the various outgroups leading to Theria (e.g., *Dimetrodon* spp., monotremes) retain the three part primary girdle. Among therians, phenotypic expression of both the procoracoid and metacoracoid becomes dramatically diminished. This reduction reflects a decrease in pre-skeletogenic cell proliferation. The procoracoid rudiment detaches from the coracoid-scapular plate and either forms a vestigial element (the praeclavium of marsupials) or becomes subsumed into the manubrium sterni (eutherians). In contrast, the therian metacoracoid returns to the primitive condition of remaining joined with the scapula, giving rise to the coracoid process, acromion and

likely contributes to the glenoid. At least among some eutherians, different genes appear to play roles in patterning the metacoracoid rudiment (e.g., *Pax1*, *Hoxc6*) compared with the scapula condensation (*Emx2*), consistent with the aforementioned homology argument.

Among reptiles, most skeletally mature individuals demonstrate only a single coracoid element, herein considered to be the metacoracoid. The procoracoid is not lost *per se*, but is retained as a rudiment that does not detach from the scapular portion of the coracoid-scapular plate. Retention of the combined scapula + procoracoid is in part achieved by a reduction in the duration of pre-skeletogenic cell mitosis (resulting in a decrease in size of the presumptive procoracoid) and an acceleration of osteogenesis (resulting in fusion of the procoracoid and scapula). Observations gleaned from experimental work on turtles and avians suggest that the reptilian scapula is a derivative of both the somites (forming the blade) and lateral plate mesoderm (forming the region around the glenoid).

Unique to avians the procoracoid rudiment may subdivide to join with both the metacoracoid (as the coracoid process) and possibly the scapula (at the glenoid). This partitioning of the procoracoid reflects either a further delay in osteogenesis or a delay in aggregation of the condensation or both. As in eutherians there is evidence to imply a patterning role of the procoracoid and metacoracoid components by *Pax1* and *Hoxc6*. In the absence of data it remains unclear if crocodylians and most lepidosauromorphs retain the procoracoid rudiment (integrated into the scapula) or if this component is lost (i.e., a failure of the presumptive skeletogenic cells to proliferate and/or differentiate).

FUTURE DIRECTIONS

Whereas the newly conceived scenario of amniote pectoral evolution is well supported, important data are lacking in several key areas. As demonstrated, a comprehensive understanding of development, in particular the role of cell condensations, forms the critical underpinning to an understanding the evolution of morphologically complex structures. Regrettably, our knowledge of the membranous skeleton in many reptilian taxa, especially lepidosauromorphs and crocodylians, remains incomplete. Another important area for consideration is the use of experimental embryology. With the

exception of turtles, most non-avian reptiles are infrequent experimental subjects. Even among avians, the diversity of taxa commonly employed is overwhelmingly dominated by a single species, *Gallus gallus*. This despite previous (and in the case of turtles, ongoing) successes with the use of tissue grafts and culturing, gene expression and extirpation experiments, and chimeric surgeries in various non-model taxa (Gans, 1985 and references therein; see also Burke, 1991b; Vincent, et al., 2003; Nagashima, 2005). Increased application of such experimental methods holds great promise as a virtually untapped resource of developmental and evolutionary data.

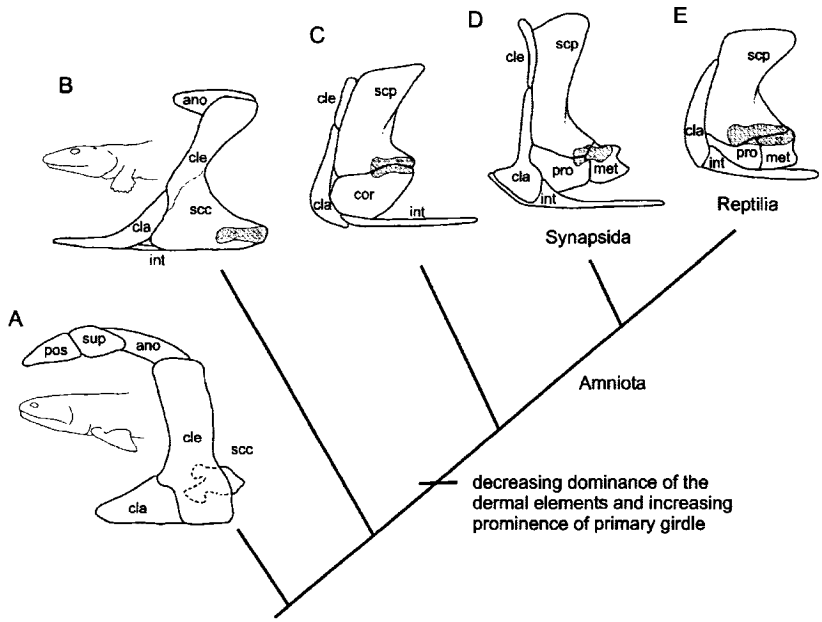

Figure 1. Evolution of the tetrapod pectoral apparatus. Among basalmost non-digit bearing tetrapods (A), the pectoral apparatus is dominated by dermal elements; the scapulocoracoid is small and obscured laterally. With the advent of digits (B), taxa demonstrate a trend towards enlargement of the scapulocoracoid while diminishing the dermal contributions. Characteristically, many of these early digit-bearing taxa fuse the scapulocoracoid with the cleithrum (indicated by dashed line). Among sister taxa to amniotes (C), the once unified scapulocoracoid is partitioned into a dorsal scapula and ventral coracoid, with the glenoid nested at the caudal border between the two. Basal members of both major amniote lineages, Synapsida (D) and Reptilia (E), demonstrate a three part primary girdle consisting of a scapula, procoracoid and metacoracoid. Abbreviations: ano (anocleithrum), cla (clavicle), cle (cleithrum), cor (coracoid), int (interclavicle), met (metacoracoid), pos (posttemporal), pro (procoracoid), scp (scapula), scc (scapulocoracoid), sup (supracleithrum). Glenoid shaded. Phylogeny based on Ruta et al. (2003). Sources for images: (A) *Eusthenopteron foordi* modified from Jarvik (1980); (B) *Acanthostega gunnari* reproduced by permission of the Royal Society of Edinburgh and M.I. Coates from Transactions of the Royal Society of Edinburgh: Earth Sciences, volume 87 (1996), pp. 363-421; (C) *Seymouria* sp. modified from Williston (1925); (D) *Dimetrodon* sp. modified from Romer and Price (1940) reproduced with fair use permission from the Geological Society of America; (E) *Captorhinus* sp. modified from Gaffney (1990) reproduced with permission from the American Museum of Natural History. Not to scale.

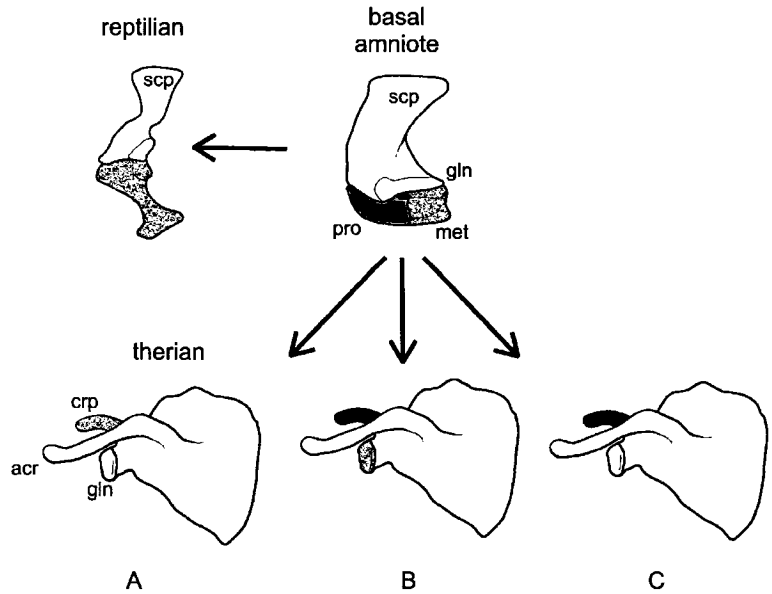

Figure 2. Competing hypotheses of coracoid homology. A: Among many early workers (e.g., Parker, 1868) the procoracoid of basal taxa was assumed to be lost in more deeply nested forms. Consequently, the coracoid process of therians and the coracoid element of modern reptiles were both considered homologous with the metacoracoid. B: Howes (1887, 1893) later argued that in therians the procoracoid gave rise to the coracoid process while the metacoracoid contributed to the glenoid. C: Alternatively, Lydekker (1893) suggested that the procoracoid formed the coracoid process of therians and the metacoracoid was the equivalent of the reptilian coracoid. Abbreviations: acr (acromion), cpr (coracoid process), gln (glenoid), met (metacoracoid [gray]), pro (procoracoid [black]), scp (scapula [white]). Sources for images: basal amniote: *Captorhinus* sp. modified from Gaffney (1990) reproduced with permission from the American Museum of Natural History; therian: *Bathyergus* sp. modified from Parker (1868); reptile: *Alligator mississippiensis* modified from Mook (1921b) reproduced with permission from the American Museum of Natural History. Not to scale.

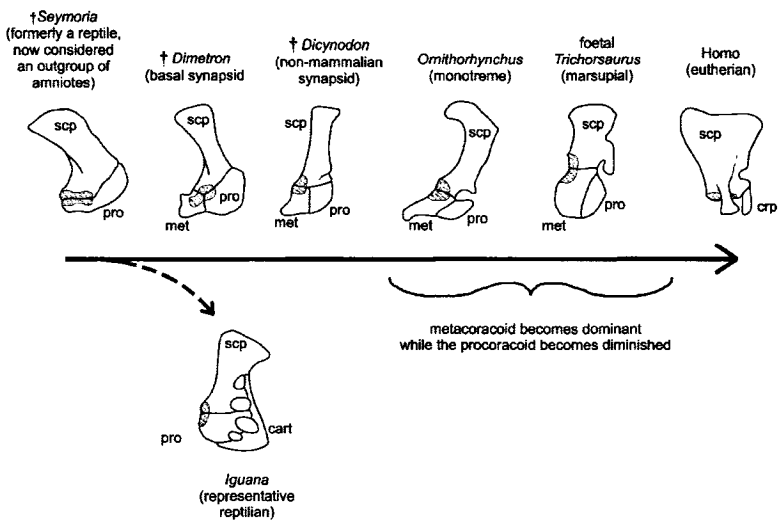

Figure 3. Romer's interpretation of amniote primary girdle evolution. Building on the work of Williston (1911, 1925), Romer hypothesized that the primitive coracoid of non-amniote tetrapods such as *Seymouria* spp., the procoracoid, was retained as the coracoid of modern reptiles. Among synapsids a second element evolved, the metacoracoid. Whereas synapsids eventually lost the primitive reptilian procoracoid, the newly evolved metacoracoid was retained by therians as the coracoid process. Although this hypothesis has long been accepted, it is not supported by the data presented herein. Abbreviations: cart (epicoracoidal and suprascapula cartilages), cpr (coracoid process), met (metacoracoid), pro (procoracoid), scp (scapula). Glenoid shaded. Source for image: modified from The comparison of mammalian and reptilian coracoids, A.S. Romer (1922, © Journal of Morphology); Reprinted with permission of Wiley-Liss, Inc., a subsidiary of John Wiley & Sons, Inc. Not to scale.

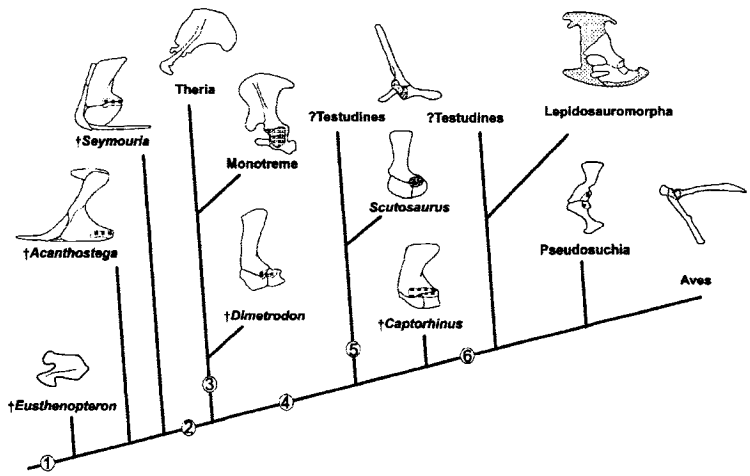

Figure 4. Revised amniote phylogeny based on the work of Brochu (2001), Lee (1996), Luo et al. (2003), Rieppel and Reisz (1999) and Ruta et al. (2003). As the phylogenetic position of turtles remains confused both competing hypotheses are presented (i.e., turtles as diapsids and turtles as proganosaurs). Nodes: 1, Tetrapoda; 2, Amniota; 3, Synapsida; 4, Reptilia; 5, Proganosauria; 6, Diapsida; 7, Archosauromorpha. Sources for images, from left to right: *Eusthenopteron foordi* modified from Jarvik (1980); *Acanthostega gunnari* reproduced by permission of the Royal Society of Edinburgh and M.I. Coates from Transactions of the Royal Society of Edinburgh: Earth Sciences, volume 87 (1996), pp. 363-421; *Seymouria* sp. modified from Williston (1925); *Priodontes maximus* modified from Flower (1876); *Tachyglossus aculeatus* reproduced by permission of F.A. Jenkins, Jr. from The postcranial remains of *Eozostrodon*, *Megazostrodon* and *Erythrotherium*, figure 19 (p. 419), 1976, published by the Royal Society; Dimetrodon sp. modified from Romer and Price (1940) reproduced with fair use permission from the Geological Society of America; *Macroclemys temminickii* modified from Gaffney (1990) reproduced with permission from the American Museum of Natural History; Scutosaurus reproduced by permission of M.S.Y. Lee from The homologies and early evolution of the shoulder girdle in turtles, figure 2 (p. 113), 1996, published by the Royal Society; *Captorhinus* sp. modified from Gaffney (1990) reproduced with permission from the American Museum of Natural History; *Shinisaurus crocodilurus* modified from Postcranial anatomy of *Shinisaurus crocodilurus* (Squamata: Anguimorpha), J.L. Conrad (In press, © Journal of Morphology); Reprinted with permission of Wiley-Liss, Inc., a subsidiary of John Wiley & Sons, Inc.; *Alligator mississippiensis* modified from Mook (1921a) reproduced with permission from the American Museum of Natural History; *Sturnus vulgaris* modified from Jenkins (1993) 'The evolution of the avian shoulder joint' reprinted by permission of the American Journal of Science. Not to scale.

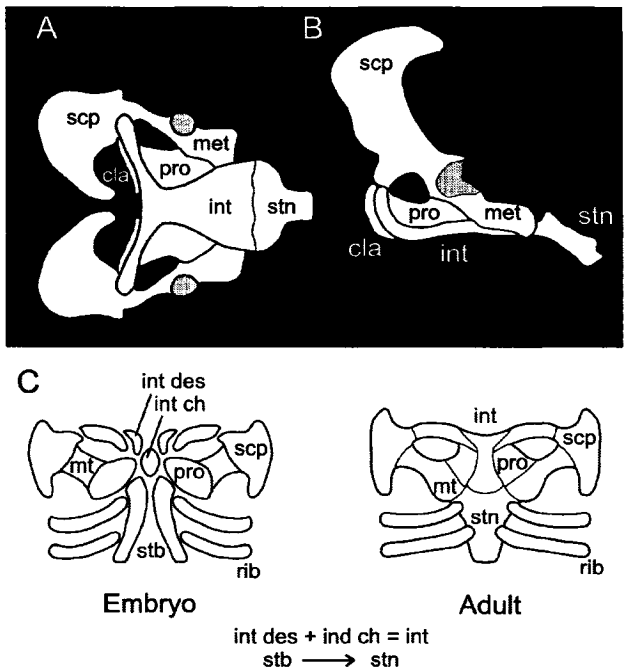

Figure 5. Monotreme pectoral apparatus. An adult *Ornithorhynchus anatinus* pectoral apparatus in ventral (A) and left lateral (B) views. Among skeletally mature monotremes, the pectoral apparatus is composed of six elements; an unpaired sternum and interclavicle, and bilateral clavicles, scapulae, procoracoids and metacoracoids. The glenoid for articulation with the humerus is positioned between the scapula and metacoracoid at the exclusion of the procoracoid. Early during skeletogenesis (C) the cellular condensations (membranous skeleton) giving rise to the pectoral apparatus include a median unpaired pars chondralis interclaviculae and bilateral pars desmalis interclaviculae, clavicular condensations, coracoid-scapular plates, sternal bands and rib primordia. The singular pars chondralis interclaviculae and paired pars desmalis interclaviculae coalesce to form the skeletally mature interclavicle. The majority of the coracoid-scapular plate forms the scapula, with more medial portions becoming segregated to form the procoracoid and metacoracoid (see text for details). Glenoid shaded Abbreviations: cla (clavicle), gln (glenoid), int (skeletally mature interclavicle), int ch (pars chondralis interclaviculae), int des (pars desmalis interclaviculae), met (metacoracoid), pro (procoracoid), rib (rib), scp (scapula), stb (sternal band), stn (sternum). Sources for images: (A, B) modified from Parker (1868); (C) reprinted from Functional Morphology in Vertebrates, volume 1, M. Klima, Development of the shoulder girdle and sternum in mammals, pp. 81-83, (1985).

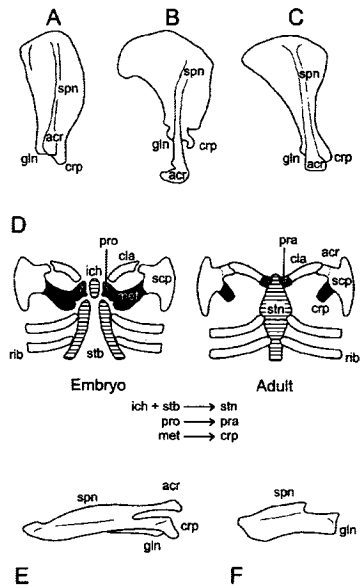

Figure 6. Therian scapula morphology and pectoral apparatus development. Adult (right) scapulae of *Canis lupus* (A), *Priodontes maximus* (B) and *Mus musculus* (C) in lateral view, demonstrating the morphological variation of this element. D: Early during skeletogenesis the cellular condensations (membranous skeleton) giving rise to the pectoral apparatus include a median unpaired pars chondralis interclaviculae and bilateral coracoid-scapular plates, clavicular condensations, sternal bands and rib primordia. The bulk of the coracoid-scapular plate gives rise to the scapula, although a rudiment homologous with the procoracoid joins with the cranialmost portion of the coalescing sternal bands and pars chondralis interclaviculae to form the manubrium sterni. In addition, procoracoid may give rise to vestiges adjacent to the clavicular-sternal contact (the praeclavia). The portion of the coracoid-scapular plate homologous with the metacoracoid gives rise to the coracoid process and, at least in some eutherians, the acromion and part of the glenoid Dorsal view of adult (left) scapula in *M. musculus*, (E) wildtype and (F) *undulated* (*Pax1* deficient) mutant (see text for details). Abbreviations: acr (acromion), cla (clavicle), cpr (coracoid process), gln (glenoid), ich (pars chondralis interclaviculae), met (metacoracoid), pra (praeclavium/suprasternal), pro (procoracoid), rib (rib), scp (scapula), spn (scapular spine), stb (sternal band), stn (sternum). Source for images: (A) and (B) modified from Flower (1876); (C, F, G) modified from Timmons et al. (1994), reproduced with permission from The Company of Biologists Ltd.; (D) reprinted from Functional Morphology in Vertebrates, volume 1, M. Klima, Development of the shoulder girdle and sternum in mammals, pp. 81-83, (1985).

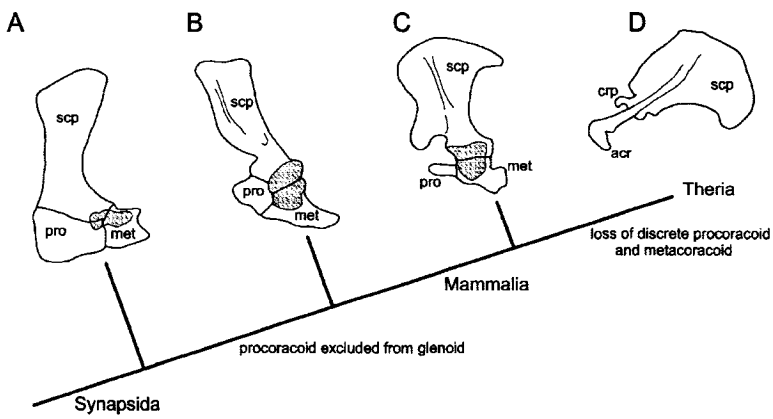

Figure 7. Evolution of the synapsid primary girdle. Among basal synapsids (A), the primary girdle consists of the scapula and the large, plate-like procoracoid and metacoracoid. All three elements contribute to the glenoid. Among more deeply nested non-mammalian synapsids (B), the procoracoid contribution to the glenoid is relatively reduced. For modern mammals, only monotremes (C) retain the procoracoid and metacoracoid as discrete elements. However, the procoracoid is excluded from the glenoid. In therians the scapula dominates the primary girdle, with the metacoracoid rudiment contributing to the coracoid process and (at least in some eutherians) the acromion and part of the glenoid. Abbreviations: acr (acromion), cpr (coracoid process), gln (glenoid), met (metacoracoid), pro (procoracoid), scp (scapula). Glenoid is dark grey stippled. Phylogeny based on Luo et al. (2003). Sources for images: (A) *Dimetrodon* sp. modified from Romer and Price (1940) reproduced with fair use permission from the Geological Society of America; (B) unidentified 'cynodont' and (C) *Tachyglossus aculeatus* reproduced by permission of F.A. Jenkins, Jr. from The postcranial remains of *Eozostrodon*, *Megazostrodon* and *Erythrotherium*, figure 19 (p. 419), 1976, published by the Royal Society; (D) *Priodontes maximus* modified from Flower (1876). Not to scale.

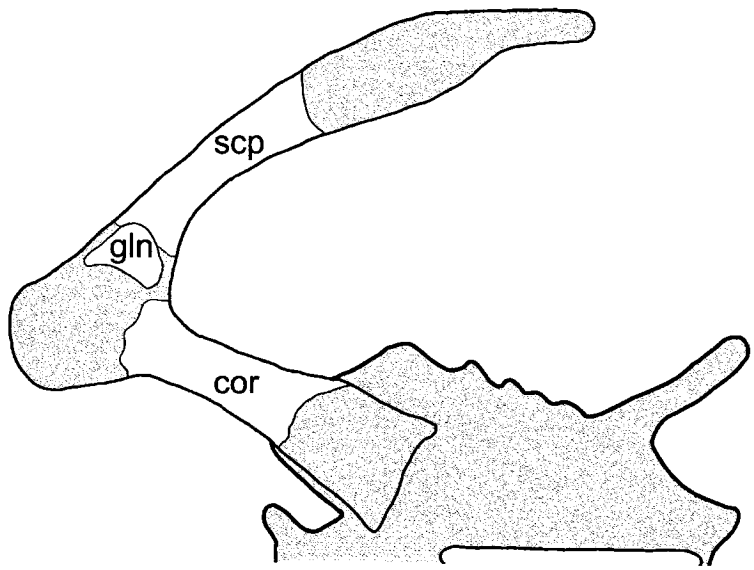

Figure 8. The avian primary girdle and sternum. Although the scapula and coracoid initially begin as a common condensation, the two elements separate from one-another and ossify independently. Furcula not depicted. Cartilage shaded. Abbreviations: cor (coracoid), gln (glenoid), scp (scapula), stn (sternum). Source for image: embryonic *Linota cannabina*, left primary girdle and left half of sternum in ventral view, modified from Parker (1868).

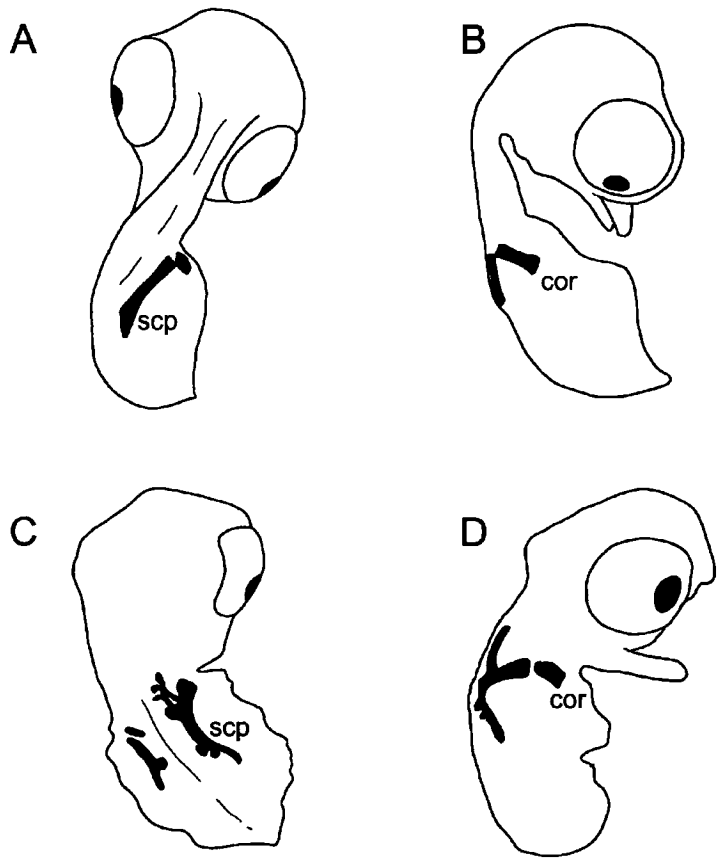

Figure 9. Normal and abnormal development of the scapula and coracoid in 11-day old *Gallus gallus* embryos stained for cartilage, with all other elements omitted and limbs removed. Normal embryos, in dorsal (A) and lateral (B) views. *Talpid3* mutant embryos, in dorsal (C) and lateral (D) views. Note the extraordinary morphology of the coracoid in talpid3 mutant embryos compared with somewhat abbreviated coracoid. Abbreviations: cor (coracoid), scp (scapula). Source of images: modified from Ede and Kelly (1964) reproduced with permission from The Company of Biologists Ltd. Not to scale.

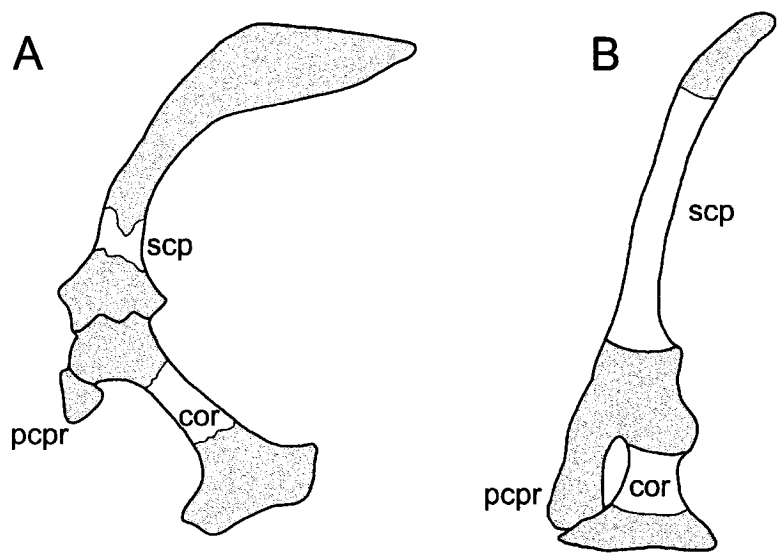

Figure 10. Development of the avian procoracoid process. Many avian taxa have been observed to develop a discrete skeletal centre for the procoracoid process (A), a medial projection that contacts the furcula. B: In *Struthio camelus* the procoracoid process is hypertrophied and reoriented ventrally to contact the sternum. It remains unclear if the procoracoid process of *S. camelus* develops independent of the scapula or as a ventrally oriented projection (see text for details). Cartilage shaded. Abbreviations: cor (coracoid), pcpr (procoracoid process), scp (scapula). Source for images: (A) embryonic *Linota cannabina* in lateral view and (B) embryonic *S. camelus* in cranial view modified from Parker (1868).

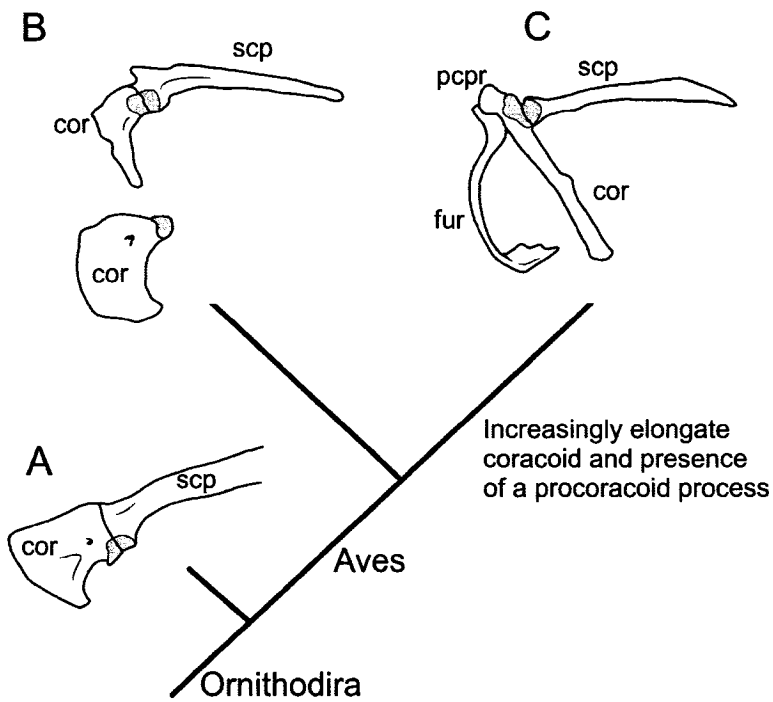

Figure 11. Evolution of the ornithodiran primary girdle. A: Among non-avian ornithodirans (e.g., *Deinonychus antirrhopus*) the primary girdle consists of a strap-like scapula and a large, plate-like coracoid. B: The coracoid of the basal avian *Archaeopteryx lithographica* remains broad, but has become reoriented with respect to the rest of the pectoral apparatus. C: For modern avians (e.g., *Sturnus vulgaris*) the coracoid is elongate and somewhat tubular. The furcula is unknown (and thus unillustrated) but presumed present in *D. antirrhopus* and has been omitted for *A. lithographica*. Abbreviations: cor (coracoid), fur (furcula), pcpr (procoracoid process), scp (scapula). Phylogeny based on Brochu, 2001. Glenoid shaded. Sources for images: (A, B, C) modified from Jenkins (1993) 'The evolution of the avian shoulder joint' reprinted by permission of the American Journal of Science; (B) *A. lithographica* coracoid modified from Ostrom (1976). Not to scale.

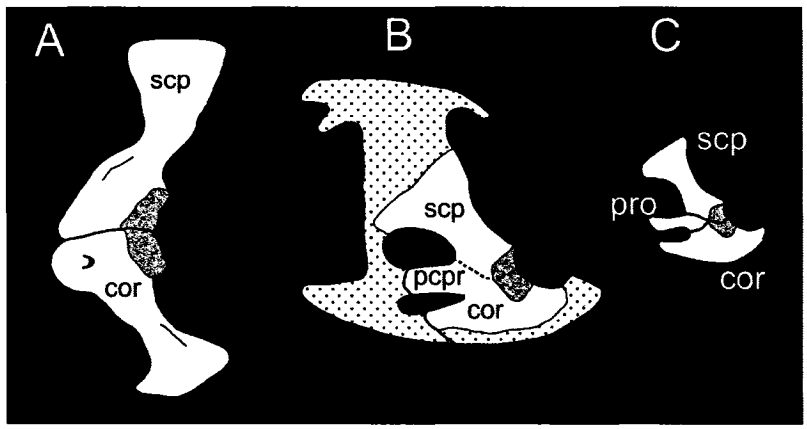

Figure 12. Non-avian reptile scapulae and coracoids. The pseudosuchian (crocodylian) *Alligator mississippiensis* (A) and lepidosauromorphan (squamate) *Shinisaurus crocodilurus* (B, C). C: Evidence from an osteological study of *S. crocodilurus* indicates that the procoracoid process of the scapula is derived from a discrete skeletal element, herein considered to be the homologue of the procoracoid (see text for details). Abbreviations: cart (epicoracoidal and suprascapula cartilages), cor (coracoid), pcpr (procoracoid process), pro (procoracoid), scp (scapula). Glenoid shaded, cartilage stippled. Sources for images: (A) *A. mississippiensis* modified from Mook (1921a) reproduced with permission from the American Museum of Natural History; (B) adult and (C) subadult *S. crocodilurus* modified from Postcranial anatomy of *Shinisaurus crocodilurus* (Squamata: Anguimorpha), J.L. Conrad (In press, © Journal of Morphology); Reprinted with permission of Wiley-Liss, Inc., a subsidiary of John Wiley & Sons, Inc. Not to scale.

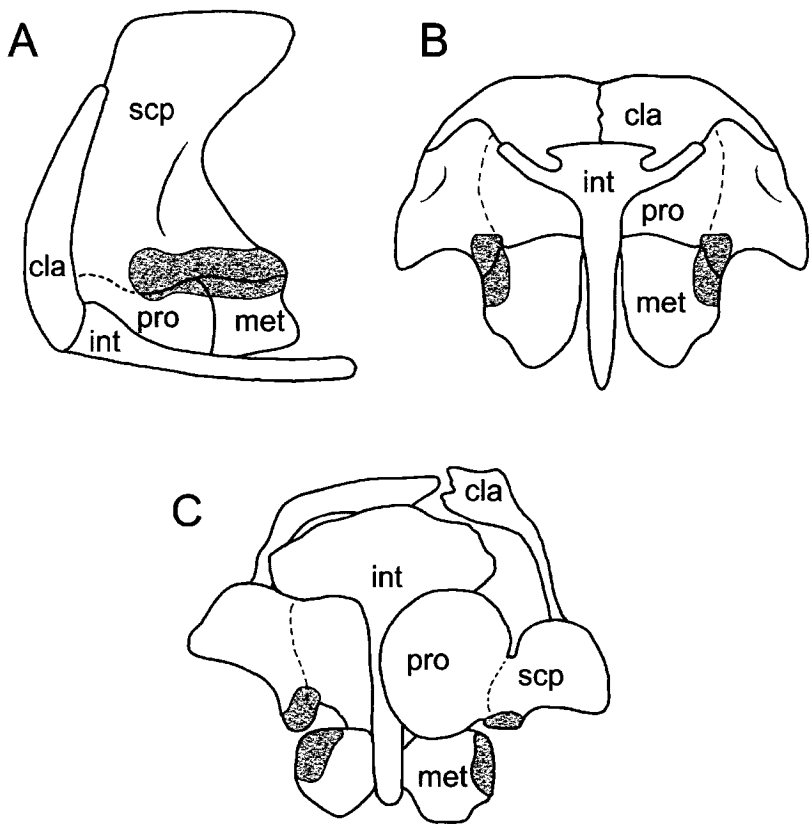

Figure 13. Basal reptilian pectoral apparatus as exemplified by *Captorhinus* sp. Adult in lateral (A) and ventral (B) views, subadult in ventral (C) view. The dashed line separating the procoracoid from the scapula denotes that these elements are often fused or tightly sutured, even in subadult specimens. Abbreviations: cla (clavicle), int (interclavicle), met (metacoracoid), pro (procoracoid), scp (scapula). Glenoid is dark grey stippled. Sources for images: (A, B) modified from Gaffney (1990) reproduced with permission from the American Museum of Natural History; (C) modified from The osteology and musculature of small captorhinids, R. Holmes © (1977, Journal of Morphology); Reprinted with permission of Wiley-Liss, Inc., a subsidiary of John Wiley & Sons, Inc. Not to scale.

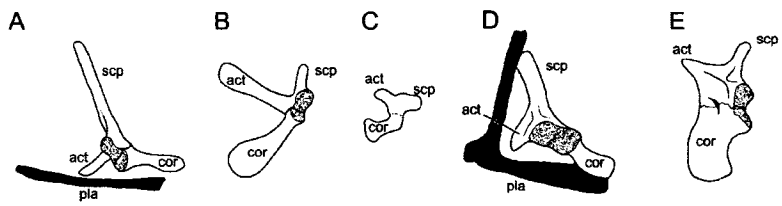

Figure 14. Testudines pectoral apparatus. *Macroclemys* (= *Macrochelys*) *temminickii*, adult in lateral (A) and ventral (B) views, subadult (C) in ventral view. *Proganochelys quenstedti*, adult in lateral (D) and ventral (E) views. Abbreviations: act (turtle acromial process), cor (coracoid), pla (plastron), scp (scapula). Glenoid shaded, cartilage stippled, plastron black. Sources for images: (A, B, D, E) modified from Gaffney (1990) reproduced with permission from the American Museum of Natural History; (C) modified from Skeletal development of *Macrochelys temminckii* (Reptilia: Testudines: Chelydridae), C.A. Sheil (2005, © Journal of Morphology); Reprinted with permission of Wiley-Liss, Inc., a subsidiary of John Wiley & Sons, Inc. Not to scale.

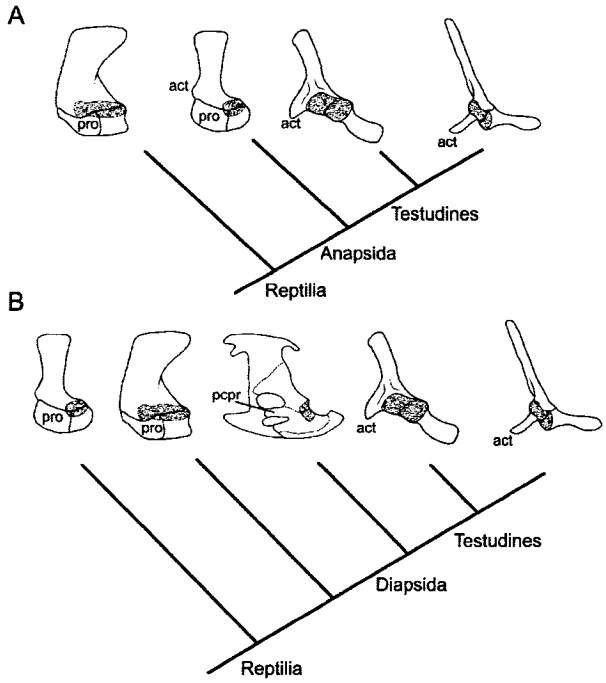

Figure 15. Evolution of the turtle primary girdle. A: The proganosaur hypothesis as proposed by Lee (1996), wherein Testudines share a close common ancestry with pareisaurs. According to this hypothesis, the evolution of the acromial process of turtles precedes the loss of the procoracoid (see text for details). B: The diapsid hypothesis as proposed by Rieppel and others (Rieppel and deBraga, 1996; deBraga and Rieppel, 1997; Rieppel and Reisz, 1999), wherein turtles share a close common ancestry with lepidosauromorphs. According to this hypothesis, the evolution of the acromial process of turtles is linked with loss of the procoracoid. Cartilage shaded. Abbreviations: act (turtle acromial process), pro (procoracoid), pcpr (procoracoid process). Sources for images, *Captorhinus* sp., *Proganochelys quenstedti*, *Macroclemys temminickii*, modified from Gaffney (1990) reproduced with permission from the American Museum of Natural History; *Scutosaurus* sp. reproduced by permission of M.S.Y. Lee from The homologies and early evolution of the shoulder girdle in turtles, figure 2 (p. 113), 1996, published by the Royal Society; *Shinisaurus* modified from Postcranial anatomy of *Shinisaurus crocodilurus* (Squamata: Anguimorpha), J.L. Conrad (In press, © Journal of Morphology); Reprinted with permission of Wiley-Liss, Inc., a subsidiary of John Wiley & Sons, Inc.

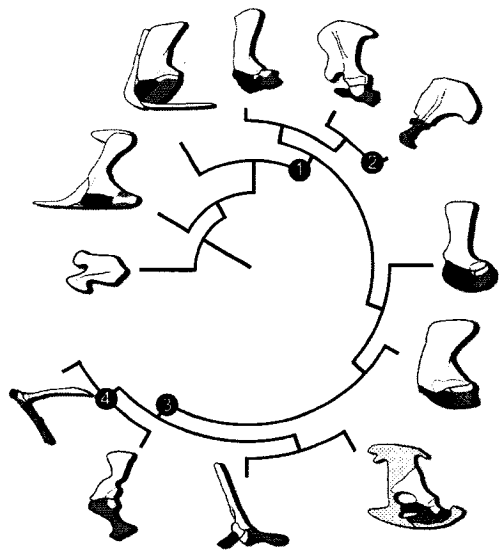

Figure 16. Evolution of the amniote scapula, procoracoid and metacoracoid; a new scenario. Amniote phylogeny based on the work of Brochu (2001), Lee (1996), Luo et al. (2003), Rieppel and Reisz (1999) and Ruta et al. (2003). Beginning with the unified scapulocoracoid of *Eusthenopteron foordi* (far left, white) and continuing in a clockwise progression; *Acanthostega gunnari*; *Seymouria* sp.; *Dimetrodon* sp.; *Tachyglossus aculeatus*; *Priodontes maximus*; *Scutosaurus* sp.; *Captorhinus* sp.; *Shinisaurus crocodilurus*; *Macroclemys temminickii*; *Alligator mississippiensis*; *Sturnus vulgaris*. The phylogenetic arrangement follows the hypothesis of Testudines as diapsids; alternatively, *M. temminickii* could be positioned as the sister group to *Scutosaurus* sp. in accordance with the turtles as proganosaurs hypothesis (see text for details). Nodes: 1, delay in osteogenesis and/or the differentiation of skeletogenic cells results in the formation of sutures and the discrete development of each of the scapula, procoracoid and metacoracoid; 2, integration of the procoracoid rudiment into the sternum combined with reduction in pre-skeletogenic cell proliferation of each of the procoracoid and metacoracoid rudiments results in the scapula dominating the primary girdle; 3, reduction of pre-skeletogenic cell mitosis and accelerated osteogenesis of the procoracoid condensation results in this element remaining linked with the scapula, albeit as a vestige; 4, delay in procoracoid osteogenesis and/or reaggregation of the procoracoid condensation alongside the presumptive metacoracoid results in coalescence of the two elements. See text for details. Glenoid shaded, cartilage stippled, scapula yellow, procoracoid red, metacoracoid blue. For sources of images please consult figure 2.4. Not to scale.

Table 1. Synonyms (and source listings) of the cranialmost and caudalmost coracoid elements present in basal amniotes and monotremes, and their inferred homologues in therians and reptiles.

	coracoid		amniote	
source	cranialmost coracoid	caudalmost coracoid	Therian coracoid process	Reptilian coracoid
Parker, 1868	epicoracoid	coracoid	coracoid	coracoid
Flower, 1876	epicoracoid	coracoid	coracoid	coracoid
Howes, 1887	epicoracoid	coracoid	epicoracoid	coracoid
Howes, 1893	epicoracoid	metacoracoid	epicoracoid	coracoid[1]
Lydekker, 1893	coracoid	metacoracoid	coracoid	metacoracoid
Broom, 1899	precoracoid	coracoid	coracoid	coracoid
Broom, 1912	precoracoid	coracoid	coracoid	precoracoid
Williston, 1911, 25	procoracoid	metacoracoid	coracoid (=procoracoid)	procoracoid
Watson, 1917	procoracoid	metacoracoid	metacoracoid	procoracoid
Gregory and Camp, 1918[2]	epicoracoid	coracoid	coracoid	coracoid
Romer, 1922	epicoracoid	coracoid	coracoid	epicoracoid
Romer, 1956	procoracoid	coracoid	coracoid	procoracoid
Klima, 1973, 1987	procoracoid	metacoracoid	metacoracoid	procoracoid
current hypothesis	**procoracoid**	**metacoracoid**	**metacoracoid**	**metacoracoid**[3]

[1]Howes regards the extant reptile coracoid as a combined epicoracoid and metacoracoid (before the two elements have separated from one another)

[2]Gregory suggest that a third coracoid, the metacoracoid, was present in basal synapsids and that a neomorphic 'subcoracoid' was also also present in placentals

[3]including minor contributions from the procoracoid

CHAPTER 3. HOMOLOGY OF THE FURCULA: A RECONSIDERATION OF THE DEVELOPMENT AND EVOLUTION OF THE UNPAIRED DERMAL ELEMENTS OF THE AMNIOTE PECTORAL APPARATUS

INTRODUCTION

"...in morphology general principles are founded on matters of quite intricate detail and require detail for their illustration..." (de Beer, 1937, p. vii).

Among tetrapods, the pectoral apparatus (shoulder girdle plus sternum; Vickaryous and Hall, 2006 [Chapter 2]) is complex in form and function. In part, the morphological and functional diversity appears to be related to the multipartite composition and origin of the pectoral apparatus, the developmental flexibility of each individual element, and that it is the only skeletal region outside the skull to contain elements of both the endoskeleton and dermal skeleton.

Underpinning the otherwise bilateral arrangement of skeletal elements in adult tetrapods, at least plesiomorphically, is an unpaired, midventrally positioned dermal bone. In non-avian reptiles and monotreme mammals this dermal keystone is the interclavicle, or its homologue, the entoplastron of turtles, while birds and their closest dinosaurian ancestors, non-avian theropods, have a furcula. Each element arguably represents the most morphologically variable component of the pectoral apparatus, with the interclavicle alternatively cruciform, T-shape, or a bar-like element without lateral processes (Fig. 17A; see also Lécuru 1968a), whereas the furcula may resemble a U, V, or Y that is planar (Fig. 17B, C), strongly bowed, or some form in between (Russell and Joffe 1985; Hall 2001). Curiously, while the interclavicle is plesiomorphic for tetrapods (dating back to the earliest forms such as *Acanthostega gunnari*; Coates 1996) and occupies a similar position within the pectoral apparatus as the furcula, the two elements are not regarded as comparable. Historically, the furcula has either been considered a neomorph or homologous with the fused clavicles.

Pierre Belon of Le Mans (1517-1564), one the earliest known comparative anatomists, was the first to publish on the subject (Singer 1957). Using a pair of

woodcuts, Belon (1555) compared the skeletons of a bird and a human and set about matching the corresponding elements (this work is also considered to be the oldest depiction of homology; Panchen 1994.) Of the avian furcula Belon stated "*L'os qu'on nomme la Lunette ou Fourchette n'est trouve en aucun autre animal, hors mis en oyseau*" (Panchen 1994, fig. 8) – that the bone of birds described as a fork (or half-moon) is not found in other animals.

As comparative anatomy evolved, Belon's interpretation was replaced with the notion of the furcula as homologous with the fused clavicles or the clavicles fused with the interclavicle, the latter forming the hypocleideum (Parker 1868). This so-called 'furcula-equals-clavicles' hypothesis (Bryant and Russell 1993) has proven to be remarkably potent and influential, including a defining role in historic evaluations of the origin of birds (e.g., Heilmann 1926; Gauthier 1986; Dodson 2000; see below).

The practical basis of the clavicles as a furcula homologue is generally summarized in three points: (1) both share a common topographic relationship to other elements of the pectoral apparatus; (2) both share a common mode of skeletogenesis (i.e., intramembranous ossification; Russell and Joffe 1985; Hall 1986, 2001; Tran and Hall 1989); and (3) neither element co-exists with the other in the same organism (Bryant and Russell 1993). Coupled with the widespread acceptance of the dinosaurian origin of birds (e.g., Gauthier 1986; Qiang et al. 1998; Xu et al. 1999; Sereno 1999; Dodson, 2000), the furcula-equals-clavicles hypothesis has become firmly established, to the exclusion of all other possibilities. Indeed, the presence of a furcula is often cited to demonstrate the proximate genealogy of modern birds relative to fossil theropods. Consequently, there has been little incentive to evaluate alternative evolutionary transformation scenarios. In one of the few dissenting opinions, Bryant and Russell (1993) reconsidered the issue by employing Patterson's (1982) three tests of homology. The first two tests are observational: the "test" of similarity infers putative homology based on resemblance in structure, development, and/or topology (see also Lee 1996; Rieppel 1996; arguably not a test, but rather a rationale for speculating homology), while the test of conjunction holds that putative homologues cannot coexist in the same organism. The third test, the test of congruence, requires that the feature in question be inherited from a common ancestor (i.e., a synapomorphy) and not represent an example

of convergent evolution. Bryant and Russell (1993) noted that while the furcula-equals-clavicles hypothesis passes the tests of similarity and conjunction, the test of congruence had yet to be fully considered. Furthermore, they raised the concern that among fossil taxa, the notion of congruence becomes problematic if and when a feature is considered present yet not preserved. Finally, Bryant and Russell (1993) questioned the accuracy of the fossil data suggesting a clavicles-to-furcula transformation. Alternatively, they identified two competing hypotheses: the furcula as a neomorph; and the furcula as a homologue of another element previously considered lost.

Since the publication of Bryant and Russell (1993) there have been numerous discoveries of non-avian theropod taxa with an unpaired, boomerang-shaped furcula, including coelophysoids, allosaurids, dromaeosaurids, oviraptorids, troodontids, and tyrranosaurids (Fig. 17C; see also Chure and Madsen 1996; Makovicky and Currie 1998; Norell et al. 1997; Qiang et al. 1998; Xu et al. 1999; Carrano et al. 2005). However, while convincingly demonstrating the presence of the furcula outside of Aves (supporting the test of congruence among fossil non-avian theropods) these data do not address homology of the furcula *per se*. To date the alternative hypotheses raised by Bryant and Russell (1993) remain unexplored and untested.

In this chapter I investigate the alternative hypotheses of furcula homology and in doing so, provide greater insight into the study of pectoral apparatus development and evolution. This work begins by exploring the hypothesis that the furcula is homologous with the interclavicle, an element previously considered lost in the lineage leading to theropods. To address the observational tests of similarity and conjunction, early skeletogenesis of *Alligator mississippiensis* interclavicle and *Gallus gallus* (the domestic fowl) furcula are compared. The advantages of comparing early skeletal formation are two-fold. First, such a comparison provides data on the mode of development and initial topology (test of similarity). Second, previous work on the pectoral apparatus (e.g., Klima 1985; Vickaryous and Hall 2006a [Chapter 2]) has demonstrated that in some instances elements absent among skeletally mature adults are present, albeit transiently, as discrete cell condensations early during the embryonic period. For example, whereas the furcula is not present in adult *Struthio camelus* (ostrich), an ephemeral rudiment comparable to this element has been identified in embryos (Holmgren 1955; Glutz von

Blotzheim 1958). Therefore, in order to effectively test for conjunction it is necessary to confirm the absence of putative homologues, including elements only temporarily present during development. Following the evaluation of observational data, several alternative (competing) tests of congruence are carried out, to determine which hypotheses is most parsimonious and/or which proposal(s) demonstrate evidence of convergence.

MATERIALS AND METHODS

For the tests of similarity and conjunction, development of the unpaired dermal element of the pectoral apparatus (viz., the interclavicle and furcula) was explored in *Gallus gallus* (domestic fowl) and *Alligator mississippiensis* (American alligator) using histology and histochemistry. Staging of embryos was conducted using appropriate Tables of Normal Development. *G. gallus* embryos were staged according to the Table established by Hamburger and Hamilton (1951) (HH). I examined HH 33-39. *A. mississippiensis* embryos were staged according to the Table established by Ferguson (1985) (FS); FS 15-24 were examined (see also Chapter 5, Appendix 1). All embryos were fixed in 10% neutral buffered formalin and stored in 70% ethanol prior to histological analysis. Dried adult skeletal materials from both *A. mississippiensis* and *G. gallus* were also consulted.

HISTOLOGY AND HISTOCHEMISTRY

Representative specimens of *Alligator mississippiensis* and *Gallus gallus* from each embryonic stage (see below) were processed for whole-mount single or double staining with Alizarin red for calcified structures (most commonly bone) alone or in combination with Alcian blue for tissues rich in glycosaminoglycans (GAGs; characteristic of the extracellular matrix [ECM] of cartilage and, to a lesser extent, osteoid), following the protocol of Klymkowsky and Hanken (1991). Comparable staged materials were also explored with serial histology.

Several histological techniques were employed to identify the tissue and cellular composition of the pectoral elements. Preparation of serial sections included decalcification in Tris-buffered 10% EDTA (buffered to pH 7.0) for 5+ days, dehydration to 100% ethanol, clearing in CitriSolv (Fisher No. 22-143975) and embedding in low

melting paraffin at 54^{O}C (Paraplast X-tra, Fisher No. 23-021-401). Sections were cut at 6-7 microns and mounted on 3-aminopropytriethoxy-silane or Haupt's coated slides. Following the staining protocols (see below), sections were mounted with DPX (Fluka No. 144581).

The most common connective tissue stain protocols used were the Hall-Brunt Quadruple (HBQ) stain (Hall 1986; Witten and Hall 2003), Mallory's trichrome, and a new pentachrome stain (AC pentachrome; Cole and Hall 2004). HBQ was used to permit the early discrimination of cartilage (with Alcian blue, pH 2.5) and bone. Mallory's trichrome is a general-purpose connective tissue stain that was carried out as follows: once hydrated, deparaffinized sections were mordanted in saturated aqueous mercuric chloride ($HgCl_2$) for 10 minutes and then rinsed in distilled water. Sections were briefly stained with acid fuchsin (15 seconds), differentiated in distilled water, then placed in phosphomolybdic acid (1 minute) and rinsed again in distilled water. The sections were then stained in an aqueous solution of 4 parts orange G: 1 part aniline blue for 1 minute to 75 seconds, before being rinsed again in distilled water, and dehydrated with 90% and then twice with 100% ethanol (10 seconds each, total of 30 seconds). The AC pentachrome (developed by A. Cole; Cole and Hall 2004) combines the utility of a general-purpose connective tissue stain (Masson's trichrome) with Verhoeff's elastin stain, substituting Bismarck brown for Haematoxylin. Significantly, whereas both Bismarck brown and Alcian blue visualize GAGs, they do not demonstrate identical staining properties (Conklin 1963). For example, when staining hyaline cartilage, Alcian blue is most effective at demonstrating capsular, territorial, and the granular portion of the interterritorial matrices, with a low affinity for the amorphous portion interterritorial matrix. The opposite is true for Bismarck brown (high intensity for the amorphous portion interterritorial matrix, otherwise low affinity; see Conklin 1963).

PHYLOGENETICS

The test of congruence is used to demonstrate that putative homologues share a common descent (i.e., they did not evolve convergently; Patterson 1982; de Pinna 1991; Bryant and Russell 1993; Shubin, 1994; Rieppel 1996). However, as observed by Rieppel (1996), the test of congruence is limited in that it will only test for the proposed

homology under consideration. Consequently, alternative competing hypotheses must be explored separately by changing the proposed homology of the furcula and then rerunning the analysis.

The test of congruence was investigated using the data matrix of Benton (2004), coding for 95 characters of Triassic archosaurs, including the presence/absence of the both the clavicles and the interclavicle. The analysis was then modified as follows: only eleven of the 24 listed taxa were scored, removing various basal archosauriforms and pseudosuchians but retaining *Hyperodapedon*, *Euparkeria*, Crocodylomorpha, *Scleromochlus*, Pterosauria, *Lagerpeton*, *Marasuchus*, *Herrerasaurus*, Sauropodomorpha, Ornithischia, and Theropoda. Appropriate to Benton (2004) and Langer (2004; contra Sereno 1999) *Herrerasaurus ischigualastensis* is considered to lie outside of theropods. In accordance with Gauthier (1986), the coding for crocodylomorphans was altered to reflect the absence of clavicles in these forms. All the analyses were conducted using PAUP* 4.0b10 (Swofford 2000), using the branch and bound search algorithm to find an exact solution, with all multi-state characters treated as unordered. The analyses were optimized to favour both reversals over parallelisms (i.e., accelerated evolutionary transformation or ACCTRAN) and parallelism over reversals (delayed evolutionary transformation or DELTRAN). All the other character states, except as noted above, were left unaltered.

In order to address the issue of accepting negative evidence for fossil taxa, five separate hypotheses considered (Table 2):

(1) clavicles = furcula, synapomorphy of theropods
(2) clavicles = furcula, plesiomorphic for dinosaurs
(3) furcula is a neomorph of theropods
(4) interclavicle = furcula, synapomorphy of theropods
(5) interclavicle = furcula, plesiomorphic for dinosaurs

After all five analyses were run, the number of evolutionary steps (tree length, TL) and the 'fit' of the data (consistency index, CI) were compared (Table 2).

TESTS OF SIMILARITY AND CONJUNCTION – RESULTS

DEVELOPMENT OF THE INTERCLAVICLE IN *ALLIGATOR MISSISSIPPIENSIS*

In skeletally mature *Alligator mississippiensis*, the interclavicle (Fig. 17A) resembles a flattened rod with a distinct cranial end offset by a tapering neck. The stem-like caudal remainder of the element, the parasternal process, is nested immediately ventral (superficial) to the midline of the cartilaginous (or partially mineralized; Mook 1921b) sternum. Along with the sternum, the interclavicle serves as part of the origin for M. pectoralis (Meers 2003; Jasinoski et al. 2006) and the hyobranchial muscles M. episternobranchiotendinous and M. episternobranchialis (Schumacher 1973).

The earliest appearance of the interclavicle is at FS 19, coinciding with the mineralization of various dermatocranial elements including the premaxilla, maxilla, pterygoid, angular, coronoid, and dentary (Chapter 5). In whole-mount preparations, the interclavicle begins as a bilateral pair of small, comma-shaped condensations positioned cranial and medial to the developing (and widely divergent) sternal bands and (meta)coracoids (Fig. 18A). At this stage in development, the interclavicular condensations are negative for Alizarin red but appear to be weakly positive for Alcian blue. Similarly, HBQ stained serial sections are also weakly positive for Alcian blue (Fig. 18B). The poor visualization of Alcian blue in the condensations differs considerably from the intense Alcian blue colouration of the adjacent replacement elements. Each condensation consists of an aggregation of plump, spherical osteoblastic cells and thin collagen fibres that stain dark blue for Mallory's trichrome (Fig. 18C) and green with the AC pentachrome. Using AC pentachrome the condensations were not visualized with Bismarck brown, nor do they demonstrate any elastin fibres within or surrounding the condensation. Surrounding each condensation is a distinctive field of loose mesenchyme, composed primarily of thin, fusiform cells. Even at this initial stage of skeletogenesis there is evidence of a cranio-caudal maturation pattern, with several cells at the cranial-most end becoming firmly embedded within the ECM. Other, more rounded cells are aligned around the periphery of the ECM, creating the osteogenic (cambial) layer of the presumptive periosteum.

By FS 20 the interclavicular condensations have become increasingly elongate, and while not obvious in whole-mounts, the cranial ends are beginning to merge, linked to one another by thin spicule. In serial section, the coalescing primordia are light blue to pinkish-blue using the HBQ protocol, dark blue with Mallory's trichrome, and green to mottled green brown with AC pentachrome (Fig. 18D, E). Longitudinal blood vessels are often found adjacent to the coalescing interclavicle. Unification of the bilateral condensations continues in subsequent stages, well in advance of the sternal bands, although the caudalmost extremity may remain bifurcated until well after hatching.

By late FS 21 the cranial end of each of the coalescing interclavicular primordia demonstrates a single centre of Alizarin red-positive tissue in whole-mount; otherwise none of the pectoral apparatus is Alizarin red-positive. In serial section, these Alizarin positive areas have a mottled colouration with each of HBQ (mottled light blue and pink) and AC pentachrome (mottled green and brown), and are dark blue with Mallory's. The developing interclavicle is nested within a bone territory (Pritchard, 1974), an obvious field of ossification bounded by fibroblasts and collagen fibres (the future fibrous periosteum). At the outermost horizon, these fusiform cells provide attachment for the developing muscle fibres (myotubes) of the M. pectoralis and (towards the cranial end of the presumptive interclavicle) the hyobranchial muscles. By late FS 21 – early FS 22, the Alizarin positive portion of the interclavicular head has enlarged to become spade-like (Fig. 18F), and the fusing presumptive parasternal processes lie ventral (superficial) to the (still unfused) sternal bands.

At FS 22 the interclavicle is well formed, except for the cranialmost margin and the caudal (the parasternal) process, which remains bifurcated (Fig. 18F). In section, the cranial end of the interclavicle is still notably concave dorsally/convex ventrally. The surrounding periosteum is readily distinguishable into osteoblastic and fibroblastic horizons. By FS 23-24 the interclavicle is well mineralized (Fig. 18G, H), effectively resembling the adult structure, and the surrounding non-skeletal tissues have become fully differentiated (as evidenced histochemically). At no time during skeletogenesis are there any signs of clavicles or clavicular rudiments developing, nor are there any signs of cartilage (primary or secondary).

DEVELOPMENT OF THE FURCULA IN *GALLUS GALLUS*

In adult *Gallus gallus*, the furcula (wishbone or merrythought) has a prominent, ventrally oriented midpoint projection, a sternal process or hypocleidium and a pair of obliquely diverging epicleideal rami, resulting in a Y-shaped morphology (Fig. 3.1B). Although the hypocleideum does not articulate directly with the sternal keel, it may be linked by ligaments and as the shared origin for the M. pectoralis. The epicleideal processes of the furcula also serve as part of the origin for several heads of the Mm. deltoideus (Jasinoski et al. 2006).

The furcula is present by HH 33 as a bilateral pair of condensations that have not fused in the midline (Fig. 18I). In whole-mount preparations the furcula is weakly visible and has begun to take up Alizarin red, primarily midlength along each epicleideal ramus; the distal (epicleideal) and proximal (midline) ends are not mineralized. Concurrently, parts of the dermatocranium, including the quadratojugal, dentary, and splenial, are undergoing mineralization (Jollie, 1957; Murray, 1963; pers. obs.). In serial section each furcular condensation stains pinkish-blue for HBQ (Fig. 18J), and is composed of a dense collection of relatively large, spherical cells depositing thin collagen fibres. The collagen fibres are dark blue for Mallory's (Fig. 18I) and green for AC pentachrome. Surrounding these presumptive furcula condensations are horizons of cells that grade distally from a dense collection of sub-circular osteoprogenitor cells into a more diffuse gathering of smaller, more fusiform morphologies (the presumptive fibrous periosteum). Myotubes of the M. pectoralis are observed to originate from these presumptive periosteal cells. There is no indication of one or more separate centre(s) for the hypocleideum.

By HH 35-36, the condensations have become larger (Fig. 18K), with more ECM deposited, and are beginning to fuse in the midline (Fig. 18L, M). The presumptive periosteal cells are now readily divisible into a bilaminar boundary layer, with plump osteoprogenitor cells positioned adjacent to the developing furcula, and fusiform cambial layer cells positioned distally. Myotubes from the M. pectoralis contact this outermost layer. At the lateralmost extremity, the furcula passes medial and caudal to the distal end of the metacoracoid (the acromial process). Medially, the fusing condensations each develop a ventrally oriented outgrowth, the future hypocleideal process. In whole-mount, the hypocleideum is apparent by HH 36-37, and by HH 39 the furcula ostensibly

resembles its adult form (Fig. 18N). There are no signs of additional dermal elements developing within or adjacent to the pectoral apparatus, nor is there any evidence of primary or secondary cartilage development.

TESTS OF SIMILARITY AND CONJUNCTION – DISCUSSION

In each of *Alligator mississippiensis* and *Gallus gallus*, the pectoral apparatus has only a single dermal element, each of which is located in a similar midventral position within the pectoral apparatus and provides origin for the M. pectoralis. Whereas the adult elements are unpaired, during the earliest stages of skeletogenesis, both the interclavicle and furcula arise from bilateral (parasagittal) condensations. As for other intramembranously derived (dermal) bones (Chapter 5), these condensations begin as aggregations of plump osteoprogenitor cells secreting thin collagen fibres that stain positively with various connective tissue protocols (Fig. 18C, J; Tran and Hall 1989; Chapter 4). Initially, these condensations are negative for Alizarin red (i.e., they are not mineralized) but reveal a weakly positive reaction for Alcian blue using the HBQ protocol for serial sections (Fig. 18B, K). However, neither presumptive element has chondroblasts/-cytes. Furthermore, the condensations are always negative for Bismarck brown. Combined, these data reveal that the early visualization with Alcian blue (denoting the presence of a limited amount of GAGs) is characteristic of osteoid (Paulsen 1993) and not cartilage/precartilage. In contrast, among the adjacent replacement elements (viz. the metacoracoid, scapula, and unfused sternal band), development is characterized by intense staining for both Alcian blue and Bismarck brown.

Common to both elements, the early formation of paired condensations is promptly followed by the initiation of ossification and fusion of the paired primordia. The onset of ossification is concomitant with mineralization of parts of the dermatocranium, and occurs in advance of the adjacent replacement bones of the pectoral apparatus (e.g., scapula, metacoracoid). Mineralization is initiated prior to coalescence of the condensations, as evidenced by a positive reaction for Alizarin red in whole-mounts and mottled colouration with the HBQ and AC pentachrome protocols. As ossification continues there is marked development of the periosteum including a cell-rich cambial (cellular) layer and a fibroblastic outer layer. Unlike some dermal bones (e.g., armadillo

osteoderms [Chapter 4], crocodylian dermatocranium [Chapter 5]), the developing interclavicle lacks a thick seam of osteoid (Fig. 18G), suggesting that growth of the bone and advancement of the mineralization front is tightly correlated. Fusion of the paired condensations, and growth (elongation) of the entire element, precedes fusion of the sternal bands. For each of *Alligator mississippiensis* and *Gallus gallus*, during pectoral skeletogenesis there is only evidence of a single dermal element developing, with no signs of formation of additional, even transient, rudiments.

CROCODYLIANS

The sternum is the first of the pectoral elements to develop, beginning as a pair of longitudinal condensations situated along the ventral aspect of the rib primordia (Rathke 1848; Kälin 1929; see also Gladstone and Wakeley 1932). In agreement with previous work (Kälin 1929; Gladstone and Wakeley 1932), this study finds that paired interclavicular condensations are briefly visible prior to fusion of the sternal bands. These condensations undergo intramembranous ossification to yield the skeletally mature element. The interclavicle is the first pectoral element to ossify, and is visible as textured opaque (Alizarin red negative) condensations in whole-mount preparations as early as FS 19 (~28d post-oviposition) (Fig. 18A). My data, similar to those of Rieppel (1993b), finds that the first signs of mineralization do not occur until FS 20 (Fig. 18D). Growth continues in a cranial-caudal sequence with the caudalmost end of the parasternal process often remaining bifurcated until after hatching.

AVIANS

Amongst the first avian elements to ossify, development of the furcular condensation nevertheless slightly trails that of the rest of the pectoral apparatus (Hall 1986). However, the furcula is the first pectoral element to mineralize. Similar to Russell and Joffe (1985) and Hall (1986; see also 2001), my results demonstrate that the bilateral mesenchymal condensations of the future furcula undergo intramembranous osteogenesis (beginning at HH 33; Fig. 18I), with fusion of the bilateral components occurring in advance of the sternal bands (HH 35; see Fig. 18L, M). There is no evidence that the hypocleideum develops separately from the rest of the furcula, and thus there is no support for the homology of this feature with the interclavicle (*contra* Parker 1868).

Whereas secondary cartilage was not identified in the *Gallus gallus* embryos examined herein, it has been reported to (transiently) develop on the epicleideal processes of the furcula, adjacent to the insertion of the M. pectoralis (Hall, 1986).

TEST OF CONGRUENCE – RESULTS

That birds arose from fossil theropods has been well established and repeatedly confirmed (e.g., Gauthier 1986; Sereno 1999). Furthermore, the furcula has been documented for numerous non-avian theropods (see below). Hence, the furcula is regarded as an autapomorphy of theropods. The test of congruence was explored for each of five hypotheses (Table 2). All five analyses found the same single most parsimonious tree (Fig. 19) using both the ACCTRAN and DELTRAN optimizations. A summary of the results is presented in Table 2. The most parsimonious description of homology (with lowest TL, 122 steps) and least amount of homoplasy (highest CI, 0.7787) are generated by hypotheses 3 (the furcula as a neomorph), and 5 (interclavicle is plesiomorphic for dinosaurs and is the homologue of the furcula). The least parsimonious description of homology (TL = 124 steps) and greatest amount of homoplasy (CI = 0.7661) is generated by hypothesis 2 (clavicles are plesiomorphic for dinosaurs; clavicles fuse to form the furcula). For all other hypotheses the results are equivocal (see Table 2).

TEST OF CONGRUENCE – DISCUSSION

HYPOTHESES 1 AND 2: FURCULA-EQUALS-CLAVICLES

Without question, the furcula is most commonly (almost exclusively) considered to be the homologue of the fused clavicles. In addition to a shared position, mode of development, and failure to co-exist, in some bird taxa the contralateral epicleideal ramus do not directly fuse with one another (e.g., some psittaciforms and strigiforms; Parker 1868; Glenny 1954; Glenny and Friedman 1954), arguably giving the appearance of clavicles. Hence, ignoring phylogeny for the moment, reconstructing a transformation series from clavicle-like elements to a U, V or Y-shaped furcula is relatively straightforward, even within the avian lineage. Interestingly (and perhaps unexpectedly),

acceptance of the furcula-equals-clavicles relationship has had a profound effect on the historical interpretation of bird origins.

Shortly after dinosaurs were first described it was observed that non-avian theropods share many skeletal features with modern birds (Huxley 1870). Notwithstanding the vast number of common features, neither the furcula nor any putative homologue (viz., the clavicles) had yet to be reliably observed in these fossil forms. Using a strict (and somewhat inaccurate) interpretation of Dollo's law of irreversibility in evolution, it was argued that if "dinosaurs" lacked (a) furcula/clavicles they could not have given rise to birds (Heilmann 1926; see also Bryant and Russell 1993). The influence of this argument was considerable, effectively burying the hypothesis of a dinosaurian origin for birds for more than 40 years.

Beginning with the work of Ostrom (1973), it soon became clear that the observed similarities of birds and dinosaurs were not merely the result of convergence. Significantly, Ostrom (1973) was able to draw upon previous discoveries of a number of small carnivorous dinosaurs that appeared to have clavicles (e.g., *Segisaurus halli*; Camp 1936). At present, the occurrence of a furcula has been documented for representatives of most major lineages of non-avian theropods (see above). Furthermore, newly collected and prepared materials have also since revealed that the so-called clavicles of basal non-avian theropods such as *S. halli* actually represent a fused and unpaired furcula (Carrano et al. 2005; see also Downs 2000; Tykoski et al. 2002).

For outgroups to theropods, the situation is less clear. In *Herrerasaurus ischigualastensis*, as for other basal saurischians, dermal pectoral elements are unknown, and it remains possible that they were present and yet not preserved/recovered (Sereno 1993). Among herbivorous dinosaurs (sauropodomorphs and ornithischians) the furcula is similarly unknown for all members. Some taxa with paired clavicle-like ossifications have been collected (e.g., basal ceratopsians such as *Montanoceratops cerorhynchus*; Chinnery and Weishampel 1998) although overall the distribution appears to be limited to a few disparate species. In at least one instance, the sauropodomorph *Massospondylus carinatus*, the elements in question are preserved in articulation with the rest of the pectoral apparatus and with each other, forming a V-shaped chevron (Yates and Vasconcelos 2005). However, unlike the coalescing epicleideal rami of *Gallus gallus*,

the contralateral components do not abut; instead the right element overlaps the left in the midline. Regrettably, none of the closest successive outgroups to Dinosauria (e.g., *Marasuchus talampayensis* and *Lagerpeton chanarensis*) demonstrate dermal pectoral elements and/or are well enough preserved to rule out their presence. For one genus of pterosaur (a juvenile specimen of *Eudimorphodon* sp.) at least, it has been argued that both the clavicles and interclavicle have become incorporated into the cranial end of the sternum (Wild 1993). This has yet to be demonstrated in other taxa.

Notwithstanding the convenience of the transformation sequence and historical concurrence, our analysis indicates that the furcula-equals-clavicles hypothesis is the least parsimonious interpretation of homology (with a TL = 123 and a CI = 0.7724). Acceptance of the clavicle hypothesis requires that the loss of such elements among the ancestors to dinosaurs is either an artifact of preservation or reversed among theropods. It is also worth noting that (excluding for the moment the possibility of the furcula), there are no known examples of clavicles fusing together.

HYPOTHESIS 3: FURCULA AS A NEOMORPH

As defined by Hall (2005), a neomorph is a *de novo* feature (element, joint, or structure) that is present in most (if not all) individuals of the ingroup while being absent in the sistergroup and all their common ancestors (successive outgroups). Belon's (1555) observations notwithstanding (see also Bryant and Russell 1993) support for a *de novo* origin of the furcula stems from the test of congruence. Theropods (including birds) are unique in demonstrating a furcula and, at present, the fossil record does not reveal any comparable element(s) from the immediate outgroups. Furthermore, the inconsistent distribution among herbivorous dinosaurs reduces the obligation to interpret the furcula via a transformation sequence of clavicle-like elements. For the present analysis, the most parsimonious genealogical interpretation supports a neomorphic hypothesis for the furcula with the fewest number of evolutionary steps (TL = 122) and the most optimal phylogenetic fit (CI = 0.7787).

HYPOTHESES 4 AND 5: FURCULA-EQUALS-INTERCLAVICLE

Perhaps unexpectedly, the proposed interclavicle hypothesis poses a serious challenge to the notion that the clavicles are the only candidate homologue for the furcula.

Similar to the clavicles, the interclavicle is plesiomorphic for tetrapods, occupies a midventral position within the pectoral apparatus, undergoes an intramembranous mode of ossification, and does not co-exist with the furcula in the same individual. Furthermore, unlike the clavicles but similar to the furcula, the interclavicle is derived from paired condensations that fuse together early during skeletogenesis. And, whereas the characteristic chevron-shape of the furcula is quite unlike that of the interclavicle of modern crocodylians, this line of reasoning has many obvious shortcomings. While birds and crocodylians are sister taxa among living reptilians, each enjoys a lengthy segregated evolutionary history (e.g., Gauthier 1986; Brochu 2001). Also, as noted by Shubin (1994; see also Bock 1989), differences in morphology are poor falsifiers of homology (similarity raises the suspicion of homology, but does not make it certain). Moreover, in a review of lepidosaur pectoral osteology, Lécuru (1968a) documented an enormous range of interclavicle morphologies, including at least one species (*Agama stellio*) that approaches a V-shape. Finally, evidence from detailed investigations of the mammalian interclavicle (Klima 1973, 1985, 1987) established that the ontogeny of this element is more complex than previously understood.

Among monotreme mammals, the interclavicle begins development as three separate condensations: a pair that undergoes intramembranous ossification, the pars desmalis interclaviculae; and an azygous condensation that develops transiently into cartilage, the pars chondralis interclaviculae. These discrete aggregations can only be identified for a brief window of development and shortly after their initial appearance they insensibly combine to yield the bony interclavicle. For therians (placental and marsupials), adults lack a discrete bony interclavicle and during development there are never any signs of the pars desmalis interclaviculae. However, early during skeletogenesis an unpaired condensation comparable with the pars chondralis interclavicular is briefly present. This precartilaginous condensation coalesces with the conjoining sternal bands and with a rudiment representing a portion of the procoracoid, to form the cranialmost portion of the sternum, the manubrium sterni (Klima 1985, 1987; Vickaryous and Hall 2006a [Chapter 2]). Related to this, an unpaired cartilaginous condensation contributes to the cranial-most end of the developing carina sterni in various birds including *Melopsittacus undulatus* (budgerigar; Fell 1939), *Phalacrocorax*

carbo (great cormorant), *Larus ridibundus* (black-headed gull) and *Hirundo rustica* (barn swallow; Klima 1962). Klima (1973) suggested that these azygous rudiments were comparable with the pars chondralis interclaviculae of monotremes. In contrast, development of the crocodylian interclavicle is comparable with the pars desmalis interclaviculae, with no evidence of an equivalent to the pars endochondralis interclaviculae (Klima 1973).

With few exceptions, the relationship between the interclavicle and furcula has been overlooked. Parker (1864) initially suggested that the interclavicle (his episternum) of lizards was comparable to the avian furcula, but amended this identification to include both the clavicles and interclavicle (the latter contributing to the hypocleideum) in subsequent work (Parker 1868). In agreement with Hall (1986), our developmental work on *Gallus* finds no basis for a separate condensation contributing to the hypocleideum, and consequently we consider it an outgrowth or process of the furcula.

Perhaps the strongest evidence in opposition to the furcula-equals-interclavicle hypothesis comes from the traditional interpretation of the fossil record, with few elements interpreted as interclavicles known for dinosaurs or any immediate outgroups. To the best of our knowledge there are only two reports of dinosaur interclavicles, one that has since been identified as a furcula (from the theropod *Oviraptor philoceratops*; Osborn 1924) and one that has since been reinterpreted as a clavicle (from *Massospondylus* sp.; Cooper 1981; Sereno 1991; Yates and Vasconcelos 2005). What remains unclear is whether elements designated as 'clavicles' alternatively represent unfused remnants of the interclavicle. In the present analysis, our data were scrutinized against two tests of congruence for the interpretation of the furcula-equals-interclavicle (hypotheses 4 and 5). Although unorthodox, hypothesis 5, assuming that the interclavicle is plesiomorphic for dinosaurs (TL = 122; CI = 0.7787), was found to be equally parsimonious with the furcula as a neomorph (hypothesis 3). Alternatively, hypothesis 4, that the interclavicle is present in theropods, is equivocal with the furcula-equals-clavicles hypotheses (see above; TL = 123 and a CI = 0.7724). Acceptance of either hypothesis requires that the interclavicle was either retained by dinosaurian outgroups (the perceived non-appearance is an artifact of preservation) and theropods but lost in other dinosaur lineages, or that the absence in outgroups is real and that presence in

theropods is a reversal. Hypothesis 4 does not provide insight into the identity of the elements found in non-theropod dinosaurs, whereas hypothesis 5 requires that the clavicle-like elements of some herbivorous forms represent the independent reacquisition of the interclavicle, albeit as paired and unfused. And while there are no modern forms documented with an unfused interclavicle, paired interclavicular elements have been described in specimens of a basal tetrapod (*Discosauriscus* sp.; Klembara 1996).

COMPARISON OF HYPOTHESES

Previous discussions of furcula homology frequently make reference to the high degree of morphological plasticity and discontinuous appearance of dermal pectoral elements, raising the possibility that the apparent absence in some members may reflect multiple independent losses or reversals (e.g., Makovicky and Currie 1998). These observations are corroborated by embryological studies that demonstrate the early initiation and rapid disappearance of the furcula in modern forms such as *Struthio camelus* (e.g., Holmgren 1955; Glutz von Blotzheim 1958). The issue becomes confounded when fossil taxa are considered, as the putative absence cannot be unambiguously established as either a taphonomic artifact (not preserved or collected) or as an evolutionary loss (either as a synapomorphy or autapomorphy). Consequently, the possibility that nonappearance equals nonexistence must be considered, leading to the hypothesis that the furcula represents a *de novo* skeletal element. Furthermore, it is also plausible that even if preserved and collected, the furcula may not be recognized, particularly if it has undergone some degree of morphological transformation or is unexpected (e.g., the furcula has often been confused with fused gastralia; Chure and Madesen 1996; Makovicky and Currie 1998).

Commonly, it is understood that the furcula forms from a discrete pair of bar-like clavicles that unite into a chevron-shape. Alternatively, it is herein proposed that the furcula is a modified interclavicle. Excluding for the moment the elements present in non-theropod dinosaurs, observational support (in terms of structure, development, and topology) for each of these hypotheses is strikingly comparable. The irregular distribution of clavicle-like elements in herbivorous dinosaurs is problematic for the furcula-equals-interclavicle hypothesis only if and when they are precluded as

interclavicles *a priori*. However, as demonstrated by the tests of congruence, acceptance of the interclavicle as equivalent to the furcula is a valid and competitive alternative to the prevalent fused clavicles hypothesis. Significantly however, the *a priori* interpretation of the furcula as a neomorph is equally compelling. Accordingly, it is (reluctantly) concluded that homology of the furcula remains ambiguous.

SUMMARY AND RESOLUTION

That the homology of the furcula remains uncertain is representative of the complexity of morphological evolution and development, and is neither extraordinary nor trivial. The key to resolving the issue begins with accepting the presence of a furcula in theropods (or possibly some clade within Theropoda). The task then becomes establishing which (if any) element is comparable among outgroups. Regrettably, data regarding the contribution(s) of dermal elements to the pectoral apparatus of the stem lineages leading to Dinosauria remains conspicuously absent. Even if the notion that pterosaurs combined the interclavicle and clavicles with the sternum is accepted (Wild, 1993), this lends nothing to establishing the identity of the furcula. Furthermore, the situation within the dinosaur clade is far from clear: an unpaired dermal element unknown among non-theropods and paired elements have a limited, and disparate, taxonomic distribution.

Accepting that the presence of dermal element(s) among dinosaur outgroups is (are) unknown, three competing hypotheses were then independently considered: the furcula as the fused clavicles, the furcula as the interclavicle, and the furcula as a neomorph. To evaluate each possibility, several tests of homology are explored. The first, the test of similarity, provides the cue to construct scenarios, but does not establish, homology. This test supports each of the fused clavicles and the interclavicle as possible homologues of the furcula, and is not applicable to the neomorphic hypothesis. The second, the test of conjunction, demonstrates nonhomology (Roth 1994). This test fails to exclude any of the proposed hypotheses. The third, the test of congruence, is often viewed as the decisive criterion (Bryant and Russell, 1986; Roth, 1994). However, as demonstrated in this instance, it remains possible that independent evaluation of multiple hypotheses using the congruency principle will fail to yield unequivocal evidence supporting one postulation over the others. And while intuitively it would seem unlikely

that both the interclavicle and clavicles were lost while a new element (the furcula) evolved, in the absence of data to the contrary it is perhaps inappropriate to rule out or ignore such a hypothesis. Consequently, the homology of the furcula remains, for the time being, unresolved.

This study underscores the developmental and evolutionary complexity of the pectoral apparatus. For the furcula, undisputed and untested acceptance of homology has already led to a historic evolutionary oversight, viz., Heilmann's (1927) removal of dinosaurs from the lineage leading to Aves. As demonstrated here, the identity of the furcula remains uncertain, imparting new impetus to further explore the issue. Ultimately, fossil discoveries will provide much needed information to readdress this issue with more certainty, particularly those specimens representing the immediate outgroups to Dinosauria. In addition, it remains possible that sampling embryos from additional taxa of modern archosaurs (birds and crocodylians) may yield evidence that contradicts the test of conjunction. Another avenue for consideration is the compelling parallel between polymorphic axial patterned serial homologues such as vertebrae (e.g., cervical and thoracic) and elements of the pectoral elements. For example, it is understood that changes in Hox gene expression are correlated with changes in vertebral identity and the developmental basis of limblessness (Cohn and Tickle, 1999). Similarly, misexpression of multiple *Hoxc* genes (following the application of retinoic acid to developing *Gallus* limb buds), results in gross appendicular malformations (Nelson et al., 1996; see also Oliver et al., 1990). Thus, changes in the (overlapping) pattern of gene expression may result in changes in the identity and/or the presence or absence of various pectoral dermal element(s). In order to explore this hypothesis further however, a greater understanding of the role of axial patterning in the pectoral apparatus is required.

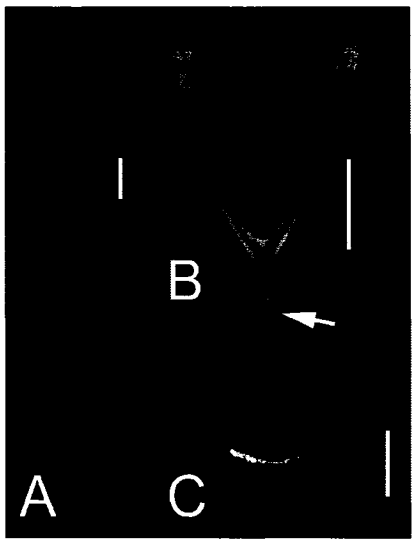

Figure 17. Dermal elements of the adult archosaur pectoral apparatus. A: *Alligator mississippiensis* interclavicle. B: *Gallus gallus* furcula with prominent hypocleideum (white arrow). C: *Gorgosaurus libratus* furcula (Royal Tyrrell Museum of Palaeontology [TMP] 94.12.602). Scale bars A, B = 20 mm; C = 50 mm.

Figure 18. Development and histology of the *Alligator mississippiensis* interclavicle (A-F) and *Gallus gallus* furcula (I-N). All whole-mounts (A, F, K, N) in ventral view with cranial towards top of image; all serial sections (B-E, G-J, L, M) with the dorsal border towards the top of the image. Visualization of the interclavicle in Ferguson stage (FS) 19 *A. mississippiensis* embryos prepared as an (A) Alizarin red and Alcian blue stained whole-mount and (B,C) serial sections. The interclavicle begins as a pair of condensations that demonstrate weak affinity for Alcian blue (A, B) indicating the presence of limited amounts of glycosaminoglycans; combined with the absence of chondrocytes/-blasts, these features are characteristic of osteoid and not cartilage. C: Same specimen as shown in B sectioned and stained with Mallory's trichrome. Scale bars for A = 1 mm, B, C = 100 μm. D: FS 20 *A. mississippiensis* embryo demonstrating the fusion of the paired interclavicular condensations, stained with AC pentachrome. Scale bar = 300 μm. E: Same specimen as shown in D, illustrating the formation of trabeculae linking the paired condensations. Scale bar = 100 μm. F: FS 22 *A. mississippiensis* interclavicle, whole-mount single stained with Alizarin red. Scale bar = 1 mm. G: FS 24 *A. mississippiensis* embryo, stained with Mallory's trichrome, demonstrating the relationship of the interclavicle with the Mm. pectoralis. Scale bar = 400 μm. H: Same specimen as shown in G, stained with HBQ and taken at a more caudal position, illustrating the relationship between the cartilaginous sternum (stn) and ossified interclavicle. Scale bar = 200 μm. I: Hamburger and Hamilton stage (HH) 33 *G. gallus* embryo demonstrating the paired condensations giving rise to the furcula, stained with Mallory's trichrome. Scale bar = 300 μm. J: Same specimen as shown in I demonstrating the weak affinity for Alcian blue characteristic of osteoid, stained with the Hall-Brunt Quadruple stain (HBQ). Scale bar = 200 μm. K: HH 35 *G. gallus* furcula, whole-mount single stained with Alizarin red. Scale bar = 1 mm. L: HH 36 *G. gallus* demonstrating the fusion of the paired condensations giving rise to the furcula in the region of the hypocleideum, stained with AC pentachrome. Scale bar = 500 μm. M: Same specimen as shown in L illustrating the formation of trabeculae linking the paired condensations giving rise to the furcula, stained with Mallory's trichrome. Scale bar = 100 μm. N: HH 39 *G. gallus* embryo demonstrating the overall morphology of the mineralizing furcula, whole-mount single stained with Alizarin red. Scale bar = 1 mm. Abbreviations: hyp (hypocleideum), int (interclavicle), mm (Mm. pectoralis).

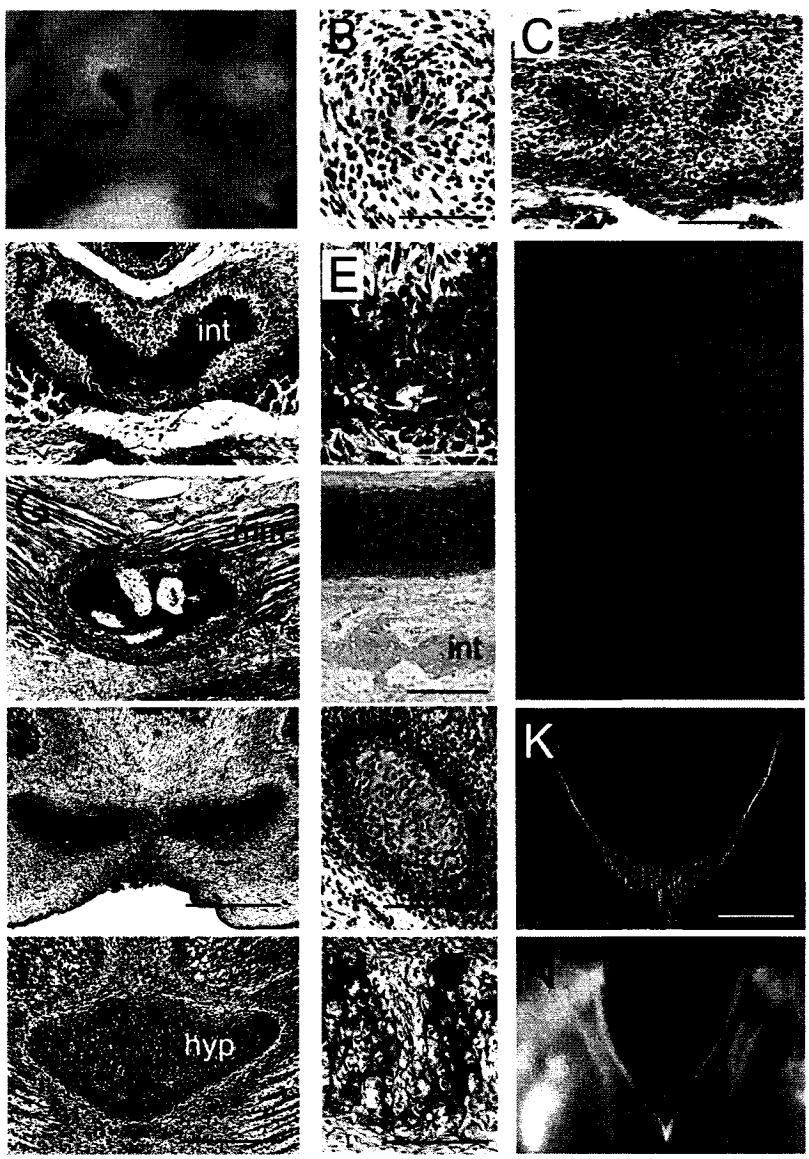

Figure 18

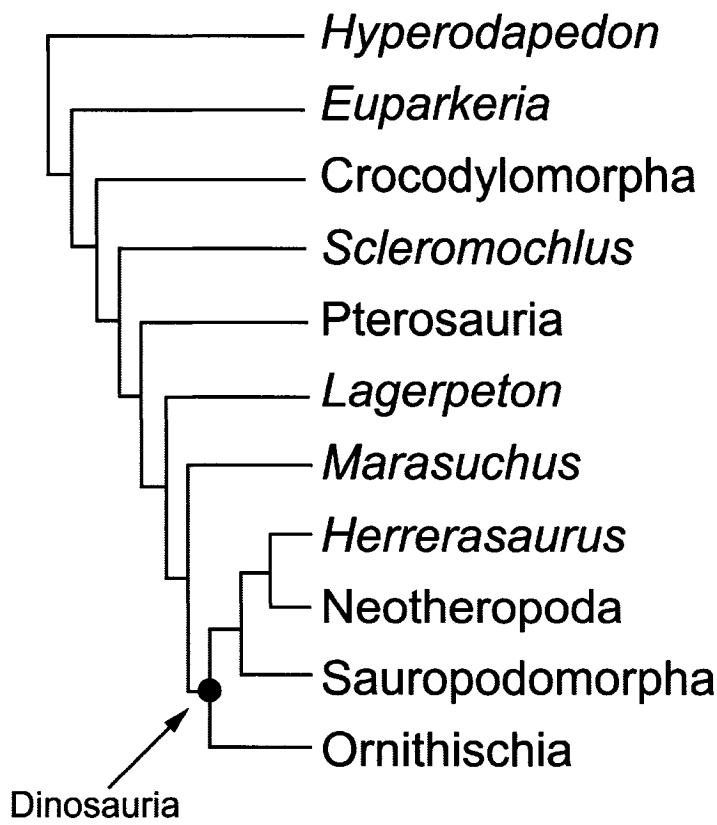

Figure 19. The single most parsimonious tree of basal archosaur genealogy generated by all five hypotheses of furcula homology. Data matrix modified from Benton (2004). In accordance with Benton (2004) and Langer (2004), *Herrerasaurus ischigualastensis* is considered a basal saurischian nested outside of Theropoda. See text for details.

Table 2. Characters modified from the data matrix of Benton (2004) for use in the test of congruence: character 38 (clavicles present [0], rudimentary/absent [1]), character 39 (interclavicle present [0], absent [1]), character 40 (interclavicle lateral processes elongate [0], reduced [1]). Clavicles are considered absent in crocodylomorphs (Gauthier, 1986). All trials were conducted using the branch and bound search algorithm and investigated for both ACCTRAN and DELTRAN.

			character			tree statistics					
Hypothesis			38	39	40	number of trees	TL	CI	HI	RI	RC
1	Theropods with clavicles (= furcula)	*Herrerasaurus*	1	1	?	1	123	0.7724	0.2276	0.8095	0.6252
		Theropoda	0	1	?						
		Sauropodomorpha	1	1	?						
		Ornithischia	1	1	?						
2	Theropods, sauropodomorphs, ornithischians with clavicles, *Herrerasaurus* uncertain	*Herrerasaurus*	?	1	?	1	123	0.7724	0.2276	0.8662	0.6242
		Theropoda	0	1	?						
		Sauropodomorpha	0	1	?						
		Ornithischia	0	1	?						
3	Furcula as a neomorph	*Herrerasaurus*	1	1	?	1	122	0.7787	0.2213	0.8151	0.6347
		Theropoda	1	1	?						
		Sauropodomorpha	1	1	?						
		Ornithischia	1	1	?						
4	Theropods with interclavicle (= furcula)	*Herrerasaurus*	1	1	?	1	123	0.7724	0.2276	0.8095	0.6252
		Theropoda	1	0	1						
		Sauropodomorpha	1	1	?						
		Ornithischia	1	1	?						
5	Theropods, sauropodomorphs, ornithischians with interclavicle, *Herrerasaurus* uncertain	*Herrerasaurus*	1	?	?	1	122	0.7767	0.2213	0.8125	0.6327
		Theropoda	1	0	1						
		Sauropodomorpha	1	0	1						
		Ornithischia	1	0	1						

CHAPTER 4. OSTEODERM MORPHOLOGY AND DEVELOPMENT IN THE NINE-BANDED ARMADILLO, *DASYPUS NOVEMCINCTUS* (MAMMALIA, XENARTHRA, CINGULATA)

The following chapter is published as: Vickaryous MK and Hall BK. 2006. Osteoderm Morphology and Development in the Nine-Banded Armadillo, *Dasypus novemcinctus* (Mammalia, Xenarthra, Cingulata). Journal of Morphology 267: 1273-1283.

INTRODUCTION

The primary role of the tetrapod integument—the stratified combination of richly keratinized epidermis and densely collagenous dermis—is to protect against mechanical, environmental, and physiological stresses (Moss, 1969; Menon, 2004; Daly and Buffenstein, 1998; Chuong et al., 2002). Nowhere are the mechanically protective properties more obvious than in representatives of the numerous lineages that reinforce the integument with localized mineralizations—*osteoderms* (= osteoscutes, dermal scutes; Vickaryous et al., 2001). Among reptiles and anurans, osteoderms are found throughout a broad and often unrelated diversity of taxa (Romer, 1956; Moss, 1969; Ruibal and Shoemaker, 1984). In contrast, among mammals osteoderms are confined to a single lineage, cingulatan edentates, with 'armadillos' (currently recognized as a paraphyletic assemblage at the base of Cingulata; Gaudin and Wible, 2006) as the only living representatives. Along with being the one of the most conspicuous apomorphies of the clade, the arrangement and morphology of osteoderms within cingulates has also been employed as a source of taxonomic information (Wetzel, 1985).

In all 21 species of extant, structural-grade armadillos (hereafter armadillos), osteoderm-bearing regions of the integument or shields include a casque-like array overtop the skull (head shield), buckler-like mosaics that enclose the pectoral and pelvic apparatuses (shoulder and pelvic shields, respectively), and an imbricated or banded section between the appendicular girdles (banded shield) (Fig. 20A) (Wilson, 1914; Cooper, 1930). Collectively, the pectoral, banded and pelvic shields form the carapace. With the exception of *Cabassous* spp., the naked-tailed armadillos (Wetzel, 1985),

armadillo osteoderms also coalesce to form a series of rings of decreasing diameter that encircle the tail (tail shield).

Perhaps unexpectedly, details regarding the development of armadillo osteoderms are poorly known. Previous work that explored the development of armadillo integument typically focused on the epidermis and epidermal derivatives, with osteoderm skeletogenesis receiving limited commentary (Leydig, 1859; Römer, 1892; Wilson, 1914; Cooper, 1930). Herein, I investigate osteoderm morphology and development in the nine-banded or common long-nosed armadillo, *Dasypus novemcinctus*.

MATERIALS AND METHODS

ARMADILLOS

All embryonic material was obtained from museum collections; adult osteoderms are from the personal collection of MKV. Three different (albeit unknown) stages of embryonic development of *Dasypus novemcinctus* Linnaeus 1758 were sampled. By chance all the specimens used in the study were male, although the results are not expected to differ between the sexes. Prior to routine histology, the formaldehyde fixed and alcohol preserved specimens were measured for total body length (sagittal plane from tip of nose to the distal end of the tail) and carapace length (sagittal plane, including the shoulder, banded and pelvic shields). The youngest (= smallest) material (University of Kansas Museum of Natural History [UKMNH] 144598) is a single specimen, body length 82 mm, carapace length 37 mm. Older (= larger) material is represented by two litters, each of four identical siblings (Texas Cooperative Wildlife Collection [TCWC] uncatalogued specimens): litter 1 average body length 216 mm, average carapace length 85 mm; and litter 2 average body length 246 mm, average carapace length 95 mm.

HISTOLOGY AND HISTOCHEMISTRY

For each embryonic stage, a head shield, tail shield and the right half of one carapace was processed for whole-mount clearing and staining with Alizarin red for calcified structures, following a modified protocol of Klymkowsky and Hanken (1991) that omitted the steps for Alcian blue staining. This permitted three-dimensional visualization of mineralized elements within the integument. In addition, cranial and postcranial

materials from both the youngest specimen (UKMNH 144598) and older material (a TCWC litter 1 specimen) were also whole-mounted, to evaluate the progression of mineralization throughout the rest (i.e., non-integumentary part) of the skeleton. Head and tail shields from siblings and the corresponding left halves of the whole-mounted carapaces, as well as carapace material from siblings, were examined with serial histology.

Various histological techniques were used to identify the tissue and cellular composition of the carapace material from all three embryonic stages and from isolated adult osteoderms. Preparation of serial sections included decalcification in Tris-buffered 10% EDTA (buffered to pH 7.0) for 5+ days, dehydration to 100% ethanol, clearing in CitriSolv (Fisher No. 22-143975) and embedding in low melting paraffin at 54^{O}C (Paraplast X-tra, Fisher No. 23-021-401). Sections were cut at 6-7 microns and mounted on 3-aminopropytriethoxy-silane coated slides. Following the staining protocols (see below), sections were mounted with DPX (Fluka No. 144581) and coverslipped.

The most common connective tissue stain protocols used were the Hall-Brunt Quadruple (HBQ) stain (Hall, 1986; Witten and Hall, 2003) and Masson's trichrome (Witten and Hall, 2003). HBQ was used to permit the early discrimination of cartilage and bone, whereas Masson's trichrome was used as a general-purpose connective tissue stain that visualizes both low and high tensile collagen fibres (Flint and Lyons, 1975). Additional tissue and cellular details were gleaned from Toluidine blue (Witten and Hall, 2003), azan (Mallory-Heidenhain) stain, Mallory's trichrome stain, the Gridley method for reticulin, the periodic acid-Schiff (PAS) technique, Sudan black B stain with polarized microscopy, and Verhoeff's elastin stain (Presnell and Schreibman, 1997).

Surface morphology of adult osteoderms was examined using scanning electron microscopy (SEM; Nanolab 2000, Bausch and Lomb) following application of a gold-coat using a sputtercoater (Samsputter-2a; Tousimis Research Corp.; Sargent-Welch Vacuum Pump).

RESULTS

GENERAL DESCRIPTION OF THE CARAPACE

Among adults, osteoderms cover most of the dorsal and lateral body surfaces, articulating to form an almost continuous mosaic of bony armour. Postcranially, the carapace is superimposed across the neck, pectoral apparatus, ribcage, and lumbar regions before enveloping the pelvis (Fig. 20A). A disconnected casque-like assemblage is situated dorsal to the cranium and the tail is completely encircled by a coalesced series of osteoderms forming a nested set of imbricating rings. With the exception of the tail rings, there are no osteoderms along the ventral surface of the body. Along the carapace, osteoderms demonstrate various geometric morphologies grading through two major phenotypes – polygonal and rectangular (Fig. 20B-F). Characteristic for both morphologies, the dorsal surface of each carapacial osteoderm is ornamented (see below) whereas the ventral surface is relatively unmarked except for one (or less commonly, two) prominent and centrally positioned neurovascular foramen (foramina).

GENERAL DESCRIPTION OF OSTEODERM

The majority of skeletally mature head, shoulder and pelvic shield osteoderms are near equidimensional polygons (hexagons and pentagons) in dorsal/ventral profile (Fig. 20B, C). When articulated, they form an orderly arranged mosaic or pavement of skeletal elements. Osteoderms of the carapace have a dorsal ornamentation that includes a number of large foramina interconnected by a series of grooves, giving rise to a rosette pattern (Fig. 20E). In most instances adjacent osteoderms do not fuse with one another—individual elements disarticulate with maceration—and the articulation surfaces appear to resemble butt joints. Upon closer inspection, it is revealed that each joint surface has a multitude of bony ridges and fingerlike projections and depressions, contributing to an interdigitating union (Fig. 20F).

Between the shoulder and pelvic shields, osteoderms of the banded shield are typically arranged in tightly grouped series of transversely arranged, imbricating bands. Notwithstanding both the common name and scientific binomen, the actual number of osteoderm-bearing bands in *Dasypus novemcinctus* is variable, ranging from 7 to 10

(Wetzel, 1985; Nowak, 1999). All specimens used in this study demonstrated the nine-banded morphology.

Individual banded shield osteoderms have an elongate, roughly rectangular morphology, with elements demonstrating up to a five to one, length to width ratio (Fig. 20D). Each osteoderm consists of a cranial portion, in life underlapping osteoderms of the proceeding cranial arrangement, and a caudal portion, superimposing (overlapping) the next successive band. The cranial (underlapping) portion is largely unmarked except by small neurovascular foramina and a few shallow, meandering furrows. The caudal (superimposing) portion is ornamented by two series of foramina arranged in caudally diverging rows. Foramina of the outermost rows are larger, interconnected by grooves outlining the position of the central triangular scale (see below), and each supports a single short, stout hair. The smaller foramina of the innermost rows are caudally offset from, yet roughly parallel to, the larger hair-bearing openings. However these apertures appear to lack follicles. At the caudalmost margin of each rectangular osteoderm, there are anywhere between two to four deep foramina transmitting long, caudally directed hairs. Similar to the polygonal osteoderms, contact between adjacent elements of each transverse phalanx (used in the original sense) appear as macroscopic butt joints reinforced by bony ridges and furrows.

Proximally, osteoderms contributing to the tail shield are rectangular, although the ratio is reduced to roughly twice as long as wide and the caudalmost margin of each osteoderm is distinctly convex. More distal elements grade into the polygonal morphology and no longer overlap one-another. Similar to the banded shield, proximal tail shield osteoderms are arranged in phalanges. Uniquely however, these osteoderms completely encircle the tail, forming a series of nested rings, with each cranial ring overlapping the caudal successor.

A single epidermal (keratinous) scale (scute) overlies each osteoderm from the head shield and the majority of osteoderms from the tail shield. In contrast, multiple scales superficially cap each carapacial osteoderm (as well as a limited number of proximal most tail shield osteoderms), and thus over this region the arrangement of scales and osteoderms is not congruous (Fig. 21; see also Fig. 20B). Similar to the osteoderms they overlie, scales of the shoulder and pelvic shields are polygonal. A rosette of scales,

matching the pattern of the bony superficial ornamentation (described above) covers each osteoderm. This arrangement includes a single slightly off-centred central (primary) scale surrounded by a series of eight smaller (secondary) scales. These secondary scales are shared between adjacent osteoderms. From the caudal border of each primary scale one to three large hairs emerge.

The morphology and pattern of scalation differs for the rectangular osteoderms of the banded shield. As each transverse arrangement of banded shield osteoderms is partially overlapped by the cranially adjacent phalanx of elements, only the exposed portion is covered by epidermis. Characteristically, there is a single large and medially positioned triangular scale with a cranially directed apex, flanked on either side by smaller triangular scales with caudally directed apices. The smaller flanking scales partially overlap adjacent rectangular osteoderms and obscure the sutural union from external view. Several large hairs penetrate the contact between adjacent osteoderms towards the caudal margin, while additional hairs pierce the middle portion of each element.

PATTERN OF APPEARANCE OF MINERALIZED OSTEODERMS

As evidenced by whole-mount stained specimens, osteoderms have a delayed onset of mineralization (calcification) as compared with the rest of the skeleton. In the youngest specimen (UKMNH 144598) there is no indication of osteoderms, although virtually the entire skeleton has formed and, in the case of many elements (e.g., skull, clavicle and limb diaphyses), is well ossified (data not shown). Among older material (the TCWC specimens from litters 1 and 2) is it clear that osteoderms do not skeletonize synchronously between or within individual shields, nor do they conform to a strictly cranio-caudal developmental sequence (Fig. 22).

Within each carapace (the combined shoulder, banded, and pelvic shields) Alizarin positive osteoderms first appear at the cranial most margin, adjacent to the sagittal plane (Fig. 22A). The sequence of carapacial osteoderm mineralization is staggered beginning with craniomedially positioned elements of the shoulder and banded shields. As osteoderms continue to mineralize caudally and laterally from these initial positions, skeletogenesis begins in the pelvic shield. The result is an asynchronous

appearance of Alizarin positive elements both within the carapace and within each shield. The more cranial and medial the position of the osteoderm (within each shield or the entire carapace), the more advanced the stage of osteogenesis (Fig. 22B): the further caudal and lateral, the more immature the state of skeletogenesis (cf. Fig. 22C-E and F-G). Significant for this study, asynchronous developmental pattern of osteoderms across the carapace results in a single embryonic specimen demonstrating multiple stages of skeletogenesis.

Among the early developing head shield osteoderms (Fig. 22H), the first signs of mineralization are localized over the parietal and caudal portion of the frontals. Interestingly, while the cranial vault is well ossified at this stage of development, incipient osteoderms are conspicuously absent from the area roughly overlying each cerebral hemisphere. In skeletally more mature specimens, osteoderms fill these vacant positions (Fig. 22I).

The last osteoderms to develop are within the ring-like integumentary arrangements of the tail shield. While there are no signs of tail shield mineralization in specimens from the TCWC litter 1, osteoderms are present in specimens from litter 2 (Figs 22K, L). Each proximal ring consists of one or two phalanges of osteoderms; when two are present the proximal most are smaller. Similar to the carapace, mineralization begins dorsomedially and proceeds ventrolaterally.

STRUCTURE OF THE INTEGUMENT PRIOR TO OSTEODERM FORMATION

Prior to osteoderm formation, the conformation of the integument surface is well established, with individual scales and shields readily distinguishable and permanent skin folds (plica cutis) developed along the banded region and tail. Although not uniform in thickness across the carapace, by this stage of development the epidermis is stratified (Fig. 23A), dominated by squamous cells and may be morphologically subdivided into a stratum corneum (four to six layers thick), stratum granulosum (one to three layers of cells), stratum spinosum (one to four layers of cells) and stratum basale (a single horizon of cuboidal-columnar cells). Nested within the stratum basale are a number of isolated melanocytes. No stratum lucidum was visible at any stage of development. In addition,

the integument has already developed numerous hair follicles and sebaceous glands. Contact between the overlying epidermis and the papillary layer of the dermis occurs at a regular junction, without epidermal ridges or dermal papillae (rete pegs).

Similar to the epidermis, prior to osteoderm formation the dermis also is well formed, and can be roughly divided into papillary (stratum papillare) and reticular (stratum reticulare) horizons (Fig. 21). The papillary dermis is cell rich and composed of thin, relatively loosely structured connective tissue, with prominent vertical collagen bundles. Deep (ventral) to the papillary layer, the more densely constructed reticular dermis is characterized by larger collagen bundles that are oriented parallel to the hypodermis (tela subcutanea) along two main axes – transverse (mediolateral) and longitudinal (craniocaudal) – resulting in an orthogonal plywood morphology. Although both layers of the dermis stain for a variety of connective tissue protocols (e.g., azan, Mallory's, Masson's), neither demonstrates any elastin (using Verhoeff's stain) or reticular fibres (using the Gridley method) (data not shown). Contact between the dermis and hypodermis is well defined as a marked transition from dense connective tissue of large collagen bundles to a looser matrix composed of reticular fibres, adipose tissue, and small blood vessels (Fig. 21).

DEVELOPMENT OF THE OSTEODERM

Presumptive osteoderms develop deep within the papillary dermis. An accumulation of plump, rounded osteoprogenitor cells and osteoblasts is the first indication of a presumptive osteoderm (Fig. 23B). These osteoblasts, and the osteoid they secrete, form the osteoderm primordium. Orientation of the osteoderm primordium parallels the epidermis; e.g., in the shoulder and pelvic shields osteoderm primordia are horizontal whereas in the banded shield primordia are obliquely oriented.

Compared with the rest of the papillary dermis, collagen bundles immediately associated with the osteoderm primordium are fewer in number and have a thinner diameter. Ventrally, cells contributing to the osteoderm primordium are juxtaposed against the reticular dermis. Although not widespread, blood vessels are present at the papillary-reticular contact, adjacent to the osteoderm. As the primordium grows, osteoblasts become trapped as osteocytes within the deposited matrix (Fig. 23C).

Characteristically, numerous thin collagen bundles radiate out of the osteoderm primordium, nested between adjacent osteoprogenitor cells.

Following the initiation of ossification, osteoderms are visible with Alizarin red as diffuse and emarginated/perforated centres (Figs. 22C, F). In section, osteoid forms an evenly distributed layer enveloping the entire osteoderm primordium, with osteoblasts along the dorsal (superficial) surface demonstrating a more spherical morphology and denser arrangement than those of the ventral (deep) surface. Collagen of the dermis and osteoid stain blue for azan and Mallory's, and green for Masson's (Figs. 24A-C). Developing osteoderms are PAS positive (Fig. 24D) but orthochromatic with Toluidine blue (Fig. 24E) and negative for alcian blue (HBQ protocol; Fig. 24F). Furthermore, there is no evidence of chondroblasts within the osteoderm primordium or elsewhere within the integument. Strong positive reactions for reticulin are present within the osteoid and the basement membrane of the epidermis (Fig. 25A).

GROWTH OF THE OSTEODERM

With continued growth and mineralization, Alizarin stained (whole-mounted) osteoderms become increasingly prominent, although their skeletal morphology remains emarginated and variably perforated (Figs. 22D-E, G, J). Among rectangular osteoderms, the caudalmost portion – that part of the element overlapping osteoderms of the successive phalanx – is the last area to mineralize, persisting as Alizarin negative while the majority of the element is well calcified (Fig. 22G).

In section, osteoderm growth is initially marked by an increase in the thickness of the osteoid layer. Gradually however, the distribution of osteoid becomes polarized, with the dorsal (epidermal) surface being thicker than the ventral (hypodermal) surface. In addition, there are considerable changes to the morphology of the surrounding cells. Those cells along the dorsal surface remain plump and rounded, and may be stacked 2-3 cells deep (Fig. 25B). On the ventral surface however, cells within and adjacent to the osteoid layer are flattened and fusiform in shape. Surrounding each osteoderm is a boundary layer of loose, cell-rich connective tissue. The thin radiating fibres noted for earlier stages of development remain but are particularly prominent along the dorsal surface. Although the exact horizon between the papillary and the recticular dermis is

arbitrary, with continued maturation the two can be grossly discriminated based on the predominant size and orientation of collagen fibres; the papillary layer is characterized by relatively thin vertical bundles, whereas the reticular layer is dominated by thick bundles in a horizontal arrangement. Contact between the epidermis and the dermis remains smooth and regular, without evidence of rete pegs.

With continued growth each osteoderm demonstrates homogeneous woven bone histology, including numerous osteocytes, and remains localized within the papillary dermis. The dorsal surface of the osteoderms retain many osteoblasts whereas the ventral surfaces have very few or only bone lining cells. The collagen matrix of the papillary layer includes thinner bundles superior to the osteoderm and thicker bundles inferior to the osteoderm. The dermis architecture is dominated by three horizons based on collagen bundle orientation: upper papillary – vertical bundles; lower papillary – less distinct distribution; reticular – horizontal bundles.

Although there is no evidence of elastin fibres within the cambial layer of the periosteum or the dermis, these connective tissue fibres are present within the basement membrane and hypodermis. Furthermore, developing osteoderms are themselves weakly positive for Verhoeff's (Fig. 25B). Sudan black B stained sections examined under polarized light demonstrate that collagen fibres of the enveloping papillary dermis are not directly incorporated into the osteoderm matrix; at this stage of development there are no signs of anchoring fibres and thus the osteoderm is effective isolated from the rest of the integument (Fig. 25C,D).

ADULT HISTOLOGY

Several dried and isolated adult osteoderms were serially sectioned to provide information about the mature skeletal architecture. Skeletally mature osteoderms consist primarily of fibro-lamellar bone, with Sharpey fibre bone present at the lateral margins (Fig. 26A, B). This Sharpey fibre bone is punctuated by numerous large collagen fibres in tension (staining red with Masson's) radiating from the centre of the element. Cells nested between the Sharpey fibres are not fusiform but instead have a plump, circular morphology. Within the fibro-lamellar matrix of the core of the osteoderm are numerous primary osteons and a limited number of isolated secondary osteons (Haversian systems;

Fig. 26C). Corresponding with the presence of secondary osteons are scalloped resorption lines. Both the dorsal and ventral surfaces of the osteoderm are lined with secondarily deposited compact lamellar bone (Fig. 26D). As noted previously, each osteoderm is typically pierced by a single large neurovascular foramen. Within the osteoderm numerous radially arranged vascular canals diverge from this aperture. Osteocytes are entrenched throughout the osteoderm.

DISCUSSION

Employment of the genus *Dasypus* as a model for developmental studies provides an otherwise extraordinary opportunity to confirm data gleaned from one specimen with other genetically identical individuals from the same litter. The six species of *Dasypus* are unique among vertebrates in always reproducing by polyembryony, wherein a sexually reproduced embryo splits into two or more siblings (Newman and Patterson, 1910; Craig et al., 1997). Invariably, all members of the same *Dasypus* litter are the same sex. In *D. novemcinctus* there are typically four identical offspring, although there may be as few as two or as many as five (Newman and Patterson, 1910). Interestingly, polyembryony is not observed in the armadillo taxa *Cabassous* or *Tolypeutes* (three-banded armadillos) (Craig et al., 1997).

Corresponding with previous work (Wilson, 1914), this study finds that osteoderm formation within the carapace is asynchronous, beginning at the craniomedial margin of the shoulder shield. With continued development, osteoderms sequentially mineralize at comparable craniomedial positions within the banded and pelvic shields. Within each shield, the initiation of skeletogenesis spreads successively among elements caudally and laterally. Osteoderms are present within all shields prior to parturition. Whereas it has been reported that osteoderm primordia are present in the shields of embryos with a carapace length of only 29 mm (Wilson, 1914), we were unable to locate any evidence for incipient elements in an embryo of carapace length 37 mm. However, our data does agree with previous evidence demonstrating osteoderm ossification once the embryo reaches a carapacial length of between 75-95 mm (Wilson, 1914; Cooper, 1930). Although details for most other armadillo taxa are lacking, no osteoderms were

identified in radiographic images of a late term embryo of *Chaetophractus vellerosus* (Vickaryous et al., 2001).

SKELETAL DEVELOPMENT AND GROWTH

Similar to most intramembranously developing (dermal) elements, each *D. novemcinctus* carapacial osteoderm begins from a single condensation of plump osteoprogenitor cells secreting a thick osteoid matrix. Deposition of this matrix is initiated near the future midpoint of the presumptive osteoderm. Subsequent periosteal osteogenesis yields a woven-fibred bone matrix with loosely organized collagen fibres and randomly distributed osteocytes. Once skeletogenesis has begun, the presence of prominent plump osteoblasts, thick seams of osteoid with entrapped osteocytes suggest that growth of the osteoderm is relatively rapid and/or that advancement of the mineralization front is delayed. The deposited skeletal matrix is positive for PAS (demonstrating carbohydrates) but orthochromatic for Toluidine blue and negative for alcian blue (indicating a lack of acidic compounds such as glycosaminoglycans), and there is no evidence for any participation of chondroblasts/-cytes. In addition, while the developing bone is weakly positive for elastin (Verhoeffs), the cambial (cellular) layer of the periosteum is not. The periosteum is positive for the presence of reticular fibres. Sections stained with Sudan black B and visualized using polarized microscopy do not demonstrate the presence of anchoring fibres bridging between the bone matrix and the surrounding dermis. As growth continues, the mineralized front encircles adjacent pre-existing hair follicles, leaving foramina for the continued passage of these structures.

Osteoderm skeletogenesis in *D. novemcinctus* compares well with the development of dermal bones, including the clavicle and parts of the skull (dermatocranium) of mammals. There are however, differences in both the timing of the onset of development and the matrix environment within which skeletogenesis occurs. For most intramembranously developing bones, ossification takes place early during the embryonic period in an undifferentiated mesenchyme (Tran and Hall, 1989; Hall, 2001). In contrast, osteoderms develop relatively late during skeletal ontogeny (i.e., well after the majority of the postcranial skeleton has formed) within the well-differentiated dermis. Nevertheless, these differences have been interpreted as being relatively minor. In a

recent review on the dermal skeleton of aquatic non-tetrapod osteichthyans ('bony fish'), it was observed that all dermal skeletal elements require extrinsic support (Sire and Huysseune, 2003). Some elements (e.g., dermatocranial bones) appear to use the development of adjacent structures (e.g., the chondrocranium) as a proximity foundation. For other elements, such as postcranial dermal plates, the connective tissue matrix, the dense, well-structured dermis, is itself supportive. The timing of skeletogenesis relates to the support requirement and not the type of element per se. Thus, the delayed formation of postcranial dermal plates in bony fish relates to the slow development of the dermis. A comparable situation is observed in the development of mineralized tendons. In some anurans and birds, these skeletal elements begin to develop once the tendon (the extrinsic support) has become a collagen-rich band of dense connective tissue, sometime after hatching (Vickaryous and Olson, in press). Hence the onset of mineralized tendon skeletogenesis is considerably delayed compared to the rest of the skeleton. Similarly, in *D. novemcinctus* osteoderms appear to require a differentiated extrinsic matrix (the papillary dermis) in order to initiate skeletogenesis. As a result, osteoderm formation is delayed corresponding with development of the integument. Furthermore, as skin development is asynchronous across the body (Sengel, 1976), so too is osteoderm development.

The presence of Verhoeffs elastin positive staining of the early mineralized osteoderm cannot be currently explained, although similar results were found for the enameloid, dentine and deep dermal structures of several chondrichthyan and osteichthyan species (e.g., *Leucoraja erinacea*; Miyake et al., 1999; Miyake et al., 2001) and the dermal bone (including osteoderms) of *Alligator mississippiensis* (Chapter 5). Typically, the Verhoeff's protocol is used to stain elastin fibres, common constituents of elastic cartilage, blood vessel walls and periodontal ligaments.

Although we lack information on the histological transition from early forming osteoderms of embryos to those of the skeletally mature adult, several generalizations can be made. The production of embryonic woven bone gives way to fibrolamellar bone, as blood vessels are incorporated into the matrix. A limited amount of continued remodeling of the fibrolamellar bone matrix, as evidenced by the presence of scalloped resorption lines, is observed in the formation of secondary osteons and the lamellar bone

of the dorsal and ventral surfaces. The presence of Sharpey fibres and Sharpey fibre bone at the lateral margins of the osteoderm in adult osteoderms seems to suggest that during post-embryonic growth, preexisting collagen bundles of the dermis are incorporated into the radially expanding element. When stained with Masson's trichrome, the high tensile (red) Sharpey fibres are highly visible radiating from the centre of the element, within a larger matrix of relatively low tensile (green) collagen fibres contributing to the bulk of the osteoderm (see Flint and Lyons, 1975). Unexpectedly, the cells nested between the Sharpey fibres are rounded in morphology and not fusiform, as have been found in other examples of Sharpey fibre bone (e.g., the salmon kype; Witten and Hall, 2003). Regrettably, in the absence of specimens demonstrating the intermediate stages of osteoderm histology, the significance of this cell morphology remains uncertain.

DERMAL ARMOUR

Although often overlooked, the presence of skeletal inclusions within the integument is widespread among various representative members of most major tetrapod lineages, Aves and Caudata excluded (Moss, 1969; Romer, 1956). For most forms, including anurans, reptilians and cingulatan mammals, these elements are osteoderms, bony investments within the dermis. Alternatively, among gymnophiones, these elements are dermal scales, non-osseous flattened disks with alternating layers of unmineralized and mineralized collagen (Zylberberg et al., 1980; Zylberberg and Wake, 1990). Dermal scales have been likened to the mineralized elements of bony fish integument and are not considered to be homologous with osteoderms.

Similar to the carapace of Testudines (turtles), the (non-homologous) carapace of cingulatans is composed of a characteristic mosaic of bones and overlying keratinized scales that are not congruous; individual keratinous scales typically overlap multiple bony elements. However unlike the testudine carapace, the cingulatan carapace is completely confined to the dermis and does not receive any direct contributions from the axial skeleton (vertebrae and ribs). Furthermore, cingulatans lack a ventral counterpart to the carapace (the plastron) and, at least among pampatheres and armadillos, the carapace is moderately flexible; among glyptodonts the carapace is typically immobile (Gaudin and Wible, 2006).

In reptiles, osteoderm development includes the direct transformation of the pre-existing dense, irregular connective tissue of the dermis into bone (Moss, 1969; for a more detailed discuss see Chapter 5). Such a transformation is referred to as metaplasia. A similar mode of skeletogenesis has also been suggested for the osteoderms of anurans (Ruibal and Shoemaker, 1984). Observations made on the anguid *Heloderma horridum* (Moss, 1969; see also Vickaryous et al., 2001) and the crocodylian *Alligator mississippiensis* (Chapter 5) demonstrate that osteoderm development within the integument is asynchronous, beginning craniomedially (dorsal to the skull) before proceeding caudally and laterally.

Similar to those of reptiles, armadillo osteoderms are bony inclusions that exhibit a delayed onset of skeletogenesis. However, there are no data to support metaplasia as the initial mode of ossification. In *D. novemcinctus* osteoderms originate from a discrete primordium, consisting of plump osteoblasts. This primordium continues to expand by periosteal deposition of osteoid prior to mineralization. And whereas adult osteoderms demonstrate Sharpey fibre bone, this is a feature of post-embryonic skeletal maturity. During early osteoderm skeletogenesis, there is no evidence of collagen fibres from the surrounding dermis becoming directly integrated into the element. Whereas *D. novemcinctus* osteoderms differ developmentally from those of squamates, they are comparable with the description of postcranial dermal plate development in osteichthyans (Sire and Huysseune, 2003).

Ostensibly, all osteoderms have been regarded as remnants of the once all-encasing dermal skeleton (= exoskeleton) of structural-grade ostracoderms (Patterson, 1977; Smith and Hall, 1990, 1993; Zylberberg et al., 1992; Sire and Huysseune, 2003). During the course of evolution the dermal skeleton has undergone considerable modification and reduction, to the point where, among tetrapods, osteoderms appear to represent one of the last postcranial remnants. Alternatively, the sporadic presence of osteoderms among distantly or unrelated lineages suggests that all such elements are not homologous (Zylberberg et al., 1992; Sire and Huysseune, 2003; Hill, 2005). Regrettably, in most instances the necessary developmental and anatomical information regarding osteoderms and osteoderm formation is lacking (Smith and Hall, 1993; Sire

and Huysseune, 2003). I will return to this topic again in Chapter 5, where I offer a more complete discussion of osteoderm homology.

Figure 20. *Dasypus novemcinctus* embryonic specimen (A) and adult osteoderms (B-F). A: Right lateral profile of a specimen from the TCWC litter 2 demonstrating the position of each of the five osteoderm-bearing shields: head (hd), pectoral (pec), banded (ban), pelvic (pel), and tail (tl). Scale bar = 30 mm. B: Dorsal view of polygonal osteoderms from the pectoral shield, with and without scalation. The larger primary scales, each corresponding to a single osteoderm, are white whereas the smaller secondary scales, overlapping the articulations between adjacent osteoderms, are black. Oriented with the cranial margin to the top left of the image. C: Ventral view of the same polygonal osteoderms from figure 1B. Scale bar for B,C = 5 mm. D: Dorsal view of two rectangular osteoderms the banded shield. Oriented with the cranial margin to the right of the image. Scale bar = 15 mm. E: Dorsal view of a polygonal osteoderm examined with scanning electron microscopy. Note the surface ornamentation including foramina and furrows. F: Same specimen as figure 1E, viewed laterally with scanning electron microscopy. In this view the ossified interdigitating processes are visible. Scale bar for D, F = 3 mm.

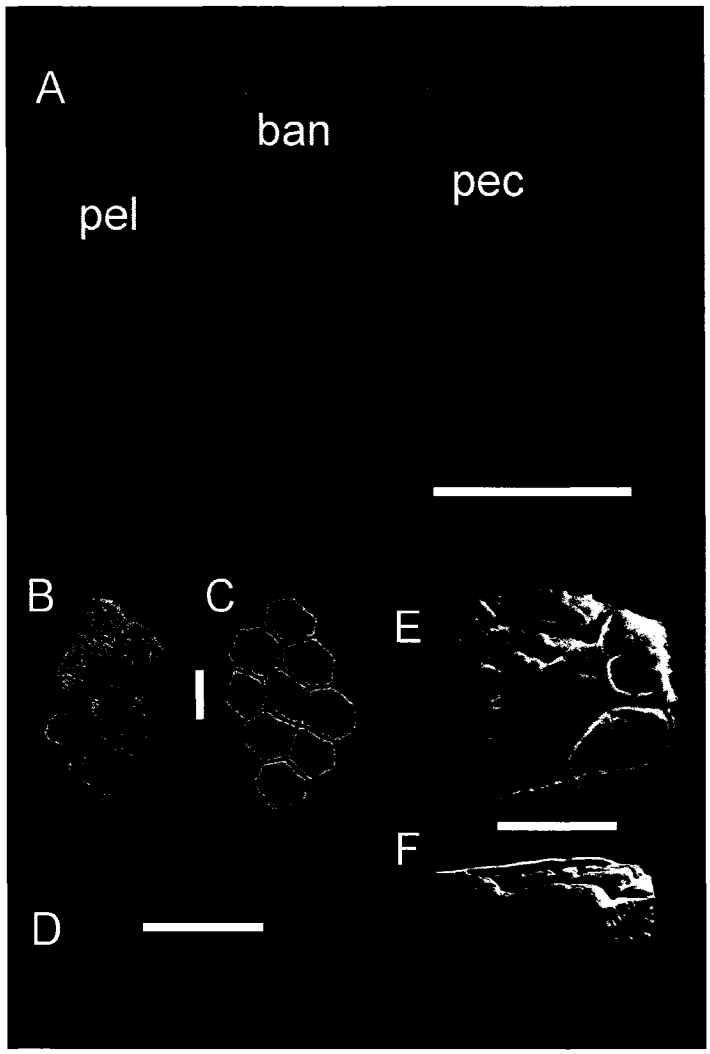

Figure 20.

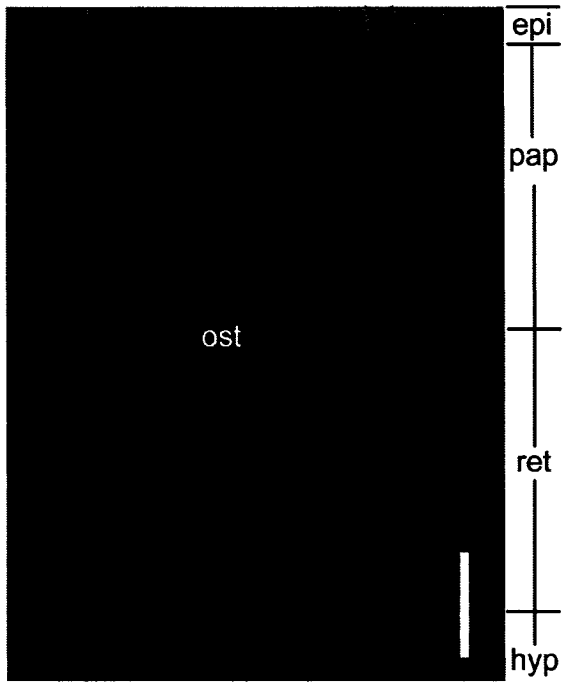

Figure 21. Serial section through the pectoral shield integument of an embryonic *Dasypus novemcinctus* (TCWC litter 2). The osteoderm is located within the papillary dermis, adjacent to the interface with the reticular dermis. Note that a small blood vessel approaches the osteoderm from the hypodermis at the bottom left of the image. The arrowhead at the top right of the image indicates the point of contact between two adjacent epidermal scales. Scale bar = 200 μm. Mallory's trichrome. Abbreviations: bv (blood vessel), epi (epidermal scale), hy (hypodermis), ost (osteoderm), pap (papillary dermis), ret (reticular dermis).

Figure 22. *Dasypus novemcinctus* Alizarin whole-mounted embryonic specimens. A, B: Right lateral profile of carapace integument from TCWC litter 1 (A) and litter 2 (B), demonstrating the distribution of Alizarin positive elements. Scale bar for A, B = 10 mm. C-E: Close up views of select polygonal osteoderms from figures 22A, B, demonstrating progressive stages of mineralization. Scale bar for C-E = 2 mm. F, G: Close up views of select banded shield osteoderms from figures 22A, B, demonstrating progressive stages of mineralization. Scale bar for F, G = 2 mm. H, I: Dorsal views of the distribution of head shield osteoderms from TCWC litter 1 (H) and litter 2 (I). Note the absence of mineralized osteoderms over the area roughly corresponding to the cerebral hemispheres in H. Scale bar for H, I = 10 mm. J: Close up view of a centrally positioned polygonal osteoderm from the head shield of figure 22I. Scale bar = 1 mm. K, L: Tail shield whole-mounts from specimens of TCWC litter 2, in dorsal (K) and left lateral (L) views. Arrowhead indicates the position of the caudalmost Alizarin positive osteoderm present in this specimen. Scale bar for K, L = 5 mm.

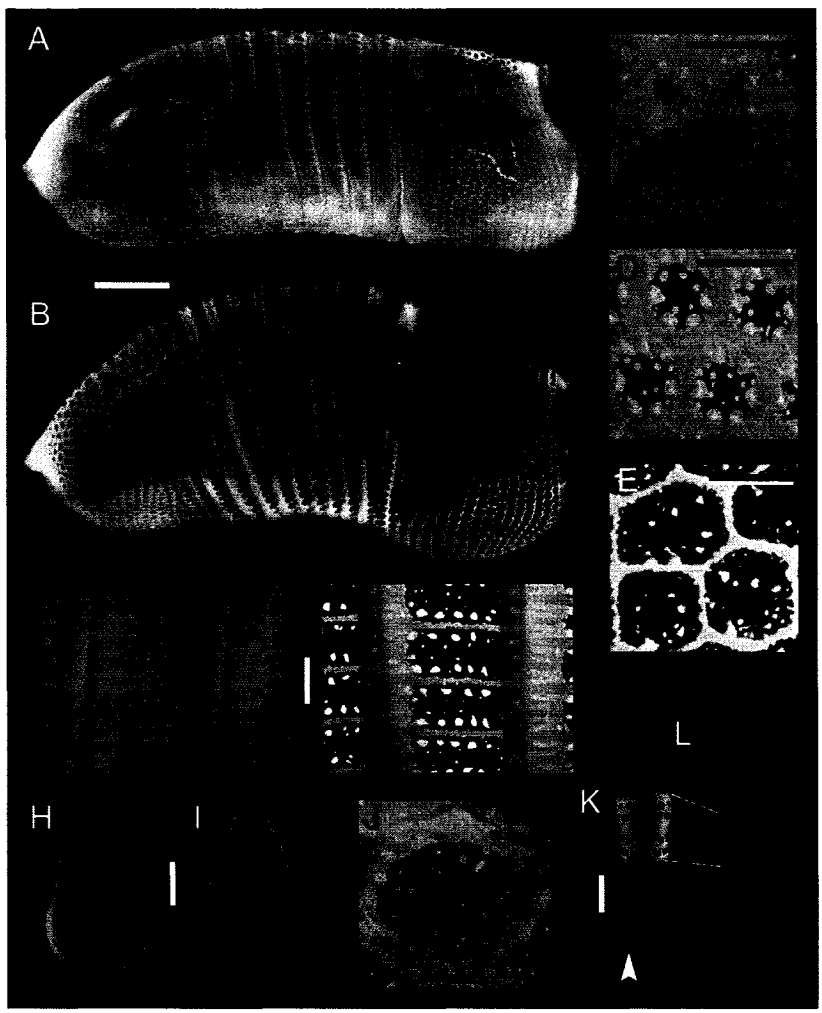

Figure 22.

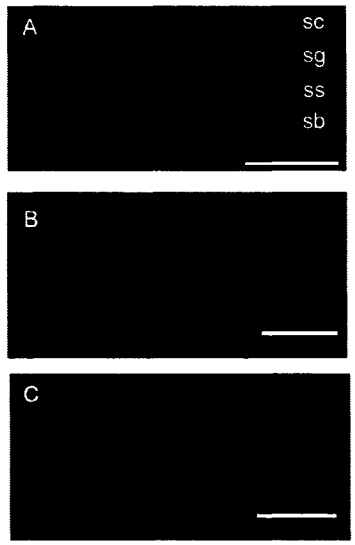

Figure 23. Histological details of *Dasypus novemcinctus* integument (TCWC litter 1). A: Prior to osteoderm development, the overlying epidermis and epidermal scales are well established. The highly stratified architecture includes a stratum corneum, stratum granulosum, stratum spinosum, and stratum basale. The underlying papillary dermis remains mesenchymal and poorly structured. Mallory 's trichome. B: Early formation of the osteoderm. Prior to mineralization the osteoderm is visible as a condensation of osteoblasts depositing osteoid. C: Slightly later during development, as the osteoderm beings to mineralize, osteoblasts become entrapped osteocytes. At this stage in development osteoid continues to be deposited evenly around the entire element. B, C: Masson's trichome. Scale bar for A-C = 50 μm. Abbreviations: sb (stratum basale), sc (stratum corneum), sg (stratum granulosum), ss (stratum spinosum).

Figure 24. Histological details of developing *Dasypus novemcinctus* osteoderms. A,B: Dorsal (epidermal) surface of developing osteoderm demonstrating the arrangement of multiple stacked osteoblasts and thin, radiating collagen fibres (A) and the thick seam of deposited osteoid (B; yellow arrowhead), stained with Azan (A) and Mallory's trichrome (B). C: Early mineralization of developing osteoderm surrounding by thick seam of osteoid (C; yellow arrowhead), stained with Masson's trichrome. D-F: Osteoderm matrix is PAS positive (D), but orthochromatic with Toluidine blue (E) and negative for Alcian blue using the Hall-Brunt Quadruple stain (HBQ) (F). There are no signs of cartilage or cartilage cells. Note that osteoblasts along the dorsal (epidermal) surface are plumper and more spherical than those along the ventral (hypodermal) surface. Scale bar for all = 40 μm.

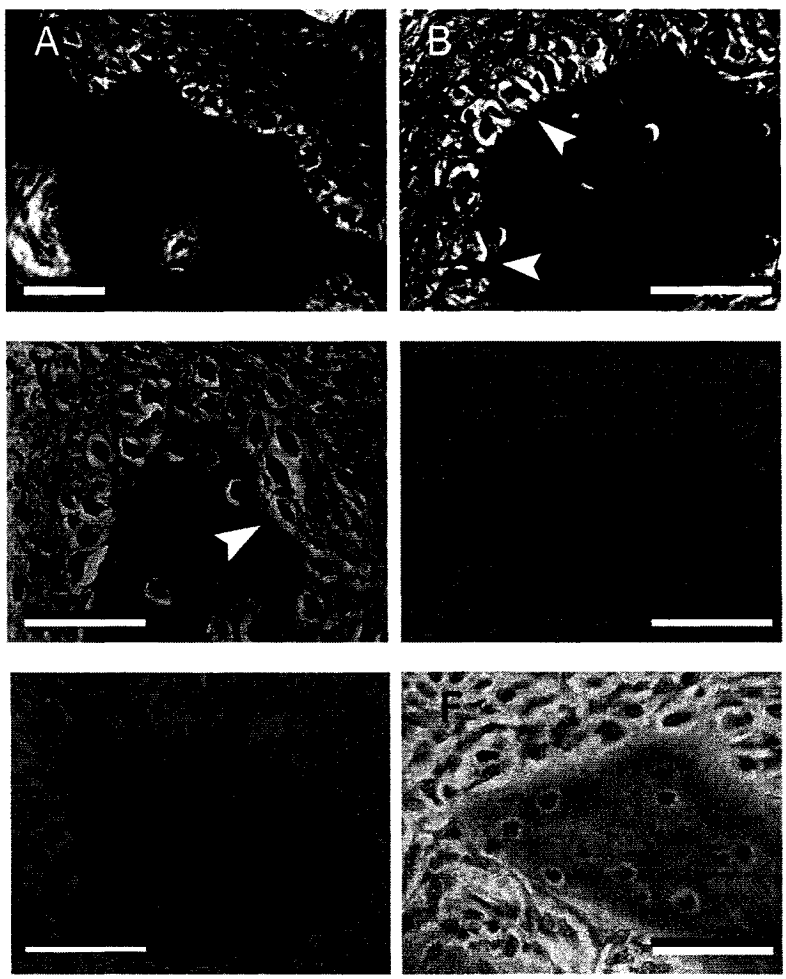

Figure 24.

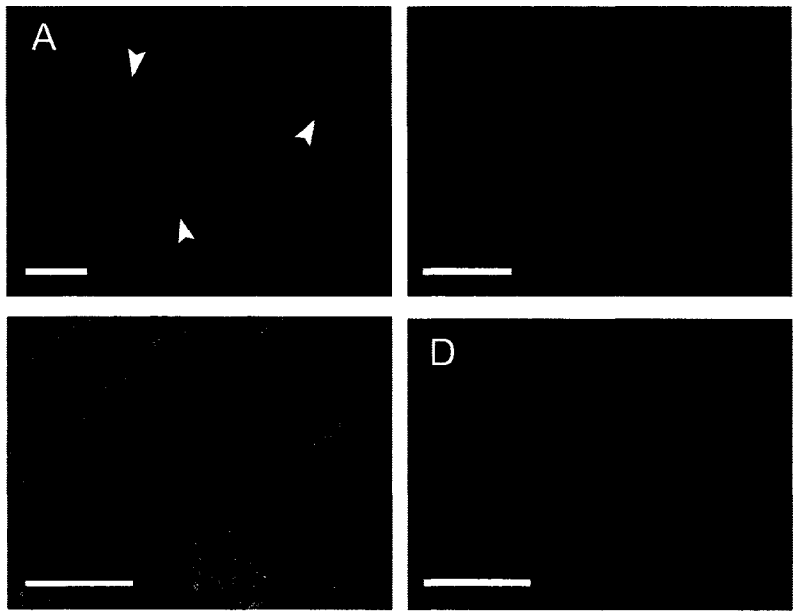

Figure 25. Histological details of developing *Dasypus novemcinctus* osteoderms. A: Reticular fibre staining (Gridley method) reveals the cambial layer of the periosteum (white arrowheads). B: Verhoeff elastin stain is not picked up by the periosteum but is by the mineralized bone, similar to some non-tetrapod vertebrates. C, D: Sudan black staining under plane (C) and polarized (D) light. The absence of collagen fibres crossing between the osteoderm and surrounding dermis indicates that at this stage in development, extrinsic collagen is not being directly incorporated into the bone matrix. Scale bar for all = 40 μm.

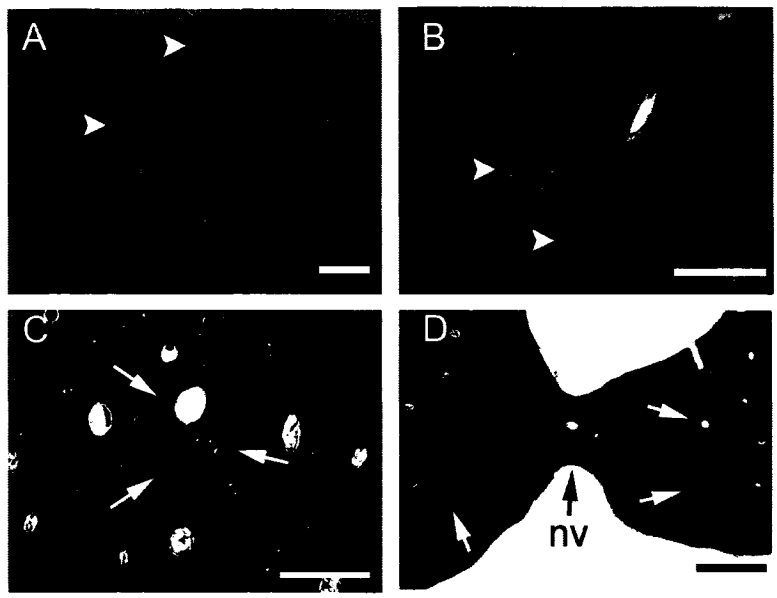

Figure 26. Histological details of a skeletally mature *Dasypus novemcinctus* osteoderm. A: The lateral margin of osteoderm (top of image) consists of Sharpey fibre bone, with many collagen fibre bundles in tension (white arrowheads) oriented parallel to one another. Deeper into the osteoderm (bottom of image), the bundles are more randomly oriented. Masson's trichrome. Scale bar = 200 μm. B: Nested in amongst the collagen fibre bundles (white arrowheads) are numerous osteocytes (with rounded morphologies) and primary osteons. Masson's trichrome. C: Deep within the osteoderm, the bony matrix has a limited number of secondary osteons (Haversian systems), characterized by the presence of scalloped resorption lines (black arrowheads). Mallory's trichome. B, C scale bars = 100 μm. D: Transverse section demonstrating the presence of secondarily deposited lamellar bone along the dorsal and ventral margins. Scalloped resorption lines (black arrowheads) are also visible. Mallory's trichome. Scale bar = 300 μm.

CHAPTER 5. DEVELOPMENT OF THE DERMAL SKELETON IN *ALLIGATOR MISSISSIPPIENSIS*, WITH COMMENTS ON OSTEODERMS

INTRODUCTION

Among craniates there are two phylogenetically independent and developmentally distinct skeletal systems: a relatively deep endoskeleton that preforms in cartilage; and a more superficial dermal skeleton (= exoskeleton, dermoskeleton) that does not (Patterson, 1977; Smith and Hall, 1990, 1993; Chapter 1). Whereas the dermal skeleton was once the predominant skeletal system, as witnessed by the all-encasing mineralized armour of many stem gnathostomes (structural-grade ostracoderms), in most modern forms it has undergone extensive reduction and modification (Romer, 1956; Moss, 1964; Zylberberg et al., 1992; Smith and Hall, 1993; Sire and Huysseune, 2003). For tetrapods, the most obvious remnants include the craniofacial skeleton (dermatocranium or desmocranium), dental tissues, and one or more elements of the pectoral apparatus. Although less common—particularly among mammals and lissamphibians—the dermal skeleton also includes bones developing within the eye (scleral ossicles), eyelid (palpebral), integument (osteoderms), and across the abdomen (gastralia). Among modern taxa, one of the most diverse collections of dermal elements is found in crocodylians.

All 23 species of extant crocodylians are characterized by a well-developed bony dermal skeleton, which, while lacking scleral ossicles and clavicles, does include an interclavicle, one or more pairs of palpebrals, numerous parasagittally arranged postcranial osteoderms, an articulating set of gastralia, and a robust dermatocranium defining the face, orbit, palate, temporal-vault region, and mandible (Table 3; see below). As in most vertebrates, the dermatocranium is the primary determinant of skull morphology, and hence a major source of phylogenetic data (Rieppel, 1993a). In a recent phylogenetic evaluation of living and fossil alligatoroid crocodylians (alligators and caiman), 48% (n = 79) of 164 characters employed, at least in part, the dermatocranium (Brochu, 1999).

Appropriate to the long standing interest in crocodylian anatomy, as the closest living relatives of birds and a convenient structural/biomechanical analogue of many fossil tetrapods, development and ontogeny of the skeleton has been the subject of numerous investigations (e.g., Parker, 1883; Meek, 1911; Shiino, 1914; Mook, 1921a; de Beer, 1937; Deraniyagala, 1939; Kesteven, 1957; Müller, 1967; Iordansky, 1973; Dodson, 1975; Bellairs and Kamal, 1981; Ferguson, 1981, 1984, 1985; Westergaard and Ferguson, 1986, 1987, 1990; Müller and Alberch, 1990; Klembara, 1991, 2001, 2004, 2005; Rieppel, 1993b). To date however, this work has primarily focused on aspects of the endoskeleton, viz. the chondrocranium, splanchnocranium, and limbs. Studies of the dermal skeleton have been limited to either the pattern and sequence of bone formation (e.g., Parker, 1882; Rieppel, 1993b), or targeted accounts of particular elements (e.g., postparietal: Klembara, 2001). As for most non-avian reptiles, comparatively few details are known about crocodylian dermal skeletogenesis and posthatching skeletal tissue ontogeny (de Ricqlès et al., 1991).

This investigation explores dermal skeleton development in *Alligator mississippiensis*, the American alligator. As development of the dentition (Westergaard and Ferguson, 1986, 1987, 1990), parasphenoid (Klembara, 1993), postparietal (Klembara, 2001), and interclavicle (Chapter 4) have been described elsewhere, the present study concentrates on documenting the remaining dermatocranial elements (Table 3), along with gastralia and osteoderms. The purpose of this study is to analyze, in detail, the pattern, sequence, and mode of dermal skeletogenesis in *A. mississippiensis*, as a representative non-avian reptile, from the embryonic period to posthatching

METHODS AND MATERIALS

The majority of *Alligator mississppiensis* specimens employed in this study were collected from the Rockefeller Wildlife Refuge, Grand Chenier, Louisiana, during the summer of 2002. Several additional embryos, also from the Rockefeller Wildlife Refuge (collected in the summers of 1987 and 1988), were kindly donated by Dr. G. B. Müller (University of Vienna). Eggs were collected from the nests of wild populations and incubated in boxes containing nesting media at 30°C and 90-95% humidity. All embryos were morphologically staged according to the Normal Table of Development of Ferguson

(1985, 1987). For *A. mississppiensis*, as for many reptiles (including birds), oviposition occurs when eggs are at a relatively advanced stage of embryogenesis (Billett et al., 1985). Furthermore, rate of development is highly dependent on ambient temperature and environmental conditions (Ferguson, 1985; Hall and Miyake, 2000). Hence, staging embryos permits more accurate comparisons between individuals than would be achieved by the use of absolute time alone. In addition to embryos, several hatchlings and subadults were dissected and select elements were processed for whole-mount histochemistry (see below). Dried skeletal material, representing multiple subadults and adults were also examined (Appendix 1). In addition, staged and serially sectioned embryos from the collection of Prof. M. W. J. Ferguson (University of Manchester) were consulted (Ferguson, 1981; see also Westergaard and Ferguson, 1986).

Anatomical terminology follows Brochu (1999; dermatocranium), Claessens (2004; gastralia), Klembara (1991; chondrocranium). Taxonomic nomenclature (e.g., Crocodylia) follows Brochu (2003).

HISTOLOGY AND HISTOCHEMISTRY

All embryos were fixed in 10% neutral buffered formalin and stored in 70% ethanol prior to histological analysis. Multiple individuals representing Ferguson (1985, 1987) stages (FS) 15-23 (Appendix 5.1) were processed for whole-mount clearing and staining with Alizarin red for calcified structures (mineralized with calcium salts; most commonly bone), alone or in combination with, Alcian blue for tissues rich in glycosaminoglycans (GAGs; characteristic of the extracellular matrix [ECM] of cartilage and, to a lesser extent, of osteoid), following the protocol of Klymkowsky and Hanken (1991). Whole-mount preparations included complete (albeit eviscerated) embryos, isolated heads, pectoral, and pelvic regions, and hemisectioned heads. For each hemisectioned head, the left half was single stained with Alizarin red while the right half was double stained with Alizarin red and Alcian blue. This permitted multiple views of the developing skeleton to be visualized in three-dimensions. In addition to embryos, cranial and postcranial materials including gastralia, osteoderms, palpebrals, and portions of the skull, from several subadults were also processed for whole-mount histology, to evaluate the progression of mineralization during posthatching development.

Various histological techniques were employed to identify the tissue and cellular composition of the developing dermal skeleton from all embryonic stages and select subadult and adult materials. Preparation of serial sections included decalcification in Tris-buffered 10% EDTA (pH 7.0) for 5+ days (up to four weeks for subadult material), dehydration to 100% ethanol, clearing in CitriSolv (Fisher No. 22-143975) and embedding in low melting paraffin at 54^{O}C (Paraplast X-tra, Fisher No. 23-021-401). Sections were cut at 6-7 microns and mounted on Haupt's or 3-aminopropytriethoxy-silane coated slides. Following the staining protocols (see below), sections were mounted with DPX (Fluka No. 144581).

The most common connective tissue stain procedures employed were the Hall -Brunt Quadruple (HBQ) stain (Hall, 1986; Witten and Hall, 2003) and Mallory's trichrome stain (Chapter 3). Additional protocols include AC pentachrome (developed by A. Cole; Cole and Hall 2004; see also Chapter 3), Toluidine blue (Witten and Hall, 2003), Masson's trichrome stain, the Gridley method for reticulin, periodic acid-Schiff (PAS) technique (with and without removing glycogen with diatase of malt), and Verhoeff elastin stain (Presnell and Schreibman, 1997). Methods employed for the Prof. M.W.J. Ferguson embryo and histology collection are discussed in Ferguson (1981; see also Westergaard and Ferguson, 1986).

RESULTS

ADULT DERMAL SKELETON MORPHOLOGY

Detailed descriptions of adult crocodylian skeletal morphology are available elsewhere (e.g., Huxley, 1860; Miall, 1878; Mook, 1921a, b; Iordansky, 1973; Cong et al., 1998); the following is presented as a brief summary of relevant bony dermal skeleton features, with emphasis on *Alligator mississippiensis*.

Among crocodylians, the distinctive dermatocranium is elongate, dorsoventrally depressed (platyrostral), and akinetic (except at the quadrate-articular jaw joint), with undulating tooth rows, a pervasive, externally embossing pitted ornamentation (see below), and a robust osseous secondary (hard) palate (Miall, 1878; Iordansky, 1973; Busbey, 1995; Cong et al., 1998) (Fig. 27A-D). The osseous secondary palate is composed of bilateral laminae from the premaxilla, maxilla, palatine, and pterygoid (Fig.

27C); in most crocodylians, including *Alligator mississippiensis*, the vomer is not visible along the palate. Paranasal sinus cavities branch off the lengthy nasal cavity to invade the rostrum, including (unique to *Alligator* spp.) the prefrontal bone (Witmer, 1995; Brochu, 1999). The external nares are subterminal and dorsally oriented, and the internal (secondary) choanae are nested exclusively within the fused pterygoids (Parsons, 1970; Witmer, 1995). In *Alligator* spp., the external nares are subdivided by a process of the nasal bone, the internarial bar (Fig. 27A).

In addition to framing the internal choanae, the fused pterygoids are characterized by an enormous, transversely oriented, caudoventrally inclined lateral flange. Although it is frequently reported that the lateral margin of this flange is capped with cartilage (e.g., Parker, 1882; de Beer, 1937; Schumacher, 1973), this has yet to be verified histologically.

Across the superficial (external) surface of the dermatocranium (and osteoderms; see below), crocodylians develop a conspicuous pattern of bony ornamentation (osteodermic relief; Iordansky, 1973) consisting of large numbers of pits and grooves (Coldiron, 1974; de Buffrénil, 1982) (Fig. 27A, B). This rugose sculpturing is restricted to those elements interfacing with the dermis, including the premaxilla, maxilla, nasal, lacrimal, prefrontal, postorbital, jugal, frontal, parietal, postparietal, squamosal, quadratojugal, dentary, angular, and surangular. The pattern of ornamentation is dynamic, becomes emphasized with growth (Mook, 1921a; de Buffrenil, 1982), and is reminiscent of the embossed the superficial surfaces of the dermatocranium, osteoderms, and even the clavicle and interclavicle of many basal tetrapods (e.g., *Acanthostega gunnari*, temnospondyls; Coldiron, 1974; de Buffrenil, 1982; Castanet et al., 2003). In crocodylians, the interclavicle and gastralia are unornamented.

Ventrally bracing the abdomen are multiple, obliquely oriented rows of rod-like gastralia (Fig. 27E, F). Each row of gastralia consists of two medial and two lateral elements arranged as parasagittal pairs. Combined, the four elements articulate to form a chevron with the apex directed cranially. Each gastralium has a round or ovoid cross-section and tapers both proximally and distally. Whereas most are relatively thin and gracile, the caudalmost gastralia are noticeably larger and more robust. In crocodylians, the number of gastralial rows is usually eight, although some variation has been reported

(e.g., Cong et al. [1998] identified seven rows in *Alligator sinensis*; see also Chiasson, 1962; Claessens, 2004). Not uncommonly, gastralia may fuse, develop abnormal morphologies, or even fail to form (e.g., Claessens et al., 2004) (Fig. 27F). As in *Sphenodon punctatus* (the tuatara), crocodylian gastralia are embedded within the superficial layers of the M. rectus abdominis (Claessens, 2004); the last two rows also receive slips from the M. truncocaudalis and M. ischiotruncus.

Along the dorsal and dorsolateral body surfaces, from immediately caudal to the skull, past the sacral region and the base of the tail, crocodylian integument is invested with large numbers of osteoderms (Fig. 27G, H). With the exception of the palpebral (see below), osteoderms do not develop within the integument covering the skull. In *Alligator mississippiensis*, unlike other alligatorids (e.g., *A. sinensis*; Cong et al., 1998; Brochu, 1999) and many species of *Crocodylus*, osteoderms do not develop across the abdomen. Similar to gastralia, osteoderms are arranged in transverse rows. The medialmost (parasagittal) elements often articulate (but do not fuse), whereas more laterally positioned osteoderms are increasingly distant. Among sequentially adjacent rows, cranially successive osteoderms may imbricate on their caudal counterparts.

In general, crocodylian osteoderms are disc-like plates of bone, varying in size and dorsal/ventral profile (circular to ovoid and square) depending on their topographic position. Characteristically, the superficial (external) surface of each osteoderm demonstrates a similar pattern of ornamentation as previously noted for dermatocranial elements (numerous round pits), plus a point and/or keel of varying prominence (Fig. 26G). Ventrally, osteoderms are relatively unmarked except for several small foramina for passage of blood vessels and nerves. Among osteoderms that imbricate, the area of articulation has reduced ornamentation and instead develops longitudinally oriented striae suggestive of a synarthrosis. Superimposing each osteoderm is a single keratinous scale derived from the epidermis. These scales substantially augment the profile of the points and keels, particularly among the post-occipital and nuchal elements.

The pattern of osteoderm distribution, particularly along the cervical region, is taxonomically informative (Huxley, 1860; Ross and Mayer, 1983). For *Alligator mississippiensis*, the normal configuration includes two or three transverse rows of post-occipital osteoderms immediately caudal to the occiput, a distinct cluster of large

articulating elements dorsal to the cervicals (the nuchal shield), followed by a near contiguous distribution caudal to the cervical-thoracic vertebral transition. Work by Ross and Mayer (1983) demonstrated that most osteoderms caudal to the cervical region demonstrate a one-to-one relationship with the underlying vertebrae. Based on this correlation, Ross and Mayer established a scheme for numbering transverse rows of osteoderms, beginning with precaudal osteoderm row 1 (PC 1), the caudalmost transverse row situated dorsal to (and musculotendinously linked with) the caudalmost sacral vertebra. In practice, PC 1 can be identified by either palpation (it overlies the caudal edge of the iliac blades) or dissection. Transverse osteoderm rows cranial to PC 1 are numbered sequentially, with the largest nuchal shield osteoderms as PC 20 and 21 (Fig. 27H).

In many crocodylians, one or more small bony elements develop within the upper eyelid, the palpebral(s) (supraciliary/-ies) (Deraniyagala, 1939; Brochu, 1999). Similar to postcranial osteoderms, the palpebral is overlain by a single scale, and while the deep (orbital) surface is relatively unmarked, the superficial surface demonstrates an obvious pitted ornamentation (Fig. 27I). In *Alligator mississippiensis*, the palpebral is a single element with a suboval dorsal/ventral profile and, similar to other crocodylians, articulates with the prefrontal bone.

SKELETAL DEVELOPMENT PART I: PATTERN AND SEQUENCE

For the sake of convenience, the description of dermal skeleton development is split into two major sections. In the first, the pattern and sequence of skeletogenesis are described. The second investigates the mode of skeletal development at the level of histology. Within each section, each of the dermatocranium, gastralia, and osteoderms are discussed separately. A summary of the earliest onset of each dermatocranial element (as determined using serial histology) is presented in Table 3.

DERMATOCRANIUM

Preceding the development of dermal bone, pre-cartilaginous condensations representing the chondrocranium and splanchnocranium are reportedly visible beginning FS 14, concurrent with the formation of epithelial thickenings or dental placodes representing the earliest evidence of the (non-functional) dentition (Westergaard and Ferguson, 1986,

1990). By FS 16, much of the chondrocranium, splanchnocranium, sclerotic cartilages, as well as parts of the postcranium (e.g., stylopodium, zeugopodium, some of the autopodium; Müller and Alberch, 1990), are well-formed and stain positively for Alcian blue in whole-mount preparations.

FS 17 (~22-23d)

None of the dermal elements are positive for Alizarin red at FS 17. However, the angular and dentary are recognizable in whole-mount preparations as textured, weakly opaque splint-like condensations occupying positions adjacent to Meckel's cartilage (caudoventrolaterally and rostrolaterally, respectively; Fig. 28A, B). In addition, the presence of the pterygoid (Fig. 28C) and coronoid (Fig. 28D) is confirmed in serial sections, with the pterygoid positioned alongside the medial surface of the processus pterygoideus of the palatoquadrate (of the chondrocranium), and the coronoid lying caudomediolateral to Meckel's cartilage (medially adjacent to the angular). All four presumptive elements are readily identifiable as discrete condensations of osteoblasts and osteoid within the otherwise loose mesenchyme. A small condensation of osteoprogenitor cells in the initial stages of synthesizing collagen marks the earliest evidence of the maxilla (Fig. 28E). Unlike the angular, dentary, coronoid, and pterygoid, the maxillary condensation is achondral, and not positioned adjacent to any cartilaginous element. Instead the maxilla is located in close proximity to the maxillary branch of the trigeminal nerve (CN V2), various blood vessels, and the developing dentition.

FS 18 (~24-26d)

In FS 18 whole-mount preparations, the most prominent Alizarin red-positive elements are the calcified endolymphatic ducts, visible within the occipital region of the cranium. Less manifest are the white, opaque to weakly Alizarin red-positive condensations corresponding to the premaxilla, maxilla, pterygoid, angular, dentary, and coronoid. Additional elements of the orbit and mandibular series are visible in serial section (see below).

Each premaxilla is a small quadrangular condensation, restricted to the rostroventrolateral margin of the upper jaw adjacent to the lamina transversalis rostralis of the nasal capsule. At this stage, the premaxilla does not underlie the primordium of

the caruncle, nor is it directly associated with any teeth and/or dental placodes. The dental arcade continues caudally (i.e., towards the jaw joint) as the maxilla. Thin and tapering in whole-mount preparations, the maxilla is beginning to expand transversely when observed in section, corresponding with the closure of the (soft tissue) secondary palatal shelves (Ferguson, 1985). The maxilla remains closely associated with the maxillary branch of the trigeminal (CN V2) and the developing dentition at the oral epithelium. The nasal bone has yet to form.

Among the elements bounding the orbital cavity, condensations representing each of the (presumptive) prefrontal, frontal, postorbital, and jugal are identifiable in section by late FS18, and in whole-mount preparations by early FS 19. At FS 18, these elements lack characteristic morphological features, and their identity is based solely on their topographic relationship to the orbital cavity and scleral cartilage.

The largest and most complex dermal element to have developed thus far is the pterygoid (Fig. 28F). Compared with other dermal bones, growth of the pterygoid is relatively rapid, resulting in the formation of a lengthy, tapering palatine process rostrally and, at the caudal margin, the prominent lateral pterygoid flange. Continued growth of the lateral pterygoid flange has ventrally enclosed the distal end of the (cartilaginous) processus pterygoideus of the palatoquadrate. As a result, cartilage at the lateral margin of this flange is becoming rapidly overgrown. Late during FS 18, condensations representing the presumptive vomer and palatine bones develop, with the vomer nested against the ventrolateral margin of the interorbital septum and the palatine forming along the dorsolateral border of the nasopharynx.

Among the mandibular elements, the most prominent is the dentary, nested parachondrally along the rostrolateral border of Meckel's cartilage. At the opposite end of the presumptive mandible, the angular continues to develop within a distinctive, caudoventrally positioned cell-rich band. Both the dentary and angular demonstrate multiple centres of ossification. Growth of the coronoid corresponds with increased skeletogenesis of the dentary and angular. By late FS 18, the long, blade-like splenial condensation is present along the medial mandibular margin. The surangular is present as a condensation dorsal to the presumptive Meckelian fossa.

FS 19-20 (27-30d)

By FS 19, the majority of elements from the facial, orbital, palatal, and mandibular series are present. In whole-mount, most of these condensations are identifiable as white textured or weakly Alizarin red-positive condensations, and many demonstrate a characteristically pitted/fenestrated surface texture (Fig. 28G-J). The premaxilla remains restricted to the rostroventrolateral margin of the nasal capsule but has formed a conspicuous and well-mineralized ventral (oral) margin (Fig. 28H). The opposite border, the dorsolateral (ascending; Iordansky, 1973) process, is weakly mineralized and composed of radiating spicules of osteoid. The maxilla is primarily visible as a dense sliver of osteoid with multiple centres of mineralization, spanning the majority of the distance between the premaxilla to the jugal (Fig. 28H). In addition to the maxillary branch of the trigeminal nerve (CN V2), the rostralmost process of the maxilla lies adjacent to the nasal capsule; otherwise the maxilla remains distant from elements of the chondrocranium. Dorsolateral growth of the maxilla continues to be negative for Alizarin red, but is weakly visible as an osteoid sheet in both serial section and whole-mount. Neither the premaxilla nor the maxilla has developed palatal laminae, nor is there any indication of the nasal bone

Among the orbital series of elements, each of the prefrontal, postorbital, and jugal bones are visible in whole-mounts by FS 19 (Fig. 28I); the lacrimal does not appear until FS 20. The prefrontal and postorbital bones frame the orbital cavity at the rostromedial and caudomedial corners respectively. In section, the prefrontal directs a deep wedge-like medial process towards the frontal bone, although the two elements do not articulate at this time. The postorbital forms a prominent triangular aggregation, with an embayment along the rostral margin corresponding with the orbit, and three distinct apices directed towards the frontal (rostrodorsally), jugal (rostroventrally) and squamosal (caudoventrally) (Fig. 28I). Contact between the postorbital and jugal (the postorbital bar) is incomplete and unossified. The jugal is first detected in serial section at FS 19 as a weakly defined condensation. By late FS 20, the jugal has formed a conspicuous triradiate span, defining the ventral border of the orbital cavity (Fig. 28I). Characteristically, the rostral process of the jugal, the maxillary ramus, is relatively deep (dorsoventrally), with a tongue-like morphology. The two caudally directed processes—

the jugal contribution to the postorbital bar (caudaodorsally) and quadratojual process (caudoventrally)—are considerably shorter and rapidly taper. The lacrimal is the last element of the orbital series to form (FS 20), initially appearing as a delicate, web-like condensation alongside the postconcha. In section, the lacrimal is observed to develop adjacent to and encircling the (pre-existing) nasolacrimal canal.

The palatal series of elements remains dominated by the pterygoid (Fig. 28J). Rostrally, the palatal process, situated medial and parallel to the palatine, and partially roofs the nasopharyngeal duct and secondary choanae. The large and well-ossified lateral pterygoid flange has encircled the (cartilaginous) processus pterygoideus of the palatoquadrate and is directed caudoventrolaterally towards the coronoid and angular of the mandibular series. The palatine has initiated skeletogenesis forming an elongate shallowly concave (ventrally) condensation, partially encircling the dorsolateral margins of the nasal cavity proper. The rostral process of the palatine ventrally underlaps the weakly developed blade-like vomer. In section, the vomerine condensations remain closely associated with ventrolateral margin of the interorbital septum.

With the exception of the frontal bone (Fig. 28J), elements of the temporal-vault series are poorly developed. The frontal bone forms a narrow arch across the dorsomedial margin of orbit, adjacent to the taenia marginalis, thus initiating the future link between the prefrontal and the postorbital. The squamosal is present as a flat, fenestrated condensation, partially overlying the lateral margin of the otic process of the palatoquadrate and the (future) external ear (Fig. 28I). The quadratojugal is weakly visible as a thin splint situated along the rostral margin of the cartilaginous quadrate. Neither the parietal nor the postparietal are present.

Among the mandibular series, all the dermatocranial elements can be identified as textured, opaque condensations; mineralization of this region remains poor. The dentary is well-formed, particularly along the alveolar margin (Fig. 28H, K). In transverse serial sectioned preparations, the medial counterpart to the dentary, the splenial, forms a thin plate (Fig. 28L). Caudal to the splenial along the medial surface of the mandible is a large, trough-like opening providing passage for the M. intramandibularis, the Mecklian (mandibular adductor) fossa. The Mecklian fossa is framed by rod-shaped condensations of the surangular (dorsally), coronoid (cranially), and angular (ventrally).

Along with the development of the dermatocranium, FS 19 marks the earliest appearance of the gastralia (see below) and interclavicle (Chapter 3). Although detailed elsewhere, it is worth noting that the interclavicle first appears as a bilateral pair of condensations nested midventrally, at the cranial end of the pectoral apparatus.

FS 21 (31-35d)

Similar to previous stages, during early FS 21 (~31-32d) elements of the dermal skeleton are visible in whole-mount preparations as textured white opaque to weakly Alizarin positive condensations (Fig. 29A-C). However, by late FS 21 (~34-35d) most dermal bones, including gastralia (see below) and the interclavicle (Chapter 3), are easily recognizable in whole-mounted specimens. For the dermatocranium, elements encircling the oral and orbital cavities demonstrate the most robust degree of development while elements of the temporal-vault series are the most weakly represented. Many of the earliest established elements (e.g., the premaxilla, maxilla, prefrontal, pterygoid) now have a trabecular-like appearance in section: each element appears as a distinctive network of interconnecting bony and/or osteoid and chondroid bone spicules (see below).

The premaxilla and maxilla have each advanced both in terms of the degree of mineralization and overall size (Fig. 29A), but remain separate from one another and their contralateral counterparts. With continued growth, each premaxilla partially underlies the recently consolidated caruncle. In whole-mount preparations, the rostral end of the maxilla has developed numerous mineralized spicules radiating dorsally to provide the earliest skeletal reinforcement of the facial (dorsolateral) process (Fig. 29A). Palatal shelves are also in the early (i.e., non-ossified) stages of development, and, in serial section, are observed to underlap the rostral end of the palatine condensation. Caudally the maxilla tapers as a lengthy rod of bone and osteoid towards the jugal. FS 21 marks the first appearance of multinucleated osteoclasts associated with dermal bone (Fig. 29D). Within each of the premaxilla and maxilla, these large cells are frequently nested alongside the bone matrix adjacent to the developing dentition and dental lamina. Osteoclasts are also found on spicules located within the canal carrying the maxillary branch of the trigeminal nerve (CN V2) through the maxilla. Although there is no sign of the nasal bone in early FS 21 (~31-32d) whole-mounts, it is present in section as an

arched lamina of osteoid several cells thick, roofing the dorsolateral border of the nasal capsule (the tectum nasi). Laterally, the nasal is overlapped by the maxilla (Fig. 29E). By late FS 21 (~34-35d), the nasal bone is present in whole-mount specimens as a thin Alizarin red-positive plate dorsal to the rostral end of the nasal capsule. As for other scarf joints of the dermatocranium, the future zone of articulation between the maxilla and nasal is filled with a relatively dense, cell-rich, connective tissue.

Similar to the facial series, the orbital series of elements are also increasingly well-developed. By the end of FS 21, the lacrimal, prefrontal, jugal, and postorbital are all distinctly present as condensations of ossified and/or osteoid spicules along the margins of the orbital cavity (Fig. 29A, B). The prefrontal is the best developed element of the orbital series, forming a prominent Alizarin red-positive mass rostroventromedial to the eye. In transverse section, the prefrontal abuts the dorsal border of the lacrimal, overlaps the developing frontal, and pinches out caudomedial to the orbital cavity. The postorbital superimposes the area between the cartilaginous sclera of the eyeball and the dorsal process of the palatoquadrate. Contact between the jugal and squamosal, combined as the postorbital bar, is incomplete. Spanning the ventral margin of the orbital cavity, the trifurcate jugal has initiated ossification within the postorbital process and quadratojugal ramus. The rostral contact with the maxilla is observed to form a scarf joint in section (jugal overlapping maxilla; Fig. 29F). Skeletogenesis of the lacrimal bone trails that of all the other orbital series elements; it does not become Alizarin-positive until late FS 21 (Fig. 29A). In serial section, numerous osteoclasts are associated with spicules lining the nasolacrimal duct.

Among the temporal-vault series, the frontal bone is the most advanced, and by early FS 21 it forms a narrow, medially deflected and dorsoventrally arch that bridges the gap between the prefrontal and postorbital condensations (Fig. 29B). Although eventually forming the dorsal rim of the orbital cavity, at this stage the frontal remains obscured from lateral view by the relatively large sclerotic cartilage. Rostrally, the frontal bone forms a thin laminar sheet, roofing the caudal portion of the nasal capsule and underlapping the prefrontal. In a caudal direction, approaching the eye, the frontal bone tapers in cross-section to form a wedge, with well-defined (uninterrupted) medial and lateral borders adjacent to the orbit and nasal capsule, and a fenestrated dorsal

surface. Both the squamosal (laterally capping the otic process of the palatoquadrate) and quadratojugal (positioned along the rostral border of the palatoquadrate) bones are present, although neither is heavily ossified. The parietal and postparietal remain undetected.

The rostral process of the pterygoid has increased in length and, when viewed in lateral profile, the distal tip of the lateral pterygoid flange lies in the same horizontal plane as the external mandibular fenestra of the mandible. In section, each of the palatine and vomer has expanded transversely. The palatine occupies a position along the lateral border of the nasal cavity, while the vomer contributes to the roof (Fig. 29C). FS 21 marks the first appearance of the ectopterygoid, partially bridging the gap between the pterygoid and jugal. The ectopterygoid has an irregular shape, with a weakly ossified ventromedial process directed towards the lateral flange of the pterygoid, and a spade-shaped craniolateral process, forming the caudal margin of the suborbital fenestra. A third, dorsal (ascending) process, contributing to the postorbital bar, is presently unossified.

Corresponding with development of the facial and palatal series, by FS 21 the mandibular series of elements are also at a relatively advanced stage of osteogenesis (Fig. 29A). The dentary continues to demonstrate multiple centres of ossification, with more intense staining rostrally. Contralateral dentaries remain separated at the mandibular symphysis. For identification of the remaining elements, the Meckelian fossa provides a convenient landmark. The cranial margin of this opening is well-defined by the inferior (caudoventral) process of the coronoid; at this stage the superior (caudodorsal) process is unmineralized. The dorsal margin of the fossa is approximated by the position of the ossifying surangular, while the ventral border is defined by the dense, rod-like angular (Fig. 29A). The splenial is positioned cranial to the coronoid as a long, thin vertically-oriented plate.

FS 22-23 (36-45d)

At FS 22, the morphology of the dermatocranium is rapidly approaching the adult condition and superficial ornamentation is well-developed (Fig. 30A, B). All of the facial series elements, including the nasal, have become ossified and are visible in whole-mount

specimens. Dorsolateral growth and continued mineralization of the premaxilla has begun to define the rostral margin of the external naris. By FS 23 (Fig. 30C-F), caudolateral growth of the premaxilla effectively isolates the external nares from the maxilla. The premaxilla overlaps both the nasal and maxilla bones to form scarf joints. In ventral (palatal) view, the dental arcade of each premaxilla is associated with the adult complement of five teeth (at FS 23), and the palatal process has begun to ossify the rostral border of the foramen incisivum (Fig. 30F). Immediately caudal, the palatal shelves of the maxilla have also begun to ossify, and by FS 23 they have nearly eliminated the large palatal fontanelle once continuous with the foramen incisivum. The future alveolar margin of the maxilla has an undulating appearance in lateral view, and, at FS 23, is associated with as many as 19 teeth. Similar to the adult condition, the first four teeth increase in size with tooth number four as the largest. The nasal bone is increasingly ossified, roofing the majority of the tectum nasi, contributing to the caudal border of the external naris, and has initiated formation of the internarial process (Fig. 30D). Ultimately, the internarial processes of the nasal with join with counterparts from the premaxilla (as of yet undeveloped) to subdivide the paired external nares. In the sagittal plane the paired nasals all but articulate, effectively isolating a large fontanelle at the proximal end of the rostrum from the external nares. Ventrolaterally, the nasal forms a scarf joint, underlapping the maxilla, while caudally it receives the rostral process of the prefrontal within a tongue and groove contact.

The prefrontal bone remains the most robust element of the orbital series. As seen dorsolaterally, it forms the rostromedial border of the orbital cavity before tapering caudally to overlap the frontal bone (Fig. 30D). At this stage, the prefrontal bone meets the lacrimal bone along a butt joint. The lacrimal bone is becoming increasingly well-ossified, nested firmly between the prefrontal and the overlapping maxilla bones (Fig. 30A, C). The medial wall of the canal for the nasolacrimal duct is the first to ossify, by FS 22; the lateral wall is Alizarin red-positive at FS 23. Similar to early stages, osteoclasts are frequently associated with spicules lining this passage. At FS 22, two of the three jugular processes have attained adult morphology: the maxillary process (rostrally) and the postorbital process (contributing to the postorbital bar) (Fig. 30B). The quadratojugal process of the jugal does not ossify until FS 23 (Fig. 30C). The

postorbital bone articulates with the squamosal via a tongue-like process beginning in FS 22. Medially, this process creates the rostrolateral border of the supratemporal fenestra.

As for all the dermal elements defining the orbital cavity, the orbital margin of the frontal is smooth and well-ossified; distal to the orbit, ossification of the frontal is comparatively diffuse and incomplete (Fig. 30D). However, by FS 23 the paired frontal bones have fused between the orbital cavities. Along with the nasal and prefrontal, this rostral contribution partially roofs the tectum nasi. Further caudal, the contralateral frontal bones follow the contour of the orbital cavity margin and rapidly diverge, creating a large fontanelle over the brain. The quadratojugal is well-developed by FS 22 (Fig. 30B), lying lateral to the quadrate. At no time does it form the small pointed spina quadratojugalis characteristic of most crocodylians. The plate-like squamosal has an embayment along its medial border, contributing to the margin of the supratemporal fenestra. Further caudal, the parietal has only just initiated ossification along its future lateral border at FS 22. By FS 23, the parietal has expanded to the point where it defines medial boundary of the supratemporal fenestra. However, the parietal remains paired with the bilateral elements separated by a large fontanelle. FS 23 also marks the first appearance of the postparietal, demarcating the caudalmost border of the dermatocranium.

In ventral (palatal) view, the vomer remains visible at FS 22, but is obscured by growth of the palatines and merging of the maxillary palatal lamina by FS 23 (Fig.5.4F). Similarly, at FS 23 the pterygoids have fused. Continued ossification of the ectopterygoid results in a contiguous ossified margin of the suborbital fenestra.

Overall, by FS 22-23 elements of the mandibular series conform to the adult morphology (Fig. 30C), except the caudal margins of the dentary and splenial (Fig. 30E), which are incompletely ossified. Each dentary has 19 teeth, and joins with its contralateral counterpart at the mandibular symphysis. The coronoid is chrevon-shaped in FS 22 Alizarin red whole-mounts, indicating that both the superior and inferior processes are ossified. By FS 23, all of the angular, surangular, and coronoid are in articulation (Fig. 30E).

GASTRALIA

Prior to the development of gastralia, the postcranial endoskeleton, including dorsal vertebrae, pelvis, and hindlimbs, is already well-formed in cartilage. Gastralia develop within a loose mesenchyme similar to that described for the dermatocranial elements, externally adjacent to epaxial (body wall) musculature. The abdominal region is dominated by an elongate spindle-shaped cleft, the umbilicus, through which the umbilical stalk, containing coils of the intestine, associated blood vessels, and the allantois, passes.

FS 19 (~27-28d)

The first gastralia to form are the paired lateral elements from the caudalmost row, followed shortly thereafter by lateral elements of the penultimate row. These successive pairs are visible in whole-mount preparations as textured rudiments, opaque or weakly positive for Alcian blue, situated cranially adjacent to the distal end of the (strongly alcianphilic) pubis (Fig. 31A). In cross-section, these caudolateral gastralia are condensations of osteoprogenitor cells and/or osteoblasts secreting thin collagen fibres and osteoid (Fig, 31B). Each gastralium is positioned along the ventrolateral margin of the epaxial (body wall) musculature and, at least for the caudalmost elements, is associated with muscle fibres originating from the pubis (one or both of the M. truncocaudalis and M. ischiotruncus; Claessens, 2004).

FS 20-21 (~29-35d)

Gastralia develop in a caudal – cranial sequence, correlated with the relative reduction in the length of the umbilicus. By late FS 20/early FS 21 the first pair of medial gastralia appears, developing in the caudalmost row. At around this time, the lateral elements from the caudalmost row begin to ossify, as demonstrated by positive reactions for Alizarin red. By mid FS 21, there are six gastralial rows, with pairs of medial elements present in the caudalmost five (Fig. 31C). Corresponding with the sequential onset of appearance, gastralia ossification is not simultaneous.

FS 22-23 (~36-45d)

Gastralia development continues in the above described caudal and lateral to cranial and medial progression. By mid FS 22, the arrangement of the Alizarin red-positive gastralial system (at this stage consisting of six lateral and four medial elements) is beginning to resemble the articulating adult morphology. In the oldest embryos examined (two specimens at FS 23), only seven rows of gastralia were present (Fig. 31D). It remains unclear at which stage the complete complement of eight rows with four elements (two pairs) per row is developed. With the uptake of Alizarin red, variability within the gastralial system becomes apparent, including the absence of elements and skeletal malformations (Fig. 31D).

OSTEODERMS AND PALPEBRALS

Compared with all other elements of the skeleton, the onset of osteoderm and palpebral calcification is significantly delayed; neither is present in embryos or newly hatched individuals. The youngest (= smallest) individual in this study demonstrating evidence of calcified postcranial osteoderms and palpebrals was 175 mm SVL (estimated at one year in age). For osteoderms, Alizarin red-positive tissue first appears among the medialmost nuchal shield elements, rows PC 20 and 21 (Fig. 31E). Concomitant with the early calcification of the nuchal shield osteoderms is the first appearance of the mineralized palpebral. When viewed dorsally, each palpebral has a roughly ovoid profile, and is positioned at the rostral apex of the semicircular eyelid (Fig. 31F), adjacent to, but separate from, the prefrontal bone.

Among increasingly larger (= older) individuals, calcified osteoderms sequentially appear at positions caudal, lateral, and cranial (e.g., post-occipital rows PC 23-25; see Fig. 27H) to the nuchal shield. Consequently, osteoderm skeletonization does not conform to a strictly cranio-caudal sequence of development, nor is it synchronous across the integument. As a corollary, the entire developmental spectrum of osteoderm formation can be explored within a single (appropriately staged) individual.

Within each osteoderm, calcification is first observed within the keel of the presumptive element. As the individual grows, the presence of Alizarin red-positive

tissue begins to spread beyond the keel, into the substance of the remainder. For the palpebral, calcification generally continues in a caudolateral direction.

SKELETAL DEVELOPMENT PART II: OSTEOGENESIS/SKELETOGENESIS

The non-dental portion of the amniote dermal skeleton is widely considered to develop via intramembranous ossification. As will be demonstrated however, osteoderm development includes calcification of preexisting connective tissues and osteogenesis via metaplasia. Accordingly, within an individual, osteoderms—as organs—are not homogenous ossified elements. In order to highlight the diversity of hard (stiff) tissues developed in osteoderms, the term skeletogenesis is employed. As for the previous section, the mode of skeletal tissue development for each of the dermatocranium, gastralia, and osteoderms are discussed separately. A summary of the histology and histochemistry of skeletal tissues is presented in Table 4.

DERMATOCRANIAL OSTEOGENESIS

Dermatocranial osteogenensis begins early in the embryonic period, in most instances before ossification of the chondrocranium and splanchnocranium (Iordansky, 1973). Prior to dermal bone formation, the extracellular matrix (ECM) is a loose homogenous mesenchyme with many argyrophilic fibres (Gridley method; Fig. 32A), forming a reticulated meshwork, but no elastin (Verhoeff elastin stain). Included within the ECM are numerous nerves and blood vessels.

The earliest sign of dermal bone is the formation of a localized aggregation or condensation of small fibroblast-like osteoprogenitor cells and fine collagen fibres (Fig. 32B). As the population of cells within the condensation increases, centrally positioned osteoprogenitor cells begin to differentiate into larger, plumper osteoblasts, synthesizing and secreting osteoid. In serial section, both the surrounding mesenchyme and osteoid stain dark blue for Mallory's trichrome, green for AC pentachrome and Masson's trichrome, and grey with Verhoeff elastin stain. Similarly, neither the mesenchyme nor osteoid stains positive for Bismarck brown (AC pentachrome). However, unlike mesenchyme, osteoid within the condensation is weakly positive for Alcian blue (pH 2.5) in both double stained whole-mounts and in serial section (HBQ protocol), and

demonstrates weak metachromasia with Toluidine blue (pH 4.5) (Fig. 32C). Prior to ossification, the condensations are negative for Alizarin red in whole-mounts, but are weakly visible with oblique illumination as textured opaque concentrations.

Following the establishment of the osteoid-rich condensation, the presumptive element begins to manifest the adult morphology. Continued growth of the condensation occurs within a fibroblastic and collagen fibre capsule, the future periosteum, defining what has been termed the bone territory (Pritchard, 1974). Spicules of osteoid are surrounded by numerous osteoblasts (Fig. 32D-F), and organized into a ramified trabecular-like framework within the bone territory. With continued growth, some (but not necessarily all) spicules within the bony territory become engorged with clusters of cells that abruptly change their morphology from plump to hypertrophic. These very large and irregularly arranged spherical cells are tightly packed within a thin deposit of intercellular matrix (Fig. 32G, H). Morphologically, this tissue closely resembles a hypertrophic cartilage undergoing interstitial growth, with dilated cells arranged in doublets and (non-columnar) isogenous groups; furthermore cell processes/canaliculi are not readily demonstrable. However, histochemically the intercellular matrix stains identically to osteoid, although with no selective affinity for Alcian blue. This combination of chondrocytic cells in a bone matrix is characteristic of chondroid bone (Huysseune and Verraes, 1986; Huysseune and Sire, 1990; Huysseune, 2000; Gillis et al., 2006; see also Hall, 2005).

As islands of osteoid and chondroid bone within the bone territories become mineralized, the growing spicules are visualized with Alizarin red. In whole-mounts, elements at this initial stage of ossification typically appear as highly emarginated and fenestrated rudiments. In section, ossifying spicules and intercellular matrix are mottled red with most connective tissue stains (Mallory's trichrome [Fig. 32G, H], Masson's trichrome, AC pentachrome [Fig. 32I], and HBQ), and grey-black with Verhoeff elastin stain. Histologically, bone territories contain chondroid bone, osteoid, and woven bone. Woven (and chondroid) bone is weakly PAS positive, following removal of glycogen, and orthochromatic with Toluidine blue, except for the territorial (capsular) matrix of woven bone lacunae, which are metachromatic. Using the Gridley stain, ossifying elements are grey to grayish-brown, with black reticular fibres passing through the

osteoid and into the periosteum and surrounding connective tissue (Fig. 32J). Within an individual dermatocranial bone territory, the mesenchyme between adjacent spicules is composed of thin fibres positive for Alcian blue (HBQ protocol; Fig. 32F).

Shortly after mineralization begins, elements interfacing with the presumptive dermis (particularly those of the facial and orbital series) demonstrate a distinctive histo-architectural polarity. While deep bone surfaces are relatively smooth and uninterrupted, the superficial (integument) surface is often irregular with radiating and branching spicules (Fig. 32K, L). Macroscopically, these spicules combine to form the numerous pits and depressions ornamenting the dermatocranium.

Continued growth occurs as the entire element undergoes appositional (centrifugal; *sensu* Francillon-Vieillot et al., 1990) ossification, with the most obvious accumulations of osteoblasts and osteoid associated with the tips spicules along the superficial surface of the element; elsewhere osteoblasts form a continuous layer one cell thick (Fig. 32F, H, I, L). The once loose reticulation of osteoid-rich spicules and chondroid bone masses becomes increasingly robust and well-mineralized with peripherally deposited woven bone.

In some regions of the dermatocranium, the large numbers of osteoblasts and osteocytes are contrasted by the presence of multinucleated osteoclasts (with 2 to 25+ nuclei each) (Fig. 32M). Multinucleated osteoclasts are found in association with osteoid, woven bone, and chondroid bone, but unlike osteoblasts they are rarely observed along superficial surfaces of the dermatocranium. Instead, they are found at the tips of deeply (inwardly) directed spicules lining passages for large nerves (e.g., the maxillary branch of the trigeminal, CN V2), ducts (the nasal epithelium of the nasolacrimal duct), and alveolar bone (Figs. 29D, 32M).

Shortly after mineralization begins, presumptive elements have acquired the basic adult morphology, and are increasingly well-stained with Alizarin red. Although originally separate, expansion of adjacent bone territories ultimately leads to contact between the outer, fibrous portion of the periostea, giving rise to sutures (Pritchard, 1974). The innermost cell-rich (cambial) portions of periostea remain distinct and independent.

By one year posthatching, patches of lamellar bone have been deposited adjacent to the pre-existing woven and chondroid bone, giving rise to fibrolamellar architecture. Adding to the heterogeneity are numerous primary osteons, scalloped resorption lines, and deeply nested seams of bone distinctly cell-rich and weakly metachromatic (for Toluidine blue; Fig. 32N). In addition, osteocytic lacunae are surrounded by an unossified territorial matrix. Sutural contacts between adjacent elements are reinforced by dense connective tissue (Fig. 32O) that lacks both reticular fibres and elastin. The histo-architectural polarity first identified early during skeletogenesis remains, with parachondral surfaces relatively smooth and superficial rugose (Fig. 32P-Q). Multinucleated osteoclasts are absent from the superficial dermatocranial surfaces but adjacent to (and associated with) alveolar bone (Fig. 32R).

GASTRALIAL OSTEOGENESIS

Development of gastralia closely parallels that of the dermatocranium. Gastralia begin to develop shortly after the initiation of elements in the dermatocranium, concurrent with the earliest signs of interclavicle formation (Chapter 3). Similar to dermatocranial elements, gastralia begin as condensations of osteoprogenitor cells (Figs. 31B, 33A) that differentiate into larger, plumper osteoblasts and begin secreting osteoid. Early on, the condensation ECM stains similar to the surrounding mesenchyme (dark blue for Mallory's trichrome, green for Masson's trichrome), is weakly PAS positive, and negative for Bismarck brown (AC pentachrome). However, unlike mesenchyme (but similar to the pre-bone matrix of dermatocranial elements) gastralial osteoid is also metachromatic (with Toluidine blue; Fig. 33B) and weakly positive for Alcian blue in both serial section (with HBQ) and double stained whole-mount preparations.

With continued synthesis, the osteoid-rich condensations are concentrated into long, splint-like morphologies, predictive of the future bony element (see Fig. 31A). Similar to the bone territories of dermatocranial elements, each presumptive gastralium is sheathed in a fibroblastic-collagenous fibre capsule. However, unlike dermatocranial elements, gastralia do not develop branching spicules or trabecular-like frameworks; they remain as compact rods. Overall, the osteoid has many entrapped osteocytes with

spherical morphologies resembling chondroid bone tissue previously described for the dermatocranium (Fig. 33C, D).

As ossification begins, it is concentrated in the peripheral margins of the osteoid matrix. In cross-sections stained with HBQ, the cell-rich central portion of the condensation retains a weak affinity for Alcian blue, suggesting the presence of osteoid, whereas the remainder of the element is pink and less cellular, comparable with woven bone (Fig. 33C). Similarly, in Toluidine blue-stained sections, ossification is accompanied by orthochromatic staining, except for the capsular matrix of osteocytes. In subadults and adults, ossified gastralia are composed primarily of woven bone, with deposits of parallel-fibred bone present adjacent to neurovascular channels (Fig. 33E). The central core of each gastralium remains relatively cell-rich, and, conspicuously, the capsular and interterritorial matrix of this area is diffusely mineralized and metachromatic with Toluidine blue (Fig. 33F). There is no sign of cartilage associated with any of the gastralia at anytime.

OSTEODERM SKELETOGENESIS

Scalation begins early during the embryonic period (FS 19-23; Alibardi and Thompson, 2000), and thus the conformation of the integument is well established in advance of osteoderm formation. Prior to osteoderm (and palpebral) calcification, the integument (including that over the eyelid) has already matured into well structured fibrillar network, readily divisible into epidermis and dermis horizons. The epidermis is composed of a superficial stratum corneum (of variable thickness), and a single layer of cells forming the regenerative stratum germinativum. The dermis includes a stratum superficiale (superficial dermis), stratum compactum, and stratum laxum. The strata compactum and laxum combined to form the stratum profundum (the deep dermis). In section, the deep dermis adjacent to the hypodermis is composed of large diameter, tightly packed collagen fibres, organized to form highly stratified orthogonal ('herringbone') horizons. Moving distally towards the epidermis, the deep dermis grades into the looser, more poorly stratified superficial dermis. In contrast to the deep dermis, the superficial dermis is characterized by thinner fibres of collagen that appear to lack a common pattern of orientation. In addition, the superficial component of the dermis is more cellular than

deeper horizons. The entire dermis stains well with various connective tissue stains, although there is little evidence of elastin or reticular fibres. Blood vessels are observed throughout the dermis but glands are absent.

As the results obtained for both osteoderm and palpebral development are similar, they are described together. Early on, each presumptive osteoderm begins as a distinct dome of connective tissue, with elements immediately flanking the sagittal plane frequently demonstrating a midline keel and an acute cross-sectional profile. The first signs of skeletogenesis begin within the osteoderm keel or the rostromedial border of the eyelid, with the formation of dense a knot of irregular connective tissue, the osteoderm primordium (Fig. 33G, H). Notwithstanding its compact structure, this primordium is otherwise indistinguishable from the surrounding dermis: histochemically both the osteoderm/palpebral primordium and dermis have the same affinities for connective tissue stains. Interspersed within the dermis and osteoderm/palpebral primordium are fusiform fibroblast-like cells (Fig. 33H). These cells are not organized into any particular horizons nor do they aggregate to form condensations. Furthermore, there is no evidence of these cells depositing osteoid.

With continued growth, the centre of the primordium begins to calcify. Calcification proceeds radially (centrifugally), directly incorporating collagen fibres from the surrounding dermis (Fig. 33I, J). As a result, the osteoderm/palpebral primordium is securely anchored within the connective tissue matrix of the integument. At this stage of skeletogenesis, the primordium is primarily a diffusely calcified dense irregular connective tissue, lacking the consolidated histological appearance of true bone. However, similar to bone there are entrapped osteocyte-like cells within lacunae, interconnected by canaliculi (Fig. 33K) and the capsular matrix is weakly positive for Alcian blue (Fig. 33L). The boundaries of the mineralization front are discernable, but negative for the presence of reticular fibres and, as noted above, lack osteoid and cell-rich osteogenic horizons. Histochemically, the osteoderm/palpebral primordium stains similar to diffusely calcified bone with various connective tissue stains (e.g., Masson's trichrome, Mallory's trichrome; Fig. 33J, K). The territorial matrix surrounding each lacuna is unossified and weakly metachromatic with Toluidine blue; otherwise the osteoderm primordium, like the dermis, is weakly orthochromatic. The PAS reaction is

faint but positive, suggesting low amounts of carbohydrates. There is no evidence for chondroblasts/-cytes within either the dermis or the developing osteoderm.

In whole-mounted specimens, Alizarin-positive tissue is observed to spread throughout the keel, before invading the remaining substance of the (non-mineralized) osteoderm (Fig. 31E). Numerous ossified spicules radiate from the original centre of mineralization. Similar to earlier stages of osteoderm skeletogenesis, development of spicules occurs in the absence of cells phenotypically identifiable osteoblasts. The entire element remains enshrouded with a dense, irregular connective tissue that lacks argyrophilic fibres (Gridley method). Within the osteoderm, areas between the spicules are filled with an open, loose tissue that closely resembles mesenchyme.

As the osteoderm develops further, spicules anastomose and become increasingly robust, and the mineralization front spreads deeper into the surrounding dense, irregular connective tissue (Fig. 33M-N). In section, the mineralization front is defined along most of the superficial surface of the osteoderm by a thin basophilic line. However, at the apex of the keel and along the deep (proximal) margins, the basophilic line is less distinct. Merging inseparably with the calcified dense irregular connective tissue are patches of woven bone, identifiable as structurally consolidated and histochemically well-ossified (e.g., red with Mallory's trichrome, AC pentachrome, and HBQ, and grey with Verhoeff elastin stain). Throughout the osteoderm matrix (including both calcified dense irregular connective tissue and woven bone) wherever multiple lacunae are closely-spaced, the interterritorial matrix between them is mottled purple with Toluidine blue (Fig. 33O); otherwise the osteoderm is orthochromatic.

Among skeletally mature osteoderms, the tissue architecture and degree of matrix mineralization of is remarkably heterogeneous (Fig. 33P-R). The majority of each element is composed of an inseparable combination of woven bone and diffusely mineralized dense irregular connective tissue. The latter demonstrates variegated staining: Mallory's, red with blue mottles; AC pentachrome, red with green-grey mottles; Verhoeff's, grey with black mottles (Fig. 33P). In some areas (most commonly along the superficial surfaces of the osteoderm distal to the apex), this tissue combination has undergone resorption, as evident from the scalloped lines, and is replaced by lamellar bone (Fig. 33P). In addition, lamellar bone is also deposited around vascular channels of

the primary (and secondary) osteons. Cells in lacunae are entrenched throughout the fibrolamellar bone - calcified connective tissue matrix (Fig. 33P, Q). Notwithstanding the presence of scalloped lines, no multinucleated osteoclasts are observed.

Interspersed within the mineralized matrix are seams of unmineralized dense irregular connective tissue (Fig. 33R). Characteristically, the cells associated with these seams are more rounded and densely organized than cells throughout the remainder of the element, although this tissue does not conform to the previous described histology for chondroid bone. At the deepest surface of the osteoderm (the base), the ventral and lateral margins have many large, penetrating Sharpey fibres that pass uninterrupted into the dermis. Compared with earlier stages of skeletogenesis, the dense connective tissue encapsulating each osteoderm is relatively thin and the large collagen fibres of the dermis immediately adjacent to each osteoderm are in tension (staining red with Masson's and AC pentachrome; Flint and Lyons, 1975). Osteoderms do not demonstrate any signs of cartilage at anytime during their development (*contra* Kleister, 1992).

DISCUSSION

One of the principle aims of this study was to provide details on the pattern and sequence of crocodylian dermal element formation. To this end, serial histology and multiple whole-mounted specimens were employed, including single-stained (Alizarin red), double stained (Alizarin red and Alcian blue), and hemisectioned preparations. The results herein agree with data from other studies in demonstrating the importance of serial histology for discriminating early skeletal tissue (e.g., Haluska and Albrech, 1983; Hanken and Hall, 1988; Rieppel, 1993a, b), although it should be noted that the role of epigenetic (environmental) and/or genetic factors accelerating the rate of embryonic development (leading to the earlier observation of dermal bones) cannot be discounted (see below). The use of hemisectioned heads permitted a controlled comparison of single (Alizarin red) versus double (Alizarin red and Alcian blue) whole-mount staining methods. Each method was found to have distinct advantages: once ossification is initiated, single stained specimens demonstrate a greater affinity for Alizarin red than double stained specimens, suggesting that omission of Alcian blue, which includes glacial acetic acid as a solvent and fixative, removes a source of decalcification.

However, prior to mineralization, opaque (Alizarin red-negative) condensations are easier to visualize against the Alcian blue-positive endoskeleton of double stained materials. In addition, double stained specimens provide topographic details (i.e., the relationship of dermal elements to the endoskeleton) unavailable on single stained specimens.

PATTERN OF DERMAL SKELETOGENESIS

DERMATOCRANIUM

Among components of the dermal skeleton, the dermatocranium is the best known and most widely studied. The basic pattern and sequence of dermatocranial element formation reported in this study corresponds well with previous efforts (e.g., de Beer, 1937; Bellairs and Kamal, 1981; Klembara, 1991; Rieppel, 1993b). Minor differences, where noted, relate to the developmental stage at which the earliest onset is observed based on serial histology (Table 3). As the study of Rieppel (1993b) provides the most comprehensive overview of staged patterns of ossification in *Alligator mississippiensis*, this will form the bulk of the comparative discussion. Other comparisons will be made where relevant.

Among the facial series of elements, the sequential pattern of development reported here, viz. maxilla (FS 17) > premaxilla (FS 18) > nasal (FS 21), is the same as that recorded by Rieppel (1993b; Table 3), although he consistently observed each element one Ferguson developmental stage later. Early formation of the maxilla (at early FS 18) and premaxilla (at mid FS 18) was also noted by Westergaard and Ferguson (1990). The earliest detection of the nasal bone comes from the work of Klembara (1991), at FS 20. It is also worth noting that formation of the internarial bar, a synapomorphy of *Alligator* spp., begins at FS 22; previous work had suggested that most crocodylians were nearly identical until FS 24 (Ferguson, 1987).

Combined with the palatal series, the premaxilla and maxilla produce the osseous secondary palate. The functional importance of this structure is reflected in the early onset of formation noted for all the participating elements: pterygoid (early FS 17) > maxilla (late FS 17) > premaxilla, palatine, and (underpinning the configuration) vomer (FS 18). The early formation of the pterygoid noted here also corresponds with observations by Müller (1967) on *Crocodylus cataphractus*. The last palatal series

element to develop is the ectopterygoid, recorded here at FS 21, although Klembara (1991) has detected it as early as FS 20. With the exception of the pterygoid (identified at FS 18) Rieppel (1993b) did not record other palatal series elements prior to FS 21. The results obtained here for the onset of orbital series elements were also dissimilar to those of Rieppel (1993b). Whereas Rieppel (1993b) reported that all the elements developed at or around FS 20, this study observed a staggered onset of development: prefrontal and postorbital (FS 18) > jugal (late FS 18) > lacrimal (FS 20).

Matching the dentigerous elements of the upper jaw, and correlating with the previous development of the dentition (FS 15; Westergaard and Ferguson, 1990), the dentary also develops early during embryogenesis (at FS 17). The sequence of onset for the mandibular series is: angular, dentary, and coronoid (FS 17) > splenial (FS 18) > surangular (FS 19). The sequence documented by Rieppel (1993b) is: angular (FS 18) > dentary and surangular (FS 19) > splenial (FS 21). Confirming the results presented here, Westergaard and Ferguson (1990) also detected the dentary at FS 17.

As a group, the temporal-vault series includes many relatively late forming elements. The recorded succession is: frontal (FS 18) > squamosal and quadratojugal (FS 19) > parietal (FS 22). A comparable order (albeit with a delayed onset) was noted by Rieppel (1993b): frontal (FS 20) > squamosal and quadratojugal (FS 21) > parietal (FS 23). The parasphenoid reportedly begins to ossify at FS 20 (Klembara, 1991) while the postparietal is not present until FS 27 (Klembara, 2001).

In common with other reptiles (e.g., avian *Gallus gallus* [Jollie, 1957; Murray, 1963; Hamilton, 1965]; squamates *Elaphe obsoleta* [Haluska and Alberch, 1983], *Lacerta vivipara* [Rieppel, 1992], and *Naja kaouthia* [Jackson, 2002]; and turtles *Chelydra serpentine* and *Apalone spinifera* [Rieppel, 1993c; Sheil, 2003; Sheil and Greenbaum, 2005]), the dermatocranium initiates ossification prior to the endoskeletal system, in most cases beginning with the pterygoid, dentary, angular, maxilla, and premaxilla. For *Alligator mississippiensis*, there is a convenient relationship between the early develop of tooth-bearing elements (at FS 17-18) and the previously established dentition (at FS 14; Westergaard and Ferguson, 1986, 1990). A similar association almost certainly holds true for other reptiles, including (edentulous) avians and turtles. The ancestors of each of avians and turtles (whether it be a member of Proganosauria or

Diapsida; see Chapter 2) display a well-developed dentition. In addition, at least for avians, experimental studies have demonstrated that the early steps in the signaling pathways for tooth development are retained, even though true teeth are never expressed (Chen et al., 2000). Similarly, the early formation of the pterygoid may relate to the prominence of this element among basal reptiles (Rieppel, 1993a), as well as its' current role as a major attachment point for jaw adductors. Although the relationship is less clear, the uncommonly early formation of the coronoid in *A. mississippiensis* (and the squamate *L. vivipara*; Rieppel, 1992) may also relate to the musculotendinous system; the coronoid is an insertion for the mandibular adductor tendon (= stem tendon) (Iordansky, 1973). Unlike ophidians and turtles, the ectopterygoid and parietal of *A. mississippiensis* are some of the last elements to develop.

GASTRALIA

With the exception of *Sphenodon*, among modern taxa the development of discrete, articulating gastralia is unique to crocodylians; the homologue of gastralia in turtles, the hyoplastron, hypoplastron, xiphiplastron, are fused and non-movable. Whereas it has been reported that gastralia are present as early as FS 17 (Ferguson, 1987), this study was unable to identify presumptive elements until FS 19, corresponding with the onset of various elements of the dermatocranium (see above), the first appearance of the interclavicle (Chapter 3), and the regionalization of the dermis (into superficial and deep layers; Alibardi and Thompson, 2000). The initial gastralia are the lateral elements of the caudalmost row, adjacent to the pubis. Skeletogenesis then continues in a cranial and (somewhat delayed) medial sequence. This pattern of development appears to be correlated with the progressive closure ventral body wall between the pubis and the umbilical stalk, and reduction in the relative size of the umbilicus. A similar pattern of lateral to medial development permitting passage of the umbilical stalk is witnessed in the formation of the turtle plastron (Gilbert et al., 2001).

Corresponding with previous reports (e.g., Claessens, 2004), the gastralial system was observed to demonstrate variation in the number of individual elements present in each row (Fig. 31D). This variation was observed in both embryos and subadults, and included both the absence (non-formation) of individual gastralium and the asymmetrical

distribution of elements. It remains unclear if this variability has any functional implications. It is also interesting to note that gastralia do not develop secondary cartilage. As mechanically articulating dermal bones (each with its' own periosteum; Fig. 33C, D), gastralia appear to demonstrate all the necessary criteria. The unexpected absence of secondary cartilage has been noted for other non-avian reptiles, including the dermatocranium of ophidians (Murray, 1963; see also Hall, 1984).

OSTEODERMS

The pattern of osteoderm formation observed in *Alligator mississippiensis* is consistent with previous studies on structural-grade lizards (Moss, 1969; Zylberberg and Castanet, 1985; Levrat-Calviac and Zylberberg, 1986) and armadillos (Chapter 4). Osteoderms develop late during ontogeny, and are generally amongst the last skeletal elements to form. In *A. mississippiensis* the earliest sign of calcification occurs approximately one year after hatching, in the area of the presumptive nuchal shield (dorsal to the cervical vertebrae; Fig. 31E). From this craniomedial position along the dorsum, osteoderms develop caudally, laterally, and cranially (forming the post-occipital cluster). For each element, mineralization is initiated first within the keel and before spreading radially (centrifugally). Similar to postcranial osteoderms, palpebrals also develop relatively late during ontogeny.

COMPARISON OF MODE OF DERMAL SKELETOGENESIS

DERMATOCRANIUM AND GASTRALIA

Elements of the dermatocranium and the gastralia undergo a common mode of osteogenesis that is comparable with intramembranous bone formation previously noted for the interclavicle (Chapter 3), and dermal elements of other vertebrates (Pritchard, 1974; Chapter 4). Briefly, osteoprogenitor cells aggregate within a loose mesenchyme and then differentiate into osteoblasts, forming skeletal condensations. Osteoblasts of the condensation deposit seams of osteoid that may either interlace to form trabeculated networks (dermatocranial elements; Fig. 32D-F) or concentrate into rod-like splints (gastralia; Fig. 31A, C). Osteoid-rich condensations form within fibrously defined bone territories. The deposited osteoid matrix demonstrates typically affinities for connective

tissue stains (e.g., dark blue with Mallory's trichrome; Fig. 32 D, E), and is weakly positive for PAS (demonstrating carbohydrates). Although, the osteoid is always negative for Bismarck brown (AC pentachrome), early on it is weakly positive for Alcian blue (using HBQ [Fig. 32F] or in double-stained whole-mount preparations) and (weakly) metachromatic for Toluidine blue, indicating the presence of small amounts of GAG's.

Continued ossification closely resembles the osteogenic modality of the avian dermatocranium (Lengelé et al., 1996a, b). In some spicules, plump osteoblasts rapidly alter their cell morphology, becoming hypertrophic, and distribution, becoming densely packed with little intercellular matrix and no readily identifiable canaliculi or cell processes. These crowded aggregations of cells with chondrocytic morphologies closely resemble isogenous groups and doublets, thus suggesting interstitial growth prior to ossification. Conversely, the intercellular matrix is histochemically identical to bone (e.g., dark blue with Mallory's trichrome [Fig. 32G, H], weakly positive for PAS, negative for Alcian blue and Bismarck brown). For avians, the development of a cell-rich tissue histologically intermediate between classically defined bone and hypertrophic cartilage has been identified as chondroid bone (Lengelé et al., 1996a, b). A strikingly similar tissue is widespread among teleosts (Huysseune, 2000; see below). As osteogenesis in the dermatocranium continues, islands of chondroid bone become encapsulated by woven and lamellar bone matrix, ultimately persisting as cell-rich patches within the fibrolamellar bone matrix of skeletally mature individuals.

For gastralia, ossification begins in the periphery and continues medially towards the centre. Rapid appositional ossification confines chondroid bone to the core, and while interterritorial matrix is gradually deposited, this area remains distinctly cell-rich (Fgi. 33C, D). In skeletally mature gastralia, the interterritorial matrix of this central, cell-rich portion is metachromatic (with Toluidine blue; Fig. 33F) and only diffusely mineralized. Otherwise, the element is well-ossified and orthochromatic.

OSTEODERMS AND PALPEBRALS

The mode of osteoderm and palpebral skeletogenesis compares well with each other and the description provided by Moss (1969) for mineralized elements present in the integument of *Heloderma horridum*, the Gila monster. Presumptive elements begin as a

domes or thickenings of the dermis. Within the otherwise irregular arrangement of connective tissue, a dense knot of collagen fibres, the osteoderm (or palpebral) primordium, first appears (Fig. 33G, H). At no time are any phenotypically osteoblastic cells present, nor is there evidence of osteoid or a periosteum. As calcification of the primordium begins, extrinsic (pre-existing) collagen fibres from the surrounding connective tissue become progressively incorporated (Fig. 33I, J). Subsequently, patches of woven bone develop, inseparably merging with the calcified dense irregular connective tissue. The absence of osteoblastic cells and a discrete periosteum is consistent with bone formation via metaplasia (Beresford, 1981). Prior to skeletal maturation, portions of the mineralized matrix are eroded, and lamellar bone is deposited in place. In skeletally mature osteoderms, seams of unmineralized dense irregular connective tissue, having become entrapped within the advancing mineralization front, persist within the otherwise mineralized osteoderm matrix. Based on histology, histochemistry, and the pattern and mode of development, palpebrals are identified as eyelid osteoderms.

The mode of skeletogenesis described for crocodylians and structural-grade lizards osteoderms differs considerably from that recorded for the mammal *Dasypus novemcinctus* (Chapter 4). For *D. novemcinctus*, osteoderm formation begins with the formation of a condensation of numerous plump osteoblasts secreting osteoid. With continued growth, each *D. novemcinctus* osteoderm is encapsulated within a fibrous periosteum. Accordingly, the mode of osteoderm formation in *D. novemcinctus* is consistent with intramembranous ossification, closely resembling the development of dermatocranial elements.

DEVELOPMENT OF ORNAMENTATION

Similar to basal tetrapods, the crocodylian dermatocranium is characterized by an embossing pitted and grooved ornamentation. A comparable pattern of bony relief develops along the superficial (dorsal) surface of osteoderms. Based on this observed similarity, Iordansky (1973) suggested that ornamentation developed as osteoderms fused with the skull surface (although, no explanation was offer as to why osteoderms had ornamentation). The current study finds no evidence to support this hypothesis. During

development, there is no evidence of osteoderms, exclusive of the palpebrals, developing superficial to the dermatocranium. Furthermore, the pitted and grooved relief is already present prior to (postcranial) osteoderm and palpebrals formation.

An alternative hypothesis, advanced by de Buffrénil (1982), proposed that the pitted and grooved pattern represents localized resorption by osteoclasts. Although intuitively reasonable, de Buffrénil was unable to locate osteoclasts in support of her claim. Thus the identification of multinucleated osteoclasts associated with the dermatocranium (see Figs.29D, 32M, R), while not unexpected, is noteworthy. Multinucleated osteoclasts are also reported from the developing dermatocranium of murine rodents (Rice et al., 1997) and various teleosts (Sire et al., 1990). Similar to those of teleosts, in *Alligator mississippiensis*, multinucleated osteoclasts are capable of resorbing osteoid (uncalcified bone) and chondroid bone. Furthermore, it is clear that these syncytial cells regulate the shape of individual elements of the dermatocranium. However, multinucleated osteoclast distribution is restricted to passages that penetrate elements (e.g., for neurovascular bundles or ducts) and alveolar bone (Fig. 32M, R); no multinucleated osteoclasts were observed along the superficial surfaces of any dermatocranial element, gastralium, osteoderm, or palpebral. While it remains possible that mononucleated osteoclasts are present in crocodylians (and not discernable with the histochemical methods employed herein), in other vertebrates these cells are responsible for fine-scale resorption (Witten et al., 2001) and are unlikely to be responsible for the deep pitting characteristic of crocodylian ornamentation.

Development of the dermatocranial ornamentation begins early during the skull development, well in advance of palpebral and postcranial osteoderm formation. In section, the bone architecture of elements interfacing with the integument is polarized, with a highly emarginated superficial (external) surface (Fig. 32K, L, P) and a relatively smooth and uninterrupted deep (internal) surface (Fig. 32K, L, Q). Moreover, plump osteoblasts and osteoid are typically concentrated at the tips of these outwardly directed spicules (Fig. 32F), whereas the deep surface is typically associated with smaller osteoblasts reminiscent of bone lining cells.

CHONDROID BONE

Chondroid bone is common to many vertebrates, including teleosts (Huysseune and Verraes, 1986; Huysseune and Sire, 1990; Huysseune, 2000; Witten and Hall, 2003; Gillis et al., 2006), mammals (Beresford, 1981, 1993; Vinkka, 1982), and birds (Lengelé et al., 1996a, b), but hitherto considered absent from non-avian reptiles and lissamphibians. Indirect support of this hypothesis came from the observed correlation between the development of chondroid bone and secondary cartilage (Lengelé et al., 1996a). Whereas secondary cartilage is present in teleosts (Benjamin, 1990; Witten and Hall, 2003), mammals (Beresford, 1981; Tran and Hall, 1989), and birds (Murray, 1963; Hall, 1986) (see also Hall, 2001), this tissue fails to develop in non-avian reptiles and lissamphibians, even during fracture repair (Hall and Hanken, 1986; Irwin and Ferguson, 1986). In agreement with the abovementioned, no secondary cartilage was observed during this study. Perhaps unexpectedly, this included the absent of cartilage from the lateral margin of the lateral pterygoid flange (contra Parker, 1882; de Beer, 1937; Iordansky, 1973; Schumacher, 1973; Bellairs and Kamal, 1981). During embryogenesis, the pterygoid initially develops adjacent to the cartilaginous processus pterygoideus of the palatoquadrate. Rapidly however, the pterygoid overgrows its parachondral support, thus excluding this cartilage from the distal margin (contra de Beer, 1937).

In teleosts, the presence of chondroid bone is often correlated with rapid skeletal growth (Huysseune and Verraes, 1986; Huysseune, 2000; Witten and Hall, 2003; Gillis et al., 2006). It remains to be determined if this is the case for *Alligator mississippiensis*. Functionally however, the presence of isogenous cell groups within chondroid bone implies a period of interstitial growth prior to mineralization. Further consideration of this notion awaits a more rigorous assessment of mitosis (e.g., using bromodeoxyuridine [BrdU] or proliferating cell nuclear antigen [PCNA]). However, the development of chondroid bone in both *Alligator mississippiensis* and *Gallus gallus* illustrates that this tissue type is widespread among archosaurian reptiles.

THE OSTEODERM ENIGMA

As previously noted, osteoderms are common to representative members of most reptilian lineages (excluding avians), as well as some anurans and the mammalian clade Cingulata

(e.g., Moss, 1969; Ruibal and Shoemaker, 1984; Hill, 2005; Chapter 4). Although Moss (1969) originally suggested that all osteoderms are homologous, both in terms of mode of development and as structural entities, a more recent study casts (Hill, 2005) doubt on this interpretation. Hill's (2005) investigation proposed that osteoderms arose independently among at least five different lineages (Pareiasauria, Squamata, Archosauria, Placodonta, and Cingulata). In addition, postcranial osteoderms are also known from some turtles (exclusive of the carapace and plastron; e.g., the fossil form, *Proganochelys quenstedti*; Gaffney, 1990; see also Barrett et al., 2002), at least one Sphenodontidae (*Pamizinisaurus tlayuaensis*; Reynoso, 1997), a basal reptile (*Sclerosaurus armatus*; von Huene, 1912), and a basal synapsid (*Elliosmithia longiceps*; Reisz et al., 1998). Developmental data corroborates the phylogenetic pattern, at least as far as reptiles and mammals are concerned, for as noted above, the modes of skeletogenesis for the mammal *Dasypus novemcinctus* (Chapter 4) and the reptiles *Heloderma horridum* and *Alligator mississippiensis* are quite dissimilar. Unlike *D. novemcinctus*, during osteoderm development in reptiles there is no evidence of cells with an osteoblastic phenotype, no osteoid, and no periosteum (Fig. 33G-R). The initiation and continued growth of reptilian osteoderms occurs as the dermis both calcifies *in situ* and transforms into bone.

Regardless of development, skeletally mature osteoderms are not histologically uniform (Moss, 1969). In *Dasypus novemcinctus*, the adult element includes a combination of woven, lamellar, and Sharpey fibre bone (Chapter 4). In the structural-grade lizard *Anguis fragilis*, osteoderms are composed of two discrete horizons; a superficial layer of woven bone underpinned by deeper layer of lamellar bone (Zylberberg and Castanet, 1985). For both *Alligator mississippiensis* and *Heloderma horridum* (Moss, 1969), osteoderms demonstrate a broad spectrum of tissues, including woven and lamellar bone, and calcified and uncalcified dense irregular connective tissue (Fig. 32 P-R). For reptiles, presence of bone in these elements is best explained as tissue metaplasia. However, recalling the presence of calcified and uncalcified dense irregular connective tissues, it is inaccurate to refer to osteoderms as strictly metaplastic bones (*sensu* Main et al., 2005): they are not (necessarily) composed exclusively bone and they do not develop exclusive via metaplasia (e.g., the dense irregular connective tissues).

Moss (1969) sought to emphasize non-uniform histology of osteoderms by employing sclerification in lieu of ossification. Correspondingly, he considered the term osteoderm misleading. However, while Moss' argument is compelling, outright rejection of the term osteoderm is unnecessary and unlikely to be broadly embraced. Herein osteoderms are defined as a structural category of skeletal organ. However, while osteoderms are not homologous as organs between taxa, all osteoderms develop within, and remain continuous with, differentiated connective tissue of the well-structured dermis. Consequently, osteoderms share a common origin relating to latent structural and skeletogenic properties of the integument. Similar conclusions were reached by Zylberberg and Wake (1990). As such, osteoderms may be an example of what has been termed deep homology (Shubin et al., 1997; Gilbert and Bolker, 2001; Hall, 2003), with the dermis as the shared mechanism (structural foundation and a source of non-chondrogenic skeletoprogenitor cells) underlying the osteoderm phenotype.

Figure 27. *Alligator mississippiesis* adult and subadult dermal skeleton morphology. Adult cranium in dorsal (A), left lateral (B), and ventral (palatal) views, and corresponding mandible in dorsal view (D). Dorsal (A) and ventral (C) views depicting parasagittal halves the cranium only. Scale bar for A-D = 50 mm. E: Alizarin red whole-mounted gastralial system from a subadult (snout vent length = 175 mm) in ventral view, demonstrating seven of the eight articulating rows. F: Same specimen as E illustrating the relationship of between adjacent lateral and medial elements of each row. Note the absence of a lateral gastralium in the row marked with an asterisk (*). Scale bar for E = 20 mm. G: Adult osteoderms representing elements from precaudal osteoderm row (pc) 21. Scale bar for G = 30 mm. H: Dorsal view of the cervical integument from the same specimen as (E), illustrating the position of pc 16 to pc 23. I: Adult palpebral in dorsal view. Note the presence of the pitted ornamentation similar to that of the osteoderms in G. Scale bar for H, I = 10 mm.

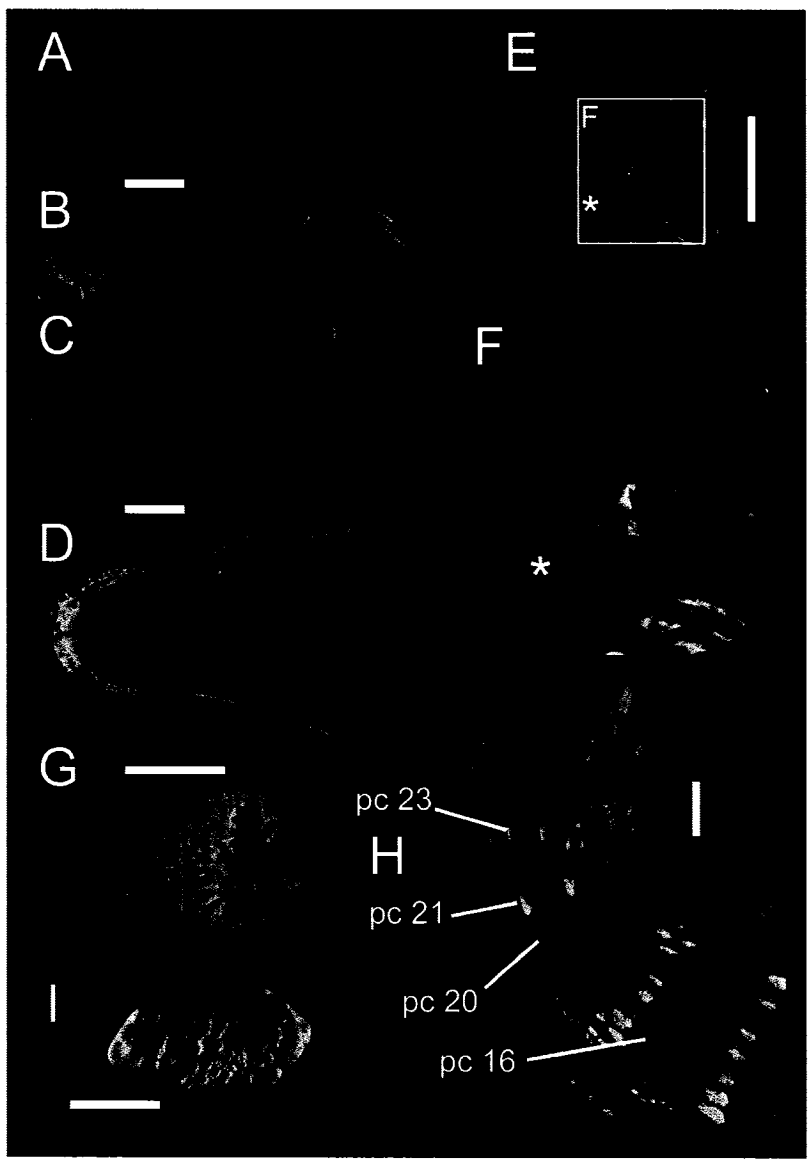

Figure 27.

Figure 28. Early development of the *Alligator mississippiensis* dermatocranium. All serial sections (A-E, K, L) cut transversely with dorsal towards the top of the image; whole-mounts (G-I) in left lateral view with cranial towards top of image; whole-mounts (F, J) in medial (parasagittal) view with cranial towards top of image. A: Ferguson stage (FS) 17 angular condensation ventrolateral to Meckel's cartilage, stained with Mallory's trichrome. B: FS 17 dentary condensation lateral to Meckel's cartilage, stained with AC pentachrome. C: FS 17 pterygoid condensation caudally adjacent to the processus pterygoideus of the palatoquadrate, stained with Mallory's trichrome. D: FS 17 coronoid condensation (small black arrow) medial to Meckel's cartilage. E: FS 17 maxilla early condensation (large black arrow) in the area of the maxillary branch of the trigeminal nerve (CN V2) (top right of image). Scale bars for A-E = 50 μm. F: FS 18 pterygoid (black arrowhead), Alizarin red single stained whole-mount. Scale bar = 1 mm. G-J: FS 19 Alizarin red and Alcian blue double stained whole-mounts of developing skull in lateral view (G), with closer views of the rostrum and mandible (H), temporal region and jaw joint (I), and a medial view of the same cranium (J). Scale bars for G-J = 5 mm. Abbreviations: an (angular), co (coronoid), dt (dentary), fr (frontal), ju (jugal), la (lacrimal), m (Meckel's cartilage), mx (maxilla), pl (palatine), pm (premaxilla), po (postorbital), pp (processus pterygoideus of the palatoquadrate), pt (pterygoid), qj (quadratojugal), sa (surangular), sp (splenial), sq (squamosal), t (tooth), vo (vomer).

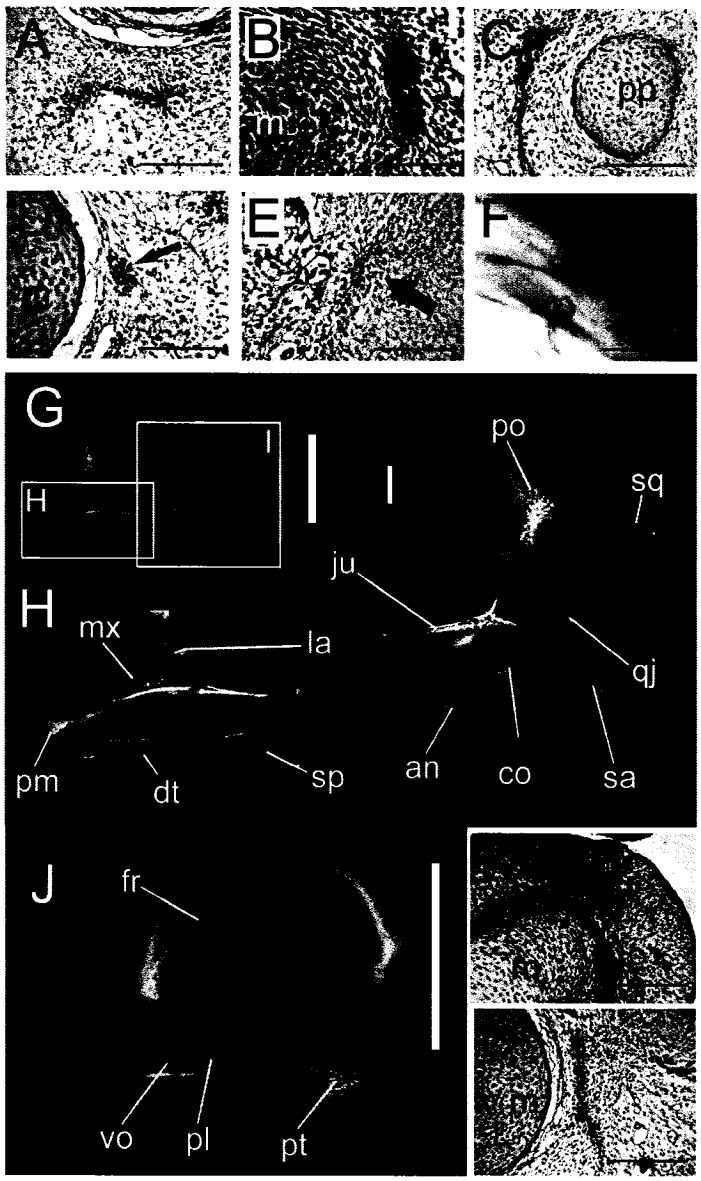

Figure 28.

Figure 29. Developing *Alligator mississippiensis* dermatocranium at Ferguson stage (FS) 21. (A-C) Alizarin red single stained whole-mount in right lateral view (A), dorsal view of orbital cavity (eyeball *in situ*) (B), and ventral (palatal) view of palate (C). Scale bar for A = 5 mm. Serial sections (D-F) cut transversely with dorsal towards the top of the image. D: Multinucleated osteoclast (black arrowhead) resorbing osteoid spicule adjacent to the developing dentition. E, F: Developing scarf joint between the nasal and maxilla (E) and maxilla and jugal (F). Scale bars for E-F = 50 μm. Abbreviations: an (angular), co (coronoid), dt (dentary), ec (ectopterygoid), fr (frontal), ju (jugal), la (lacrimal), mx (maxilla), na (nasal), pf (prefrontal), pl (palatine), pm (premaxilla), po (postorbital), ps (parasphenoid), pt (pterygoid), qj (quadratojugal) sa (surangular), sp (splenial), sq (squamosal), vo (vomer).

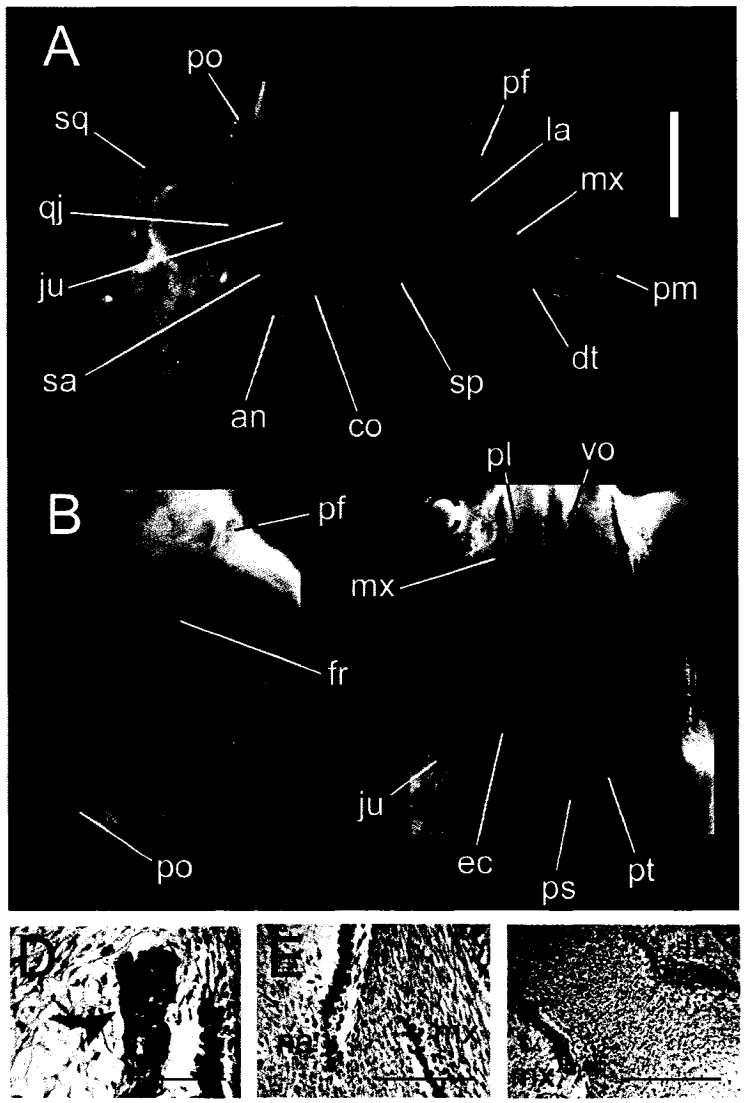
A
po
sq
pf
la
mx
qj
ju
pm
dt
sa
an
co
sp
pl
vo
B
pf
mx
fr
ju
po
ec
ps
pt
D
E
nal
mx

Figure 29.

Figure 30. Developing *Alligator mississippiensis* dermatocranium at Ferguson stages (FS) early 22 (A-B) and early 23 (C-F). Alizarin red and Alcian blue double stained whole-mounts illustrating an oblique, close-up view of the rostrum (A) and temporal-vault (B) regions. Alizarin red single stained whole-mounts illustrating a rostrolateral view (C) and dorsal view (D) of the skull, a medial view (E) of the mandible, and a ventral (palatal) view of the palate (F). Scale bar for D = 5 mm. Abbreviations: an (angular), co (coronoid) dt (dentary) eb (epibranchial), ec (ectopterygoid), fr (frontal), ju (jugal), la (lacrimal), mx (maxilla), na (nasal), pf (prefrontal), pl (palatine), pm (premaxilla), po (postorbital), ps (parasphenoid), pt (pterygoid), qj (quadratojugal), qu (quadrate), sa (surangular), sp (splenial), sq (squamosal), vo (vomer).

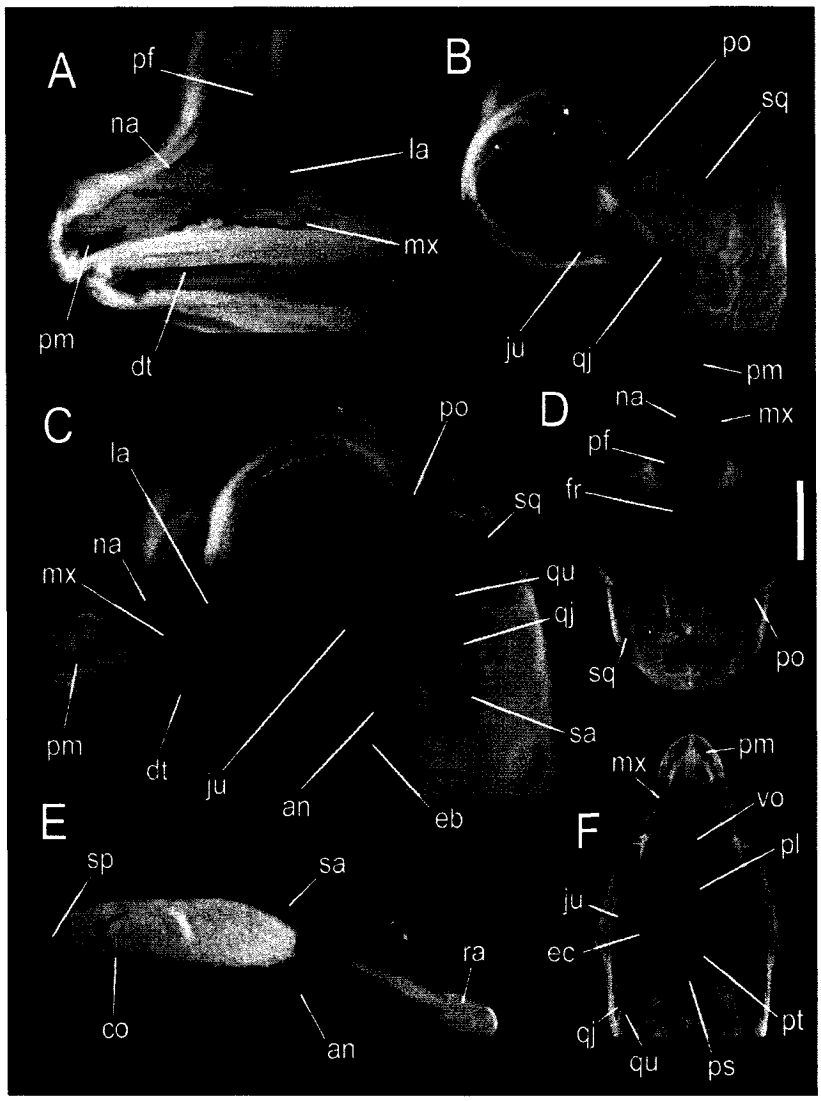
A
pf
na
la
mx
pm
dt
B
po
sq
ju
qj
pm
C
po
la
sq
na
mx
qu
qj
pm
dt
ju
an
eb
sa
D
na
mx
pf
fr
sq
po
E
sp
sa
ra
co
an
F
mx
pm
vo
pl
ju
ec
qj
qu
ps
pt

Figure 30.

Figure 31. Gastralium, osteoderm, and palpebral development in *Alligator mississippiensis*. Cranial is towards the top of the image for A, C-F. A: Ferguson stages (FS) 19 Alizarin red and Alcian blue double stained whole-mount. The first gastralium to develop is the lateral element of the caudalmost row (bottom black arrowhead), cranially adjacent to the (alcianiphilic) pubis (bottom right corner); subsequent elements develop cranially (top black arrowhead) and medially. Note the weak blue staining of the caudalmost gastralium, indicative of osteoid. Scale bar = 1 mm. B: FS 19 serial section cut transversely with dorsal towards top of image. Two sequential gastralia (black arrowheads) demonstrating the relationship of these elements to the body wall musculature. Scale bar = 70 μm. C: FS 21 Alizarin red single stained whole-mount demonstrating the development of six gastralial rows including both lateral and medial components. D: FS 23 Alizarin red single stained whole-mount in ventral view demonstrating the development of seven gastralial rows including both lateral and medial components. Note the absence of a left lateral component in the cranialmost row (top white arrow), the bifurcation of various elements, and the asymmetrical position of the gastralia identified with the bottom white arrow with asterisk. E: Subadult (snout vent length [SVL] = 175 mm) cervical integument, Alizarin red single stained whole-mount in dorsal view demonstrating the position of precaudal osteoderms (pc) 20, 21, and 23, and the overall pattern of calcification, beginning with the keel and radiating outwards. F: Subadult (SVL = 175 mm; same specimen as E) eyelid, Alizarin red single stained whole-mount in ventral view demonstrating the position of the ossifying palpebral. Scale bars for C-F = 5 mm.

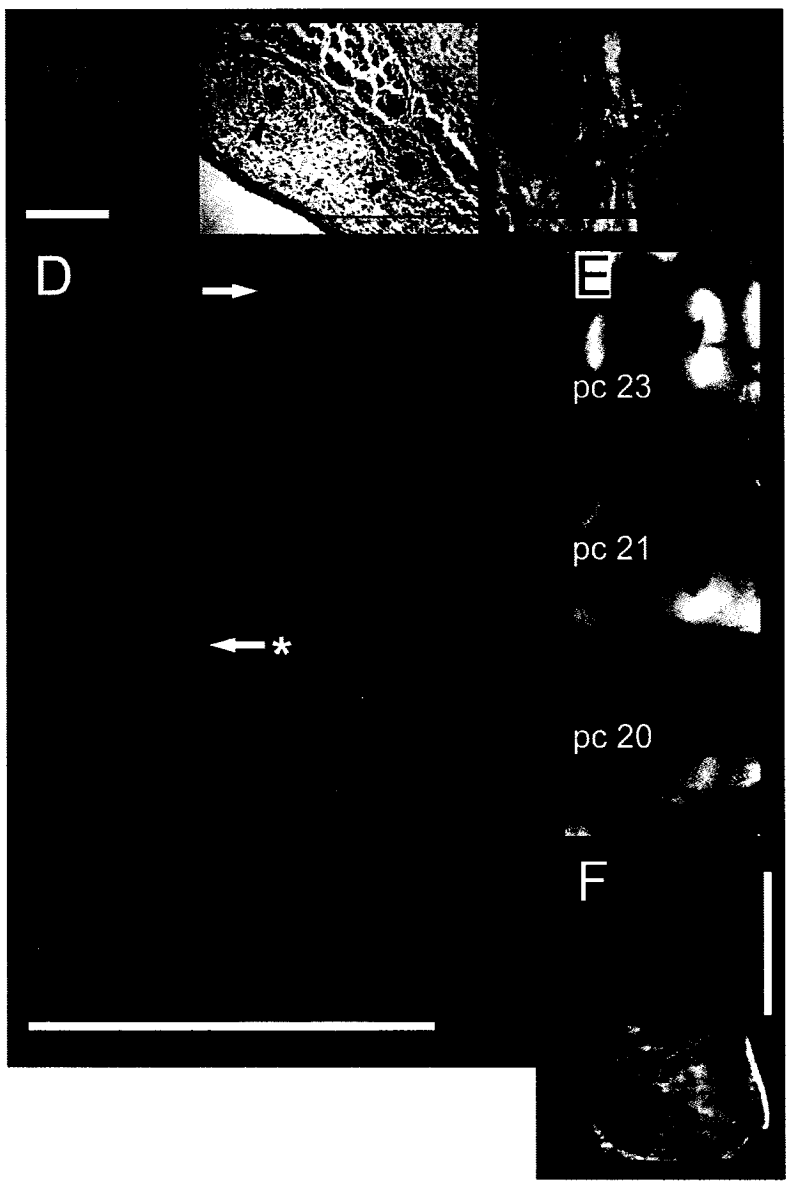

Figure 31.

Figure 32. Details of the mode of ossification and histology of the dermatocranium in *Alligator mississippiensis*. All sections with dorsal towards the top of the image. Serial sections (A, B, D, F, G, J, N-R) cut transversely; serial section (C, E, H, I, K, L, M) cut longitudinally. A: Ferguson stage (FS 16) stained with Gridley method for reticulin. Section taken from the area of the presumptive maxilla. Note the presence of many interconnected argyrophilic fibres. No dermal skeleton condensations are present at this time. B: FS 19 early vomer condensation ventrally adjacent to interorbitalcartilage (right of image), stained with Mallory's trichrome. The condensation is characterised by a growing accumulation of osteoprogenitor cells and thin collagen fibres. C: FS 18 pterygoid condensation caudally adjacent to the processus pterygoideus of the palatoquadrate (left of image), stained with Toluidine blue. Note the weak metachromatic staining of the presumptive pterygoid. Scale bars for A-C = 100 μm. D: FS 19 maxilla condensation medially adjacent to a blood vessel and the maxillary branch of the trigeminal nerve (CN V2) (right side of image), stained with Mallory's trichrome. The initial condensation is beginning to develop radiating spicules of osteoid. E: FS 19 prefrontal condensation stained with Mallory's trichrome. Scale bars for D, E = 200 μm. F: FS 20 mineralizing prefrontal spicule, stained with the Hall-Brunt Quadruple stain (HBQ). The tip of the spicule is actively growing, as demonstrated by presence of numerous osteoblasts depositing (weakly alcianiphilic) osteoid. Scale bar = 100 μm. G, H: FS 21 spicule of maxilla (G) and prefrontal (H) demonstrating the presence of large numbers of hypertrophic cells, stained with Mallory's trichrome. This cell-rich tissue is identified as chondroid bone. Note that cell density decreases in areas that have become mineralized (red). I: FS 22 section through ossifying postorbital, stained with AC pentachrome. J: FS 23 section through lacrimal, stained with Gridley method for reticulin. Various argyrophilic fibres penetrate into the surrounding extracellular matrix. Scale bars for G-J = 200 μm. K: FS 23 section through prefrontal, stained with Mallory's trichrome. Note the histo-architectural polarity, with the less interrupted ventral border (bottom of image) and radiating spicules directed dorsally (top of the image). L: FS 23 section through premaxilla, stained with Verhoeff elastin stain. This section demonstrates the early stages of histo-architectural polarity, with a less interrupted deep border (right of image) and various radiating spicules directed superficially (left of the image). Scale bars for K, L = 200 μm. M: FS 23 section through alveolar bone of the maxilla, stained with Mallory's trichrome. Multinucleated osteoclasts (black arrowheads) are often associated with remodeling the alveolar bone. Scale bar = 100 μm. N: Subadult (SVL = 195 mm) section through nasal, stained with Toluidine blue. Note the metachromatic capsular matrix surrounding most of the lacunae. In the cell-rich seam (middle of image), the interterritorial matrix is also weakly metachromatic. Scale bar = 50 μm. O: Subadult (SVL = 195 mm; same as N) section through the suture linking the angular (left) and dentary (right), stained with HBQ. Many large collagen fibres reinforce the connection between these elements. P, Q: Subadult (SVL = 195 mm; same as N) section through the angular (P) and splenial (Q), stained with AC pentachrome. Note the histo-architectural polarity of the bone, with the superficial surface of the angular (P) (interfacing with the dermis; right of image) demonstrating many radiating spicules, whereas the medial surface of the splenial (Q) (interfacing with the tissues lining the oral cavity; left of image) is smooth and unornamented. Scale bars for O- Q = 40 μm. R: Subadult (SVL = 195 mm; same as N) section through alveolar bone of the

maxilla, stained with Mallory's trichrome. Several large multinucleated osteoclasts are identified (black arrowheads). Scale bar for R = 100 μm.

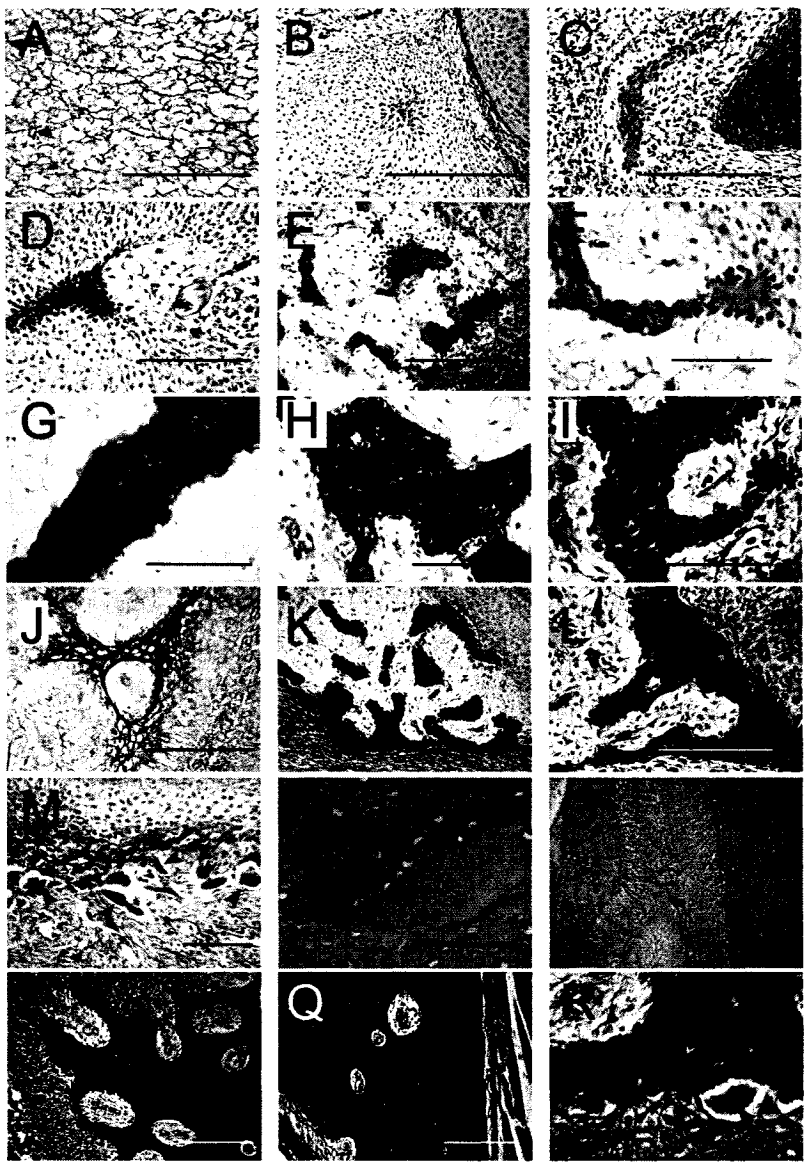

Figure 32.

Figure 33. Details of the mode of ossification and histology of gastralia (A-F), osteoderms, and palpebrals (G-R) in *Alligator mississippiensis*. All sections with dorsal towards the top of the image. Serial sections (A-J, M, R) cut transversely; serial section (K, L, O-Q) cut longitudinally. A: Ferguson stage (FS 19) gastralium condensation, stained with Mallory's trichrome. Osteoprogenitor cells are aggregating and beginning to secrete thin collagen fibres externally adjacent to the body wall musculature. B: FS 20 osteoid gastralium, stained with Toluidine blule. Note the weak metachromasia of the osteoid, particularly where lacunae are closely spaced. C: FS 21 ossifying gastralia, stained with the Hall-Brunt Quadruple stain (HBQ). Note the dense accumulation of large chondrocytic-like cells in the core of the gastralia, with weak affinities for Alcian blue; the cortex is beginning to ossify and cells are less densely arranged. Scale bars for A-C = 50 μm. D: FS 23 gastralium, stained with Mallory's trichrome. Note the large number of closely spaced cells within the core of the gastralium and the well-defined periosteum. Scale bar = 100 μm. E: Subadult (snout vent length [SVL] = 195 mm) gastralium, stained with AC pentchrome. The central canal of this image has eroded the adjacent cell-rich, poorly calcified matrix (greenish-grey). The canal is lined with newly deposited parallel-fibred bone. Woven bone surrounds the canal and poorly calcified matrix. F: Subadult (SVL = 195 mm; same specimen as E) gastralium, stained with Toluidine blue. Capsular matrix is metachromatic, as is some of the interterritorial matrix of the cell-rich, poorly calcified core region. Scale bars for E, F = 40 μm. G, H: Subadult (SVL = 175 mm) laterally (i.e., not immediately parasagittally) positioned osteoderm from precaudal row (PC) 23, stained with Masson's trichrome. The first sign of osteoderm development begins within the superficial dermis (G), with the formation of a dense knot of irregular connective tissue (H). Note the absence of phenotypically osteoblastic cells. I: Subadult (SVL = 175 mm; same as G) medially (i.e., immediately parasagittally) positioned osteoderm from PC 23, stained with AC pentachrome. Calcification (stained here as black) begins within the keel and continues to proceed radially. Scale bars for G, I = 1 mm. J: Subadult (SVL = 175 mm; same as G) medially positioned osteoderm from PC 21, stained with Masson's trichrome. Large numbers of collagen fibres pass uninterrupted into the calcified matrix, firmly securing the osteoderm within the dermis. K, L: Subadult (SVL = 195 mm) palpebral, stained with Mallory's trichrome (K) and HBQ (L). Various cells are entrapped within the mineralized matrix, surrounded by poorly mineralized, alcianiphilic, capsular matrix. Note the absence of a cell-rich osteogenic horizon and periosteum surrounding the calcifying element. Scale bars for J, K = 50 μm; scale bar for L = 40 μm. M, N: Subadult (SVL = 195 mm) medially positioned osteoderm from PC 21, stained with Mallory's trichrome. The calcified component of the osteoderm has increased in size and individual spicules are beginning to interconnect (M). Large collagen fibres continue to pass uninterrupted into the calcified matrix (N). Scale bar for M = 1 mm; scale bar for N = 40 μm. O: Subadult (SVL = 195 mm; same as K) medially positioned osteoderm from PC 21, stained with Toluidine blue. Where lacunae are closely spaced, the interterritorial matrix is weakly metachromatic. Scale bar for O = 50 μm. P-R: Adult (SVL = 1.5+ m) medially positioned osteoderm from PC 20, stained with Verhoeff elastin stain (P), HBQ (Q), and Mallory's trichrome (R). The matrix is very heterogenous, with scalloped resorption lines, parallel-fibred, lamellar, and woven, and dense irregular connective tissue. Note

the seam of unmineralized dense irregular connective tissue in R, stained here as blue. Scale bars for P-Q = 40 μm.

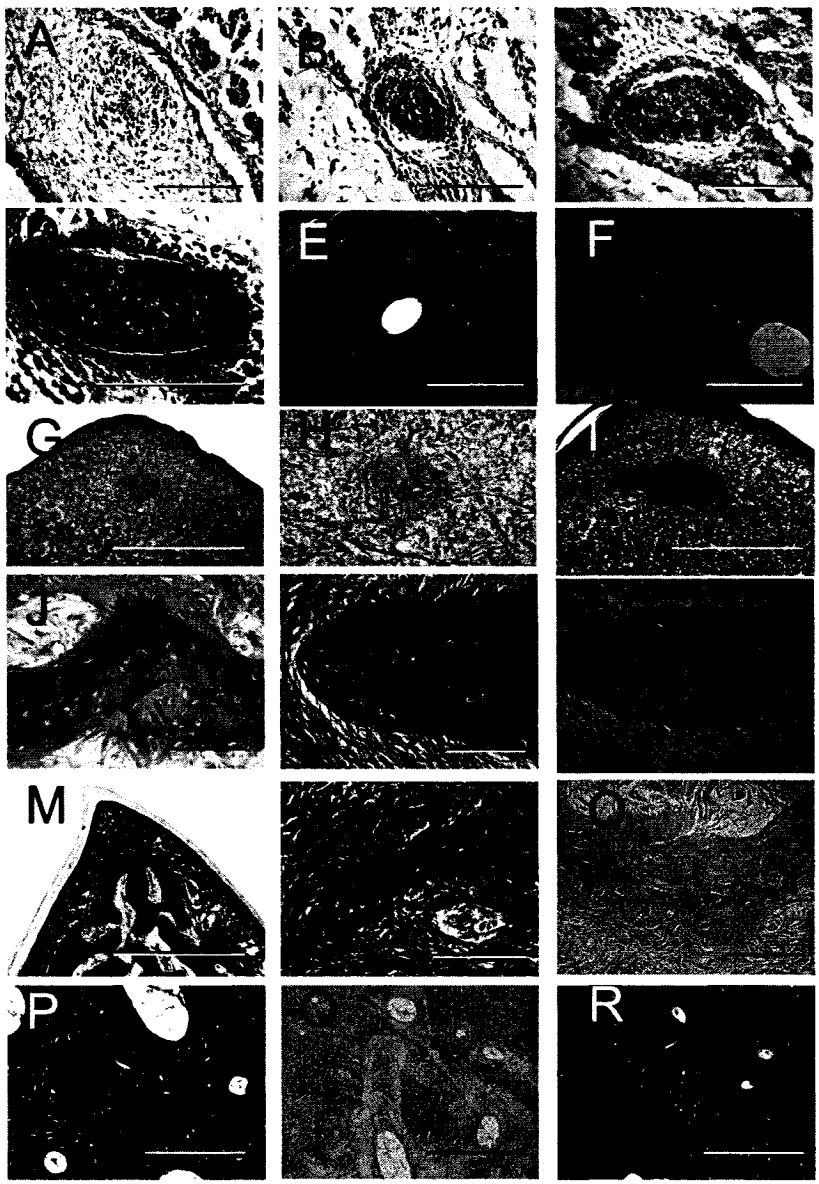

Figure 33.

Table 3. Comparison of earliest onset of osteogenesis for elements of the dermatocranium of *Alligator mississippiensis*. The results from this study, as well as the work of Klembara (1993, 2001) and Westergaard and Ferguson (1990) were obtained from serial histology; data from Klembara (1991) and Rieppel (1993b) were obtained from whole-mount preparations. See text for details. Abbreviations: FS, Ferguson (1985, 1987) Normal Table of Development stage.

Region/element	FS, this study	FS, Rieppel (1993b)	FS, other
Facial			
premaxilla	18	19	18 (Westergaard and Ferguson, 1990)
maxilla	17	18	18 (Westergaard and Ferguson, 1990)
nasal	21	22	20 (Klembara, 1991)
Orbital			
prefrontal	18	20	
lacrimal	20	20	
postorbital	18	20	
jugal	18	20	
Temporal-vault			
frontal	18	20	
parietal	22	23	
squamosal	19	21	
quadratojugal	19	21	
Palate			
vomer	18	21	
palatine	18	21	
pterygoid	17	18	
ectopterygoid	21	21	20 (Klembara, 1991)
Mandibular			
dentary	17	19	17 (Westergaard and Ferguson, 1990)
splenial	18	21	
angular	17	18	
surangular	19	19	
coronoid	17	?	

Table 4. Histology and histochemistry of skeletal tissues and the dermis of *Alligator mississippiensis*. For the purpose of comparision with the staining properties of osteoid, data from the histology/histochemistry of cartilage included.

Histological stains	Osteoid	Dermatocranium, gastralium	Osteoderm	Dermis	Cartilage	comments
Hall-Brunt Quadruple stain (Alcian blue pH 2.5)	weakly blue	red-pink	reddish pink	small fibres, colourless; large fibres, pink	blue	
Mallory's trichrome	dark blue	red with dark blue mottles; capsular matrix dark blue	red-orange with blue mottles	dark blue (red around osteoderm)	light blue	
AC pentachrome	green	red with grey mottles	red; small amounts of grey-green mottles	green (red around osteoderm)	olive green-brown	lines of resorption black
Toluidine blue (pH 4.5)	weakly purple	blue (with purple streaks); capsular matrix purple	weakly blue; capsular matrix purple	weakly blue	purple	lines of resorption deep blue
Masson's trichrome	green	red with green mottles	red; small amounts of green mottles	green (red around osteoderm)	green	
Gridley reticulin stain	n/a	grey - brown	greyish black	reticular fibres are black	grey-brown	argyrophilic fibres black
periodic acid-Schiff (PAS)	weakly pink to pink	pink	weakly pink	weakly pink to colourless	weakly pink	
Verhoeff's elastin	grey	black-grey	grey with black mottles; capsular matrix black	Grey	grey	no elastin fibres found in dermis; lines of resorption black

CHAPTER 6. CONCLUSIONS

The dermal skeleton of modern amniotes is remarkably complex in terms of the individual morphology of contributing elements, and the diversity of the contributing tissues. In addition to the dermatocranium, most amniotes develop an interclavicle and/or clavicles (or their homologues, the entoplastron and epiplastra of turtles); less common elements include gastralia, osteoderms, and palpebrals. Among the categories of tissues present in the dermal skeleton are woven, lamellar, chondroid, and Sharpey fibre bone, and calcified and uncalcified dense irregular connective tissue. Developmental studies conducted at the condensation and tissue level of this organ system provide important opportunities to address questions concerning not only the mode and pattern of element formation, but also the homology and evolution of individual components, and, by extension, the skeletal system as a whole.

In the introduction, I posed a series of questions related to the evolution and development of the dermal skeleton and pectoral apparatus. In order to summarize my work, I briefly return to each:

EVOLUTION AND DEVELOPMENT OF THE AMNIOTE PECTORAL APPARATUS

ANALYSE THE DEVELOPMENT OF THE PECTORAL APPARATUS IN AMNIOTES

The pectoral apparatus is a skeletal complex consisting of multiple elements from both the dermal and endoskeletal systems. I analyzed pectoral apparatus development at the level of the cell condensation, in order to gain a more comprehensive understanding of this compound structure. Unlike adult elements, which may fail to form or become integrated into adjacent structures, cell condensations are typically identifiable, at least temporarily, as discrete entities (Atchley and Hall, 1991; Eames et al., 2003. Consequently, it is possible to record the transient presence of elements during embryogenesis that are otherwise considered 'lost' in adults. For example, in therian mammals (marsupials + placentals), the procoracoid forms a rudiment that typically merges inseparably with the cranial end of the sternum; in skeletally mature individuals it

can not be discretely identified (Klima, 1973, 1985, 1987). Other studies have found that several of the genes responsible for patterning the coracoid are common to both mammalian and reptilian lineages (e.g., *Pax1*, *Hoxc6*; see Timmons et al., 1994; Dietrich and Gruss, 1995; Soriano, 1997; Pellegrini et al., 2001). Based on this understanding, the homology of the reptilian coracoid was reappraised (see below). Furthermore, support was found for the homology of the reptilian sternum with the acromialcoracoid ligament of turtles (Chapter 2).

READDRESS THE HOMOLOGY OF THE REPTILIAN CORACOID – IS THE REPTILIAN CORACOID HOMOLOGOUS WITH THE THERIAN CORACOID PROCESS?

Similar to monotreme mammals, the pectoral apparatus of most basal (fossil) amniotes includes two coracoid elements, a cranialmost procoracoid and caudalmost metacoracoid. Whereas for therian mammals the metacoracoid has long been accepted as the homologue of the coracoid process, among extant reptiles the metacoracoid has long been assumed lost (Romer, 1922, 1956). Herein I challenge this notion (Chapter 2). My study unequivocally supports a new conclusion: similar to the therian coracoid process, the reptilian coracoid is the homologue of the metacoracoid. In contrast, the reptilian procoracoid remains as a rudiment that is incorporated as a process of the (meta)coracoid and/or the glenoid region of the scapula early during development, prior to skeletogenesis.

REVISE THE SCENARIO OF CORACOID EVOLUTION

Drawing upon my new interpretation of coracoid homology (above; Chapter 2), I revised the scenario of coracoid evolution. I propose that changes in cell aggregation, proliferation, and differentiation, along with increases/decreases in the tempo of osteogenesis, play a major role in the evolution of the pectoral apparatus. It is hypothesized that changes in the osteogenic pattern and/or the failure of pre-skeletogenic cells to differentiate, results in the formation of sutures, thereby subdividing the once unified cell condensation giving rise to the scapulocoracoid. This results in the formation of a discrete scapula, procoracoid, and metacoracoid. In synapsids (including mammals),

cell condensations giving rise to both the procoracoid and metacoracoid are diminished. For reptiles, the procoracoid cell condensation is also lessened. In contrast, the reptilian metacoracoid remains prominent and well-formed.

DO THE FURCULA AND INTERCLAVICLE SHARE A SIMILAR TOPOLOGY, AND PATTERN AND MODE OF DEVELOPMENT (I.E., DO THE FURCULA AND INTERCLAVICLE PASS THE TEST OF SIMILARITY)?

In chapter 3, the homology of the furcula (wishbone) was reconsidered. Determination of the non-avian equivalent of the furcula is amongst the oldest documented and discussed questions in comparative anatomy. Although widely accepted as equivalent to the fused clavicles, two alternative proposals—the furcula as a neomorph or as the homologue of an element previously considered lost—have yet to be rigorously explored (Bryant and Russell, 1993). In recent years the fossil record has clearly demonstrated the presence of a furcula among non-avian theropod dinosaurs (e.g., Makovicky and Currie, 1998; Carrano et al., 2005). However, the equivalent element(s) (if any) among non-theropods remains uncertain. I investigated the competing hypotheses of furcula homology by employing Colin Patterson's (1982) three tests of homology. The observational tests of similarity and conjunction were investigated using developmental data from the crocodylian *Alligator mississippiensis* and the avian *Gallus gallus*. The test of congruence was examined using competing phylogenetic hypotheses, considering the furcula as: the homologue of the fused clavicles; the interclavicle; or as a neomorph. My study of the development of the *Alligator mississippiensis* interclavicle and *Gallus gallus* furcula illustrates that each is amongst the first skeletal elements to mineralize. For both taxa, only a single dermal element develops within the adult pectoral apparatus, situated within a comparable midventral position cranially adjacent to the sternum. Both elements begin development as a pair of condensations that initiate intramembranous ossification immediately prior to fusion. Details of the mode of ossification for both elements are similar, including identical affinities for all the histological stains employed. The interclavicle and furcula pass the test of similarity as possible homologues.

DO THE FURCULA AND INTERCLAVICLE CO-EXIST IN THE SAME ORGANISM (I.E., DO THE FURCULA AND INTERCLAVICLE PASS THE TEST OF CONJUNCTION)?

As noted above, during pectoral development, only a single dermal element is observed. I found no evidence at any time of any other dermal contribution to the pectoral apparatus. A critical examination of this literature corroborates this conclusion, and thus neither the interclavicle nor the furcula is observed to co-exist with the other at anytime during development. Hence, the interclavicle and furcula pass the test of conjunction as possible homologues.

DO THE FURCULA AND INTERCLAVICLE SHARE A COMMON PATTERN OF DESCENT, OR IS IT MORE PARSIMONIOUS TO CONSIDER THE FURCULA AS EQUIVALENT TO THE FUSED CLAVICLES, OR AS A NEOMORPH (I.E., DO THE FURCULA AND INTERCLAVICLE PASS THE TEST OF CONGRUENCE)?

My test of congruence finds that each of the neomorphic origin and furcula as the homologue of the interclavicle hypotheses to be equally parsimonious, although the results only differ by a single evolutionary step from the predominant furcula-equals-clavicles hypothesis. Hence, I find the homology of the furcula to be ambiguous. My work highlights the intricate and complicated evolution of the archosaurian pectoral apparatus and the need for continued investigation.

AMNIOTE DERMAL SKELETON DEVELOPMENT

WHAT IS THE PATTERN OF SKELETOGENESIS FOR ELEMENTS OF THE DERMAL SKELETON?

Ignoring for the moment osteoderms, my study corroborates the view that elements of the dermal skeleton develop early during embryogenesis, with most beginning ossification prior to mineralization of the endoskeleton (e.g., Iordansky, 1973; Haluska and Alberch, 1983; Rieppel, 1992, 1993b; see also Hall, 2001). As for other reptiles, my investigation

of the crocodylian dermatocranium demonstrates that circumoral elements, including the pterygoid and dentigerous elements, are amongst the first to form (Haluska and Alberch, 1983; Rieppel, 1992, 1993b; Sheil, 2003, Sheil and Greenbaum, 2005). Shortly after the onset of these dermatocranial elements, postcranial dermal elements, including the interclavicle and gastralia, initiate skeletogenesis. Ossification of the interclavicle (and the furcula) begins prior to fusion of the bilateral condensations (chapter 3). Formation of the gastralial system begins with the caudolateral element, before continuing cranially and medially (chapter 5). At present, data are lacking for the development of gastralia in other taxa, although a similar lateral-to-medial ossification sequence has been observed in the turtle plastron, homologue of the gastralial system (Gilbert et al., 2001).

DO ELEMENTS OF THE DERMAL SKELETON ARISE VIA HOMOLOGOUS DEVELOPMENTAL PROCESSES? DOES CHONDROID BONE AND/OR SECONDARY CARTILAGE DEVELOP?

Exclusive of reptilian osteoderms (see below), dermal bone initiates osteogenesis via intramembranous ossification. In addition, for many crocodylian elements, including those of the dermatocranium and gastralia, I documented the formation of chondroid bone, a tissue distinguished as having many closely packed chondrocytic-like cells in a bony (or pre-bone) matrix. Similar observations have previously been made for dermal elements of avians, mammals, and teleosts (Beresford, 1981; 1993; Huysseune and Verraes, 1986; Lengelé et al., 1996a, b; Gillis et al., 2006; see chapter 5). My study marks the first recorded presence of chondroid bone in a non-avian reptile. Functionally, at least prior to ossification, chondroid bone may permit rapid development via interstitial growth. Interestingly, I was unable to identify secondary cartilage at any stage of ontogeny examined. As a result, periosteal cells of the crocodylian dermal skeleton are either incapable of (re)differentiating into chondroblasts (i.e., they are not bipotential) or the normal developmental environment does not induce or permit such a transformation (see also Hall, 1984). With continued growth, dermal bone (including chondroid bone) and osteoid is resorbed by multinucleated osteoclasts. My studies demonstrate that the rugose ornamentation characteristic of the crocodylian dermatocranium and osteoderms

(see below) is not formed as a result of localized bone erosion by multinucleated osteoclasts—no syncytial cells were identified along the superficial bone surface (contra de Buffrénil, 1982). Instead, I documented just the opposite – that ornamentation is developed as a result of localized concentrations bone deposition by osteoblasts.

DO ALL OSTEODERMS DEMONSTRATE A SIMILAR PATTERN OF SKELETOGENESIS?

Although often overlooked, the presence of osteoderms, bony investments within the dermis, is widespread among various representative members of most major tetrapod lineages, including anurans, reptiles (such as alligators), and cingulatan mammals (such as armadillos) (Moss, 1969; Romer, 1956; Hill, 2005). In order to investigate how osteoderms develop, I used multiple specimens of the mammal *Dasypus novemcinctus*, and the crocodylians *Alligator mississippiensis*. In *D. novemcinctus*, osteoderms are organized into five discrete assemblages across the body: the head, shoulder, banded, pelvic, and tail shields. The shoulder, banded, and pelvic shields articulate to form the carapace (chapter 4; Vickaryous and Hall, 2006b). For *Alligator mississippiensis*, osteoderms form a nearly continuous (and contiguous) mosaic across the dorsal and dorsolateral body surfaces. A single osteoderm, the palpebral, develops within each *A. mississippiensis* eyelid (chapter 5). In both taxa, osteoderms demonstrate a delayed onset of development compared with the rest of the skeleton. Furthermore, osteoderm formation is asynchronous across the body, with the first elements to form situated dorsally adjacent to the cervical vertebrae. Similar findings have been reported for the structural-grade lizard *Heloderma horridum* (Moss, 1969). Broadly stated, all amniote osteoderms share a common pattern of skeletogenesis.

DO ALL OSTEODERMS ARISE VIA HOMOLOGOUS DEVELOPMENTAL PROCESSES?

Aside from the fact that all osteoderms develop within the dermis in the absence of cartilage precursors, my results demonstrate that the mode of development giving rise to these elements is not homologous among mammals and reptiles. In *Dasypus*

novemcinctus, osteoderm skeletogenesis is directly comparable with intramembranous ossification. *D. novemcinctus* osteoderms begin as a condensation of osteoblasts secreting osteoid. As development continues, each individual osteoderm develops a periosteum (see chapter 4; Vickaryous and Hall, 2006b).

In contrast, for *Alligator mississippiensis* osteoderms, there is no formation of a cell condensation, nor any cells with an osteoblastic morphology. Furthermore, *A. mississippiensis* osteoderms do not develop a periosteum. Accordingly, the mode of osteoderm development in *A. mississippiensis* is not intramembranous ossification (chapter 5). My findings indicate that where present, osseous tissue of *A. mississippiensis* arises via metaplasia, the direct transformation of the dense irregular connective tissue of the dermis into bone. Hence, not all osteoderms arise by homologous developmental processes.

ARE OSTEODERMS HOMOLOGOUS AT THE LEVEL OF THE ORGAN?

The sporadic presence of osteoderms among distantly or unrelated lineages suggests that all such elements are not homologous (Zylberberg et al., 1992; Smith and Hall, 1993; Sire and Huysseune, 2003; Hill, 2005). My developmental study corroborates this hypothesis, at least with regards to mammals and reptiles. As noted above, the mode of development differs between taxa. Furthermore, among various taxa the histological composition of osteoderms differs. For example, in my study of *Dasypus novemcinctus* (chapter 4; Vickaryous and Hall, 2006b), osteoderms were found to be composed of woven bone, lamellar bone, and Sharpey fibre bone. In contrast, for *Alligator mississippiensis* (and *Heloderma horridum*; Moss, 1969) osteoderms include woven, lamellar, and chondroid bone, and calcified and uncalcified dense irregular connective tissues (see chapter 5). Accordingly, osteoderms are not considered homologous as individual organs. However, features shared by osteoderms relate to their common origin from within the dermis, indicating that the integument maintains some structural and latent capacity for skeletal tissue formation. Thus osteoderms may represent a deep homology, sharing the dermis as a structural foundation and a source of skeletogenic cells. Furthermore, osteoderms share the process of skeletal development in the absence

of cartilage, linking these elements with the pervasive full-body external skeletons of some ancient vertebrates (see below).

The practical implications of this conclusion are medically relevant. In humans, the disease progressive osseous heteroplasia (Kaplan and Shore, 2000) is a genetic disorder characterized by uncontrolled intramembranous bone development within the dermis, hypodermis, and deeper lying connective tissues. Future studies on the genetic regulation of osteoderm formation may provide critical insights into the development of therapeutic remedies of this and many other heterotopic bone conditions.

ARE OSTEODERMS COMPONENTS OF THE DERMAL SKELETON, OR SHOULD THEY BE CLUSTERED IN AMONGST SKELETAL OUTLIERS SUCH AS MINERALIZED TENDONS?

Given their unusual distribution (taxonomic and topographic) and, at least for reptiles, mode of ossification, one might construe that osteoderms are not related to the dermal skeleton *per se*, but are purely functional/biomechanical derivatives. Based on the evidence presented herein, I argue against this statement and maintain that osteoderms are related to the broader dermal skeletal system. Although not homologous as organs, the deep homology of osteoderms within the context of the dermis connects them with the postcranial dermal plates of aquatic non-tetrapods, and ultimately the ancestral scale (Sire and Huysseune, 2003). The latent ability of the dermis to manifest (non-cartilaginous) skeletal tissue clearly requires further exploration. However, the data provided by this research provides an important and compelling foundation for continued investigation.

REFERENCES

Alibardi L, Thompson MB. 2000. Scale morphogenesis and ultrastructure of dermis during embryonic development in the alligator (*Alligator mississippiensis*, Crocodilia, Reptilia). Acta Zoologica (Stockholm) 81:325-338.

Atchley WR, Hall BK. 1991. A model for development and evolution of complex morphological structures. Biological Reviews 66: 101-157.

Barrett PM, Clarcke J, Brinkman DB, Chapman SD, Ensom PC. 2002. Morphology, histology and identification of the 'granicones' from the Purbeck Limestone Formation (Lower Cretaceous: Berriasian) of Dorset, southern England. Cretaceous Research 23:279-295.

Bellairs AdA, Kamal AM. 1981. The chondrocranium and the development of the skull in recent reptiles. In: Gans C, Parsons TS, editors. Biology of the Reptilia: volume 11. New York: Academic Press. p 1-263.

Belon P. 1555. L'Histoire de la Nature des Oyseaux, avec leurs descriptions, & naifs portraiêt retirez du naturel. Paris: Guillaume Cavellat.

Benjamin M. 1990. The cranial cartilages of teleosts and their classification. Journal of Anatomy 169:153-172.

Benton M J. 2004. Origin and relationships of Dinosauria. In: Weishampel DB, Dodson P, and Osmolska H , editors. The Dinosauria, Second Edition. Berkeley, California: University of California Press. p. 7-19.

Beresford B. 1983. Brachial muscles in the chick embryo: the fate of individual somites. Journal of Embryology and Experimental Morphology 77: 99-116.

Beresford WA. 1981. Chondroid bone, secondary cartilage and metaplasia. Munich: Urban & Schwarzenberg. 454 p.

Beresford WA. 1993. Cranial skeletal tissues: diversity and evolutionary trends. In: Hanken J, Hall BK, editors. The Skull, Volume 2: Patterns of Structural and Systematic Diversity. Chicago: University of Chicago Press. p 69-130.

Billett F, Gans C, Maderson PA. 1985. Why study reptilian development? In: Gans C, Billett F, Maderson PA, editors. Biology of the Reptilia, Volume 14, Development A. New York: John Wiley & Sons. p 3-39.

Bock WJ. 1989. The homology concept: its philosophical foundation and practical methology. Zoologische Beiträge 32: 327-353.

Brochu CA. 1999. Phylogenetics, taxonomy, and historical biogeography of Alligatoroidea. Society of Vertebrate Paleontology Memoir 6 19(2):9-100.

Brochu CA. 2001. Progress and future directions in archosaur phylogenetics. Journal of Paleontology 75(6):1185-1201.

Brochu CA. 2003. Phylogenetic approaches toward crocodylian history. Annual Reviews of Earth and Planetary Sciences 31:357-397.

Broom R. 1899. On the development and morphology of the marsupial shoulder-girdle. Transactions of the Royal Society of Edinburgh 39: 749-770.

Broom R. 1906a. Note on the lacertilian shoulder girdle. Transactions of the South African Philosophical Society 16: 373-375.

Broom R. 1906b. On the early development of the appendicular skeleton of the ostrich, with remarks on the origin of birds. Transactions of the South African Philosophical Society 16: 355-368.

Broom R. 1912. The morphology of the coracoid. Anatomischer Anzeiger 41: 625-631.

Bryant HN and Russell AP. 1993. The occurrence of clavicles within Dinosauria: implications of homology of the avian furcula and the utility of negative evidence. Journal of Vertebrate Paleontology 13: 171-184.

Burke AC. 1991a. The development and evolution of the turtle body plan: Inferring intrinsic aspects of the evolutionary process from experimental process from experimental embryology. American Zoologist 31: 616-627.

Burke AC. 1991b. Proximal elements in the vertebrate limb: Evolution and developmental origin of the pectoral girdle. In: Hinchliffe JR, Hurle J, Summerbell D, editors. Developmental Patterning of the Vertebrate Limb, volume 205. London: Plenum Press, p. 385-394.

Busbey AB. 1995. The structural consequences of skull flattening in crocodilians. In: Thomason JJ, editor. Functional Morphology in Vertebrate Paleontology. Cambridge: Cambridge University Press. p 173-192.

Camp CL. 1923. Classification of the lizards. Bulletin of the American Museum of Natural History 48: 289-482.

Camp CL. 1936. A new type of small bipedal dinosaur from the Navajo Sandstone of Arizona. University of California Publications, Bulletin of the Department of Geological Sciences 24: 39-56.

Carrano MT., Hutchinson JR, Sampson, S. D. 2005. New information on *Segisaurus halli*, a small theropod dinosaur from the Early Jurassic of Arizona. Journal of Vertebrate Paleontology 25: 835-849.

Case EC, Williston SW. 1913. A description of certain collections of bones referred to *Sphenacodon* Marsh. Carnegie Institute of Washington Publication 181: 61-70.

Castanet J, Francillon-Vieillot H, de Ricqles A, Zylberberg L. 2003. The skeletal histology of the Amphibia. In: Heatwole H, Davies M, editors. Amphibian

Biology, Volume 5: Osteology. Chipping Norton, Australia: Surrey Beatty & Sons. p 1598-1683.

Chen Y, Zhang Y, Jiang T-X, Barlow AJ, St. Amand TR, Hu Y, Heaney S, Francis-West P, Chuong C-M, Maas R. 2000. Conservation of early odontogenic signaling pathways in Aves. Proceedings of the Academy of Sciences of the United States of America 97(18):10044-10049.

Chevallier A. 1975. Role du mesoderme somitique dans le developpwment de la cage thoracique de l'embryon d'oiseau. I. Origine du segment sternal et mecanismes de la differenciation des cotes. *Journal of Embryology and Experimental Morphology* 33: 291-311.

Chevallier A. 1977. Origine des ceintures scapulaires et pelviennes chez l'embryon d'oiseau. Journal of Embryology and Experimental Morphology 42: 275-292.

Chiappe LM, Shu'an J, Qiang J, Norell MA. 1999. Anatomy and systematics of the Confusciusornithidae (Theropoda: Aves) from the Late Mesozoic of Northeastern China. Bulletin of the American Museum of Natural History 242: 1-89.

Chiasson RB. 1962. Laboratory Anatomy of the Alligator. Dubuque, Iowa: WM. C. Brown Company Publishers. 56 p.

Chinnery BJ and Weishampel DB. 1998. *Montanoceratops cerorhynchus* (Dinosauria: Ceratopsia) and relationships among basal Ceratopsians. Journal of Vertebrate Paleontology 18: 569-585.

Chuong CM, Nickoloff BJ, Elias PM, Goldsmith LA, Macher E, Maderson PA, Sundberg JP, Tagami H, Plonka PM, Thestrup-Pedersen K, Bernard BA, Schroder KR, Williams ML, Feingold KR, King LE, Kligman AM, Rees JL, Christophers E. 2002. What is the 'true' function of skin? Experimental Dermatology 11(2):159-187.

Chure DJ, Madsen JH. 1996. On the presence of furculae in some non-maniraptoran theropods. Journal of Vertebrate Paleontology 16: 573-577.

Clack JA. 2002. Gaining Ground. Bloomington, Indiana: Indiana University Press.

Claessens LPAM. 2004. Dinosaur gastralia; origin, morphology, and function. Journal of Vertebrate Paleontology 24(1):89-106.

Coates MI. 1996. The Devonian tetrapod *Acanthostega gunnari* Jarvik: postcranial anatomy, basal tetrapod interrelationships and patterns of skeletal evolution. Transactions of the Royal Society of Edinburgh 87: 363-421.

Cohn MJ, Tickle C. 1999. Developmental basis of limblessness and axial patterning in snakes. Nature 399:474-479.

Cole AC, Hall BK. 2004. The nature and significance of invertebrate cartilages revisited: distribution and histology of cartilage and cartilage-like tissues within Metazoa. Zoology 107: 261-273.

Conklin JL. 1963. Staining properties of hyaline cartilage. American Journal of Anatomy 112: 259-267.

Conrad JL. 2006. Postcranial skeleton of *Shinisaurus crocodilurus* (Squamata: Anguimorpha). Journal of Morphology 267:759-775.

Cooper MR. 1981. The prosauropod dinosaur *Massospondylus carinatus* Owen from Zimbabwe: its biology, mode of life, and phylogenetic significance. Occasional Paper, National Museum Monuments Rhodesia (Series B) 6: 689-840.

Cooper ZK. 1930. A histological study of the integument of the armadillo, *Tatusia novemcincta*. The American Journal of Anatomy 45(1):1-37.

Cope ED. 1892. On degenerate types of scapular and pelvic arch in the Lacertilia. Journal of Morphology 7: 223-244.

Craig SF, Slobodkiin LB, Wray GA, Biermann CH. 1997. The 'paradox' of ployembryony: A review of the cases and a hypothesis for its evolution. Evolutionary Ecology 11:127-143.

Daly TJM, Buffenstein R. 1998. Skin morphology and its role in thermoregulation in mole-rats, *Heterocephalus glaber* and *Cryptomys hottentotus*. Journal of Anatomy 193:495-502.

de Beer GR. 1937. The Development of the Vertebrate Skull. Oxford: Oxford University Press.

de Buffrenil V. 1982. Morphogenesis of bone ornamentation in extant and extinct crocodilians. Zoomorphology 99:155-166.

deBraga M. 2003. The postcranial skeleton, phylogenetic position, and probable lifestyle of the Early Triassic reptiles *Procolophon trigoniceps*. Canadian Journal of Earth Sciences 40: 527-556.

deBraga M, Rieppel O. 1997. Reptile phylogeny and the interrelationships of turtles. Zoological Journal of the Linnean Society 120:281-354.

Deraniyagala MA. 1939. The Tetrapod Reptiles of Ceylon, Volume I. Testudinates and Crocodilians. Colombo Ceylon: Colombo Museum of Natural History. 412 p.

Dietrich S, Gruss P. 1995. Undulated phenotypes suggest a role for *Pax1* in the development of vertebral and extravertebral structures. Developmental Biology 167: 529-548.

Dodson P. 1975. Functional and ecological significance of relative growth in *Alligator mississippiensis*. Journal of Zoology 175:315-355.

Dodson P. 2000. Origin of birds: the final solution? American Zoologist 40: 504-512.

Dollé P, Dierich A, LeMeur M, Schimmang T, Schuhbaur B, Chambon P, Duboule D. 1993. Disruption of the *Hoxd-13* gene induces localized heterochrony leading to mice with neotenic limbs. Cell 75:431-441.

Downs A. 2000. *Coelophysis bauri* and *Syntarsus rhodesiensis* compared, with comments on the preparation and preservation of fossils from the Ghost Ranch *Coelophysis* Quarry. In: Lucas SG, Heckert AB, editors. Dinosaurs of New Mexico. Albuquerque: New Mexico Museum of Natural History and Science Bulletin 17, 33-37.

Eames BF, de la Fuente L, Helms JA. 2003 Molecular ontogeny of the skeleton. Birth Defects Research (Part C) 69: 93-101.

Ede DA, Kelly WA. 1964. Developmental abnormalities in the trunk and limbs of the *talpid*^{3} mutant of the fowl. Journal of Embryology and Experimental Morphology 12: 339-356.

Elzanowski A. 1988. Ontogeny and evolution of the ratites. In: Ouellet H, editor. Acta XIX Congressus Internationalis Ornithologici, vol. II. Ottawa: University of Ottawa Press. p. 2037-2046.

Elzanowski A. 2002. Archaeopterygidae. In: Chiappe LM, Witmer LM, editors. Mesozoic Birds: Above the Heads of Dinosaurs. Berkeley, California: University of California Press. p. 129-159.

Fell HR. 1939. The origin and developmental mechanics of the avian sternum. Philosophical Transactions of the Royal Society B 229: 407-463.

Ferguson MWJ. 1981. The value of the American alligator (*Alligator mississippiensis*) as a model for research in craniofacial development. Journal of Craniofacial Genetics and Developmental Biology 1:123-144.

Ferguson MWJ. 1984. Craniofacial development in *Alligator mississippienesis*. In: Ferguson MWJ, editor. Structure, Development and Evolution of Reptiles. London: Academic Press. p 223-273.

Ferguson MWJ. 1985. Reproductive biology and embryology of the crocodilians. In: Gans C, Billett F, Maderson PFA, editors. Biology of the Reptilia, volume 14; Developement A. New York: Academic Press. p 329-491.

Ferguson MWJ. 1987. Post-laying stages of embryonic development for crocodilians. In: Webb GJW, Manolis C, Whitehead PJ, editors. Wildlife Management: Crocodiles and Alligators. Sydney: Surrey Beatty and Sons Pty Limited.

Flint MH, Lyons MF. 1975. The effect of heating and denaturation on the staining of collagen by the Masson trichrome procedure. Histochemical Journal 7:547-555.

Flower WH. 1876. An Introduction to the Osteology of the Mammalia: Being the Substance of the Course of Lectures Delivered at the Royal College of Surgeons of England in 1870. London: MacMillan and Co.

Francillon-Vieillot H, de Buffrénil V, Castanet J, Geraudie J, Meunier F, Sire J-Y, Zylberberg L, de Ricqles A. 1990. Microstructure and mineralization of vertebrate skeletal tissues. In: Carter JG, editor. Skeletal biomineralization; Patterns,

Processes and Evolutionary Trends, Volume 1. New York: Van Nostrand Reinhold. p 471-548.

Gaffney ES. 1990. The comparative osteology of the Triassic turtle *Proganochelys*. Bulletin of the American Museum of Natural History 194: 1-263.

Gans C. 1985. Biology of the Reptilia, Development A. Academic Press, New York.

Gaudin TJ, Wible JR. 2006. The phylogeny of living and extinct armadillos (Mammalia, Xenarthra, Cingulata): a craniodental analysis. In: Carrano MT, Gaudin TJ, Blob RW, Wible JR, editors. Amniote Paleobiology: Perspectives on the Evolution of Mammals, Birds and Reptiles. Chicago: University of Chicago Press. p. 153-198.

Gauthier JA. 1986. Saurischian monophyly and the origin of birds. Memoirs of the California Academy of Science 8: 1-55.

Gilbert SF, Bolker JA. 2001. Homologies of process and modular elements of embryonic construction. Journal of Experimental Zoology (Molecular and Developmental Evolution) 291:1-12.

Gilbert SF, Loredo GA, Brukman A, Burke AC. 2001. Morphogenesis of the turtle shell: the development of a novel structure in tetrapod evolution. Evolution and Development 3(2):47-58.

Gillis JA, Witten PE, Hall BK. 2006. Chondroid bone and secondary cartilage contribute to apical dentary growth in juvenile Atlantic salmon. Journal of Fish Biology 68:1133-1143.

Gladstone RJ, Wakeley CPG. 1932. The morphology of the sternum and its relation to the ribs. Journal of Anatomy and Physiology 66: 508-564.

Glenny FH. 1954. The clavicles and dorsal carotid arteries as indices of phyletic relations and levels of avian evolution. Anatomischer Anzeiger 101: 95-100.

Glenny FH, Friedmann H. 1954. Reduction of the clavicles in the Mesoenatidae, with some remarks concerning the relationship of the clavicle to flight-function in birds. Ohio Journal of Science 54: 111-113.

Glutz von Blotzheim U. 1958. Zur Morphologie und Ontogenese von Schultergurtel, Sternum und Becken von *Struthio*, *Rhea*, und *Dromiceius*. Revue Suisse de Zoologie 65(35):609-772.

Gow CE. 1972. The osteology and relationships of the Millerettidae (Reptilia: Cotylosauria). Journal of Zoology 167:219-264.

Grassé P-P. 1955. Ordre des pholidotes. In: Grassé P-P, editor. Traité de Zoologie. Paris: Masson et Cie. Vol. 17. pp 1267-1284.

Gregory WK, Camp CL. 1918. Studies in comparative myology and osteology, Part IV. Second note on the evolution of the coracoid elements in reptiles and mammals. Bulletin of the American Museum of Natural History 38:545-552.

Groβmann M, Sánchez-Villagra MR, Maier W. 2002. On the development of the shoulder girdle in *Crocidura russula* (Soricidae) and other placental mammals: evolutionary and functional aspects. Journal of Anatomy 201:371-381.

Grüneberg H. 1963. The Pathology of Development: A study of Inherited Skeletal Disorders in Animals. Oxford: Blackwell.

Hall BK. 1970. Cellular differentiation in skeletal tissues. Biological Reviews 45:455-484.

Hall BK. 1984. Developmental processes underlying the evolution of cartilage and bone. In: Ferguson MWJ, editor. The Structure, Development and Evolution of Reptiles, Symposium No 52 of the Zoological Society of London. London: Academic Press. p 155-176.

Hall BK. 1986. The role of movement and tissue interactions in the development and growth of bone and secondary cartilage in the clavicle of the embryonic chick. Journal of Embryology and Experimental Morphology 93:133-152.

Hall BK. 1998. Evolutionary Developmental Biology, second edition. Dordrecht, The Netherlands: Kluwer Academic Publishers.

Hall BK. 2001. Development of the clavicles in birds and mammals. Journal of Experimental Zoology 289:153-161.

Hall BK. 2003. Descent with modification: the unity underlying homology and homoplasy as seen through an analysis of development and evolution. Biological Reviews 78:409-433.

Hall BK. 2005. Bones and Cartilage: Developmental and Evolutionary Skeletal Biology. New York: Elsevier Academic Press. 512 p.

Hall BK, Hanken J. 1985. Repair of fractured lower jaws in the spotted salamander: do amphibians form secondary cartilage? Journal of Experimental Zoology 223:359-368.

Hall BK, Miyake T. 1992. The membranous skeleton: the role of cell condensations in vertebrate skeletogenesis. Anatomy and Embryology 186:107-124.

Hall BK, Miyake T. 2000. Craniofacial development of avian and rodent embryos. In: Tuan RS, Lo CW, editors. Methods of Molecular Biology, Volume 135: Developmental Biology Protocols, Volume 1. Totowa, New Jersey: Humana Press Inc. p 127-137.

Haluska F, Alberch P. 1983. The cranial development of *Elaphe obsoleta* (Ophidia, Colubridae). Journal of Morphology 178:37-55.

Hamburger V, Hamilton HL. 1951. A series of normal stages in development of the chick embryo. Journal of Morphology 88:49-92.

Hamilton HL. 1965. Lillie's Development of the Chick; An Introduction to Embryology. New York: Holt, Rinehart and Winston.

Hanken J, Hall BK. 1988. Skull development during anuran metamorphosis: I. Early development of the first three bones to form--the exoccipital, the parasphenoid, and the frontoparietal. Journal of Morphology 195:247-256.

Hanson FB. 1919. The ontogeny and phylogeny of the sternum. American Journal of Anatomy 26:41-115.

Hanson FB. 1920. The problem of the coracoid. Anatomical Record 19:327-345.

Heilmann G. 1926. The Origin of Birds. London: Witherby. 210 p.

Hill RV. 2005. Integrative morphological data sets for phylogenetic analysis of Amniota: the importance of integumentary characters and increased taxonomic sampling. Systematic Biology 54(4):530-547.

Hofmann C, Drossopoulou G, McMahon A, Balling R, Tickle C. 1998. Inhibitory action of BMPs on Pax1 expression and on shoulder girdle formation during limb development. Developmental Dynamics 213(2):199-206.

Holmes R. 1977. The osteology and musculature of the pectoral limb of small captorhinids. Journal of Morphology 152:101-140.

Holmgren N. 1955. Studies on the phylogeny of birds. Acta Zoologica (Stockholm) 36: 243-328.

Howes GB. 1887. The morphology of the mammalian coracoid. Journal of Anatomy and Physiology 21:190-198.

Howes GB. 1893. On the coracoid of the terrestrial Vertebrata. Proceedings of the Zoological Society of London 1893:585-592.

Huang R, Zhi Q, Patel K, Wilting J, Christ B. 2000. Dual origin and segmental organisation of the avian scapula. Development 127:3789-3794.

Huxley TH. 1860. On the dermal armour of *Jacare* and *Caiman*, with some notes on the specific and generic characters of recent *Crocodilia*. Journal of the Proceedings of the Linnean Society of London 4:1-28.

Huxley TH. 1870. Further evidence of the affinity between dinosaurian reptiles and birds. Proceedings of the Geological Society of London 26: 12-31.

Huysseune A. 2000. Skeletal system. In: Ostrander GK, editor. Microscopic Functional Anatomy. San Diego: Academic Press. p 307-317.

Huysseune A, Verraes W. 1986. Chondroid bone on the upper pharyngeal jaws and neurocranial base in the adult fish *Astatotilapia elegans*. The American Journal of Anatomy 177:527-535.

Huysseune A, Sire J-Y. 1990. Ultrastructural observations on chondroid bone in the teleost fish *Hemichromis bimaculatus*. Tissue & Cell 22:371-383.

Iordansky NN. 1973. The skull of the Crocodilia. In: Gans C, editor. Biology of the Reptilia, Volume 4, Morphology D. New York: Academic Press. p 201-262.

Irwin CR, Ferguson MWJ. 1986. Fracture repair of reptilian dermal bone: can reptiles form secondary cartilages? Journal of Anatomy 146:53-64.

Jasinoski SC, Russell AP, Currie PJ. 2006. An integrative phylogenetic and extrapolatory approach to the reconstruction of dromaeosaur (Theropoda: Eumaniraptora) shoulder musculature. Zoological Journal of the Linnean Society 146: 301-344.

Jenkins FA, Jr. 1993. The evolution of the avian shoulder joint. American Journal of Science 293-A:253-267.

Jenkins FA, Jr., Parrington FR. 1976. The postcranial skeletons of the Triassic mammals *Eozostrodon*, *Megazostrodon* and *Erythrotherium*. Philosophical Transactions of the Royal Society Series B, Biological Sciences 273:387-431.

Jollie MT. 1957. The head skeleton of the chicken and remarks on the anatomy of this region in other birds. Journal of Morphology 100(3):389-436.

Kaplan FS, Shore EM. 2000. Progressive osseous heteroplasia. Journal of Bone and Mineral Research 15(11):2084-2094.

Kearney M. 2002. The appendicular skeleton in amphisbaenians. Copeia 2002(3):719-738.

Kesteven HL. 1957. On the development of the crocodilian skull. Proceedings of the Linnean Society of New South Wales 82:117-124.

Klembara J. 1991. The cranial anatomy of early ontogenetic stages of *Alligator mississippiensis* (Daudin, 1802) and the significance of some of its cranial structures for the evolution of tetrapods. Palaeontographica Abteilung A: Paleaozoologie, Stratigraphie 215:103-171.

Klembara J. 1993. The parasphenoid and associated dermal structures of the parabasisphenoid of *Alligator mississippiensis* (Daudin, 1802). Palaeontographica Abteilung A: Paleaozoologie, Stratigraphie 228:143-164.

Klembara J. 1996. The first record of subdivided clavicles and interclavicle in the seymouriamorph tetrapod *Discosauricus* from the Lower Permian of the Boskovice Furrow (Czech Republic). Journal of Vertebrate Paleontology 16(4):787-790.

Klembara J. 2001. Postparietal and prehatching ontogeny of the supraoccipital in *Alligator mississippiensis* (Archosauria, Crocodylia). Journal of Morphology 249:147-153.

Klembara J. 2004. Ontogeny of the palatoquadrate and adjacent lateral cranial wall of the endocranium in prehatching *Alligator mississippiensis* (Archosauria: Crocodylia). Journal of Morphology 262:644-658.

Klembara J. 2005. Ontogeny of the partial secondary wall of the otoccipital region of the endocranium in prehatching *Alligator mississippiensis* (Archosauria, Crocodylia). Journal of Morphology 266:319-339.

Klima M. 1962. The morphogenesis of the avian sternum. Acta Academiae Scientiarium Cechsloveniacae 34: 151-194.

Klima M. 1968. Early development of the human sternum and the problem of homologization of the so-called suprasternal structures. Acta Anatomica 69:473-484.

Klima M. 1972. Ossa suprasternalia der Primaten und die Spezialanpassungen des Manubrium sterni bei den Brullaffen (Alouatta). Folia Primatologia 17:421-433.

Klima M. 1973. Die Fruhentwicklung des Schultergurtels und des Brustbeins bei den Monotremen (Mammalia: Prototheria). Advances in Anatomy, Embryology and Cell Biology 47:1-80.

Klima M. 1978. Comparison of the early development of the sternum and clavicle in striped dolphin and in humpback whale. The Scientific Reports of the Whales Research Institute, Tokyo 30:253-269.

Klima M. 1985. Development of the shoulder girdle and sternum in mammals. In: Duncker H-R, Fleischer G, editors. Functional Morphology in Vertebrates; Proceedings of the 1st International Symposium on Vertebrate Morphology. New York: Gustav Fischer Verlag. p 81-83.

Klima M. 1987. Early development of the shoulder girdle and sternum in marsupials (Mammalia: Metatheria). Advances in Anatomy, Embryology and Cell Biology 109:1-91.

Klymkowsky MW, Hanken J. 1991. Whole-mount staining of *Xenopus* and other vertebrates. Methods in Cell Biology 36:419-441.

Korringa P. 1938. Uber den Schultergurtel der Schildkroten. Anatomischer Anzeiger 86:259-268.

Langer MC. 2004. Basal Saurischia. In: Weishampel DB, Dodson P, Osmolska H, editors. The Dinosauria, Second Edition. Berkeley, California: University of California Press. p. 25-46.

Lécuru S. 1968a. Etude des variations morphologiques du sternum, des clavicules et de l'interclavicule des lacertiliens. Annales des Sciences Naturelles, Zoologie 10: 511-544.

Lécuru S. 1968b. Remarques sur le scapulo-coracoide des lacertiliens. Annales des Sciences Naturelles, Zoologie 10(12):475-510.

Lee MSY. 1996. The homologies and early evolution of the shoulder girdle in turtles. Proceedings of the Royal Society of London, Series B 263:111-117.

Lee MSY. 1997. Pareiasaur phylogeny and the origin of turtles. Zoological Journal of the Linnean Society 120:197-280.

Lengelé B, Schowing J, Dhem A. 1996a. Chondroid tissue in the early facial morphogenesis of the chick embryo. Acta Embryologica 193:505-513.

Lengelé B, Schowing J, Dhem A. 1996b. Embryonic origin and fate of chondroid tissue and secondary cartilages in the avian skull. Anatomical Record 246:377-393.

Levrat-Calviac V, Zylberberg L. 1986. The structure of the osteoderms in the Gekko: *Tarentola mauritanica*. The American Journal of Anatomy 176:437-446.

Leydig F. 1859. Ueber die ausseren Bedeckungen der Saugethiere. Archiv fur Anatomie, Physiologie und wissenschaftliche Medicin:677-747.

Luo Z-X, Kielan-Jaworowska Z, Cifelli RL. 2002. In quest for a phylogeny of Mesozoic mammals. Acta Palaeontologica Polonica 47(1):1-78.

Lydekker R. 1893. Note on the coracoidal element in adult sloths, with remarks on its homology. Proceedings of the Zoological Society of London 1893:172-174.

Main RP. 2005. The evolution and function of thyreophoran dinosaur scutes: implications for plate function in stegosaurs. Paleobiology 31(2):291-314.

Makovicky P, Currie PJ. 1998. The presence of a furcula in tyrannosaurid theropods, and its phylogenetic and functional implications. Journal of Vertebrate Paleontology 18: 143-149.

McGonnell IM. 2001. The evolution of the pectoral girdle. Journal of Anatomy 199:189-194.

McGonnell IM, Graham A. 2002. Trunk neural crest has skeletogenic potential. Current Biology 12:767-771.

Meek A. 1911. On the morphogenesis of the head of the crocodile. Journal of Anatomy and Physiology 45:357-377.

Meers MB. 2003. Crocodylia forelimb musculature and its relevance to Archosauria. Anatomical Record 274A:891-916.

Menon GK. 2004. The skin barrier: an evolutionary and environmental perspective. In: Forslind B, Lindberg M, editors. Skin, Hair, and Nails: Structure and Function. New York: Marcel Dekker, Inc. p 189-216.

Miyake T, Vaglia JL, Taylor LH, Hall BK. 1999. Development of dermal denticles in skates (Chondrichthyes, Batoidea): patterning and cellular differentiation. Journal of Morphology 241:61-81.

Miyake T, Vaglia JL, Witten PE, Hall BK. 2001. Elastin and/or elastin-like proteins in the skeleton of cartilaginous and teleost fishes. Journal of Morphology 248:262.

Modesto SP. 1999. Observations on the structure of the Early Permian reptile *Stereosternum tumidum* Cope. Palaeontologica Africana 35:7-19.

Modesto SP, Anderson JS. 2004. The phylogenetic definition of Reptilia. Systematic Biology 53(5):815-821.

Montero R, Gans C, Lions ML. 1999. Embryonic development of the skeleton of *Amphisbaenia darwini heterozontata* (Squamata: Amphisbaenidae). Journal of Morphology 239:1-25.

Mook CC. 1921a. Individual and age variations in the skulls of recent Crocodilia. Bulletin of the American Museum of Natural History 44:51-66.

Mook CC. 1921b. Notes on the postcranial skeleton in the Crocodilia. Bulletin of the American Museum of Natural History 44:67-100.

Moss ML. 1969. Comparative histology of dermal sclerifications in reptiles. Acta Anatomica 73:510-533.

Müller F. 1967. Zur embryonalen Kopfentwicklung von *Crocodylus cataphractus* Cuvier. Revue Suisse de Zoologie 74:189-294.

Müller GB, Alberch P. 1990. Ontogeny of the limb skeleton in Alligator mississippiensis: developmental invariance and change in the evolution of archosaur limbs. Journal of Morphology 203:151-164.

Müller J. 2001. Osteology and relationships of *Eolacerta robusta*, a lizard from the Middle Eocene of Germany (Reptilia, Squamata). Journal of Vertebrate Paleontology 21(2):261-278.

Murray PDF. 1963. Adventitious (secondary) cartilage in the chick, and the development of certain bones and articulations in the chick skull. Australia Journal of Zoology 11(3):368-430.

Nagashima H, Uchida K, Yamamoto K, Kuraku S, Usuda R, Kuratani S. 2005. Turtle-chicken chimera: an experimental approach to understanding evolutionary innovation in the turtle. Developmental Dynamics 232:149-161.

Newman HH, Patterson JT. 1910. The development of the nine-banded armadillo from the primitive streak stage to birth; with especial reference to the question of specific polyembryony. Journal of Morphology 21:359-437.

Newton A, Gadow H. 1893-1896. A Dictionary of Birds. London: Black. 836-858 p.

Nicholls EL, Russell AP. 1991. The plesiosaur pectoral girdle: the case for a sternum. Neues Jahrbuch fur Geologie und Palaontologie, Abhandlungen 182(2):161-185.

Norell MA, Makovicky P, Clark JM. 1997. A *Velociraptor* wishbone. Nature 389: 447.

Nowak RM. 1999. Walker's Mammals of the World, Sixth Editiion. Baltimore, Maryland: Johns Hopkins University Press. 836 p.

Oliver G, DeRoberts EM, Wolpert L, Tickle C. 1990. Expression of a homeobox gene in the chick wing bud following application of retinoic acid and grafts of polarizing region tissue. EMBO Journal 9(10):3093-3099.

Osborn HF. 1899. A complete mosasaur skeleton, osseous and cartilaginous. Memoirs of the American Museum of Natural History 1(4):167-188.

Osborn HF. 1924. Three new Theropoda, *Protoceratops zone*, central Mongolia. American Museum Novitates 144: 1-12.

Ostrom JH. 1973. The ancestry of birds. Nature 242: 136.

Ostrom JH. 1976. Some hypothetical anatomical stages in the evolution of avian flight. Smithsonian Contributions to Paleobiology 27:1-21.

Panchen AL. 1994. Richard Owen and the concept of homology. In: Hall BK, editor. Homology: The Hierarchial Basis of Comparative Biology. New York: Academic Press. p. 22-62.

Parker WK. 1864. On the sternal apparatus of birds and other Vertebrata. Proceedings of the Zoological Society of London, 1864: 339-341

Parker WK. 1868. A monograph on the structure and development of the shoulder-girdle and sternum in the Vertebrata. The Ray Society.

Parsons TS. 1970. The nose and Jacobson's organ. In: Gans C, Parsons TS, editors. Biology of the Reptilia, Volume 2, Morphology B. New York: Academic Press. p 99-191.

Patterson C. 1977. Cartilage bones, dermal bones and membrane bones, or the exoskeleton versus the endoskeleton. In: Andrews SM, Walker AD, editors. Problems in Vertebrate Evolution. London: Academic Press. p 77-122.

Patterson C. 1982. Morphological characters and homology. In: Joysey KA, Friday AE, editors. Problems of Phylogenetic Reconstruction. London: Academic Press. p. 21-74.

Paulsen DF. 1993. Basic Histology, second edition. Norwalk, Connecticut: Appleton & Lange. 407 p.

Pellegrini M, Pantano S, Fumi MP, Lucchini F, Forabosco A. 2001. Agenesis of the scapula in *Emx2* homozygous mutants. Developmental Biology 232:149-156.

Presnell JK, Schreibman MP. 1997. Humason's Animal Tissue Techniques, Fifth Edition. Baltimore: The Johns Hopkins University Press. 572 p.

Pritchard JJ. 1974. Growth and differentiation of bone and connective tissue. In: Goldspink G, editor. Differentiation and Growth of Cells in Vertebrate Tissues. London: Chapman & Hall. p 101-128.

Qiang J, Currie PJ, Norell MA, Shu'an J. 1998: Two feathered dinosaurs form northeastern China. Nature 393: 753-730.

Rathke H. 1848. *Über die Entwicklung der Schildkröten.* Braunschweig, Germany: Friederich Vieweg und Sohn.

Reisz R, Dilkes DW, Berman DS. 1998. Anatomy and relationships of *Elliotsmithia longiceps* Broom, a small synapsid (Eupelycosauria: Varanopseidae) from the late Permian of South Africa. Journal of Vertebrate Paleontology 18(3):602-611.

Reynoso V-H. 1997. A "beaded" sphenodontian (Diapsida: Lepidosauria) from the Early Cretaceous of Central Mexico. Journal of Vertebrate Paleontology 17(1):52-59.

Rice DPC, Kim H-J, Thesleff I. 1997. Detection of gelatinase B expression reveals osteoclastic bone resorption as a feature of early calvarial bone development. Bone 21(6):479-486.

Rieppel O. 1992. Studies of skeleton formation in reptiles. III. Patterns of ossification in the skeleton of *Lacerta vivipara* Jacquin (Reptilia, Squamata). Fieldiana: Zoology, New Series 68:1-25.

Rieppel O. 1993a. Patterns of diversity of the reptilian skull. In: Hanken J, Hall BK, editors. The Skull; Patterns of Structural and Systematic Diversity. Chicago: University of Chicago Press. p 344-390.

Rieppel O. 1993b. Studies on skeleton formation in reptiles. V. Patterns of ossification in the skeleton of *Alligator mississippiensis* Daudin (Reptilia, Crocodylia). Zoological Journal of the Linnean Society 109:301-325.

Rieppel O. 1993c. Studies on skeleton formation in reptiles: patterns of ossification in the skeleton of *Chelydra serpentina* (Reptilia, Testudines). Journal of Zoology 231:487-509.

Rieppel O. 1996. Testing the homology by congruence: the pectoral girdle of turtles. Proceedings of the Royal Society of London, Series B, Biological Sciences 263:1395-1398.

Rieppel O, deBraga M. 1996. Turtles as diapsids. Nature 384:453-455.

Rieppel O, Reisz R. 1999. The origin and early evolution of turtles. Annual Reviews of Ecology and Systematics 30:1-22.

Romanoff AL. 1960. The Avian Embryo; Structural and Functional Development. New York: MacMillan Company.

Romer AS. 1922. The comparison of mammalian and reptilian coracoids. Anatomical Record 24:39-47.

Romer AS. 1956. Osteology of the Reptiles. Chicago: University of Chicago Press.

Romer AS, Price LW. 1940. Review of the Pelycosauria. Geological Society of America Special Papers 28:1-538.

Römer F. 1892. Über den Bau und die Entwickelung des Panzers der Gürteltiere. Jenaische Zeitschift fur Naturwissenschaft 27:513-528.

Ross FD, Mayer GC. 1983. On the dorsal armor of the Crocodilia. In: Rhodin AGJ, editor. Advances in Herpetology and Evolutionary Biology. Cambridge, Massachusetts: Museum of Comparative Zoology. p 305-331.

Roth VL. 1994. With and between organisms: replicators, lineages, and homologues. In: Hall BK, editor. Homology: The Hierarchial Basis of Comparative Biology. New York: Academic Press. p. 301-337.

Ruckes H. 1929. Studies in chelonian osteology, part II; the morphological relationships between the girdles, ribs and carapace. Annals of the New York Academy of Sciences 31:81-120.

Ruibal R, Shoemaker V. 1984. Osteoderms in anurans. Journal of Herpetology 18(3):313-328.

Russell AP, Joffe DJ. 1985. The early development of the quail (*Coturnix c. japonica*) furcula reconsidered. Journal of Zoology 206: 69-81.

Ruta M, Coates M, Quicke DLJ. 2003. Early tetrapod relationships revisited. Biological Reviews 78:251-345.

Sánchez-Villagra MR, Maier W. 2002. Ontogenetic data and the evolutionary origin of the mammalian scapula. Naturwissenschaften 89:459-461.

Sánchez-Villagra MR, Maier W. 2003. Ontogenesis of the scapula in marsupial mammals, with special emphasis on perinatal stages of didelphids and remarks on the origin of the therian scapula. Journal of Morphology 258:115-129.

Schumacher G-H. 1973. The head muscles and hyolaryngeal skeleton of turtles and crocodilians. In: Gans C, Parsons TS, editors. Biology of the Reptilia: volume 4. New York: Academic Press. p 101-199.

Sengel P. 1976. Morphogenesis of the Skin. Cambridge: Cambridge University Press. 277 p.

Sereno PC. 1991. Basal archosaurs: phylogenetic relationships and functional implications. Society of Vertebrate Paleontology Memoir 2: 1-53.

Sereno PC. 1993. The pectoral girdle and forelimb of the basal theropod *Herrerasaurus ischigualastensis*. Journal of Vertebrate Paleontology 13: 425-450.

Sereno PC. 1999. The evolution of dinosaurs. Science 284: 2137-2147.

Sheil CA. 2003. Osteology and skeletal development of *Apalone spinifera* (Reptilia: Testudines: Trionychidae). Journal of Morphology 256:42-78.

Sheil CA. 2005. Skeletal development of *Macrochelys temminckii* (Reptilia: Testudines: Chelydridae). Journal of Morphology 263:71-106.

Sheil CA, Greenbaum E. 2005. Reconsideration of skeletal development of *Chelydra serpentina* (Reptilia: Testudinata: Chelydridae): evidence for intraspecific variation. Journal of Zoology 265:235-267.

Shiino K. 1914. Studien zue Kenntnis des Wirbeltierkopfes. I. Das Chondrocranium von *Crocodilus* mit Berücksichtigung der Gehirnnerven und Kopfgefasse. Anat Hefte 50:254-381.

Shubin NH. 1994. History, ontogeny, and evolution of the archetype. . In: Hall BK, editor. Homology: The Hierarchial Basis of Comparative Biology. New York: Academic Press. p. 250-271.

Shubin N, Tabin C, Carroll S. 1997. Fossil, genes and the evolution of animal limbs. Nature 388:639-648.

Singer C. 1957. A Short History of Anatomy from the Greeks to Harvey. New York: Dover Publications, Inc., 209 p.

Sire J-Y. 2001. Teeth outside the mouth in teleost fish. How to benefit from a developmental accident. Evolution and Development 3:104-108.

Sire J-Y, Huysseune A. 2003. Formation of dermal skeletal and dental tissues in fish: a comparative and evolutionary approach. Biological Reviews 78:219-249.

Sire J-Y, Huysseune A, Meunier FJ. 1990. Osteoclasts in teleost fish: light- and electron-microscopical observations. Cell and Tissue Research 260:85-94.

Skinner JH. 1959. Ontogeny of the breast-shoulder apparatus of the South African lacertilian, *Microsauria pumila pumila* (Daudin). Annals of the University of Stellenbosch 35(1):5-66.

Smith MM, Hall BK. 1990. Developmental and evolutionary origins of vertebrate skeletogenic and odontogenic tissues. Biological Reviews 65:277-374.

Smith MM, Hall BK. 1993. A developmental model for evolution of the vertebrate exoskeleton and teeth: role of cranial and trunk neural crest. Evolutionary Biology 27:387-448.

Soriano P. 1997. The PDGFalpha receptor is required for neural crest cell development and for normal patterning of the somites. Development 124:2691-2700.

Stokely PS. 1947. Limblessness and correlated changes in the girdles of a comparative morphological series of lizards. American Naturalist 38:725-754.

Stone JR, Hall BK. 2004. Latent homologues for the neural crest as an evolutionary novelty. Evolution and Development 6(2):123-129.

Sumida SS. 1989. The appendicular skeleton of the early Permian genus *Labidosaurus* (Reptilia, Captorhinomorpha, Captorhinidae) and the hind limb musculature of captorhinid reptiles. Journal of Vertebrate Paleontology 9:295-313.

Swofford, D. L. 2000. PAUP*. Phylogenetic Analysis Using Parsimony (* and Other Methods). Version 4. Sunderland, Massachusetts: Sinauer Associates.

Timmons PM, Wallin J, Rigby PWJ, Balling R. 1994. Expression and function of *Pax1* during development of the pectoral girdle. Development 120:2773-2785.

Tran S, Hall BK. 1989. Growth of the clavicle and development of clavicular secondary cartilage in the embryonic mouse. Acta Anatomica 135:200-207.

Tykoski RS, Forster CA, Rowe TB, Sampson SD, Munyikwa D. 2002. A furcula in the coelophysoid theropod *Syntarsus*. Journal of Vertebrate Paleontology 23: 728-733.

Vaughn PP. 1955. The Permian reptile *Araeoscelis* restudied. Bulletin of the Museum of Comparative Zoology 113:305-467.

Vickaryous MK, Fedak TJ, Franz-Odendaal T, Hall BK, Stone J. 2003. Dusting off bone ontologies; considering skeletons in the palaeo-closet. Palaeontological Association Newsletter 53:48-51.

Vickaryous MK, Hall BK. 2006a. Homology of the reptilian coracoid and a reappraisal of the evolution and development of the amniote pectoral apparatus. Journal of Anatomy 208: 263-285.

Vickaryous MK, Hall BK. 2006b. Osteoderm morphology and development in the nine-banded armadillo, *Dasypus novemcinctus* (Mammalia, Xenarthra, Cingulata). Journal of Morphology 267: 1273-1283.

Vickaryous MK, Olson WM. (in press). Sesamoids and ossicles in the appendicular skeleton. In: Hall BK, editor. Fins and Limbs: Evolution, Development, and Transformation. Chicago: University of Chicago Press. 42pp.

Vickaryous MK, Russell AP, Currie PJ. 2001. The cranial ornamentation of ankylosaurs (Ornithischia: Thyreophora): reappraisal of developmental hypotheses. In: Carpenter K, editor. The Armored Dinosaurs. Bloomington: Indiana University Press. p 318-340.

Vincent C, Bontoux M, Le Douarin NM, Pieau C, Monsoro-Burq A-N. 2003. Msx genes are expressed in the carapacial ridge of turtle shell: a study of the European pond turtle, *Emys orbicularis*. Development Genes and Evolution 213:464-469.

Vinkka H. 1982. Secondary cartilages in the facial skeleton of the rat. Proceedings of the Finnish Dental Society 78 (supplement 7):1-137.

von Huene F. 1912. Die Cotylosaurier der Trias. Palaontolographica 59:69-102.

Walker WF. 1947. The development of the shoulder region in the turtle, *Chrysemys picta marginata*, with special reference to the primary musculature. Journal of Morphology 80:195-249.

Walker WF. 1973. The locomotor apparatus of Testudines. In: Gans C, Parsons TS, editors. Biology of the Reptilia, Morphology D. New York: Academic Press. p 1-100.

Westergaard B, Ferguson MWJ. 1986. Development of the dentition in *Alligator mississippiensis*. Early embryonic development in the lower jaw. Journal of Zoology 210:575-597.

Westergaard B, Ferguson MWJ. 1987. Development of the dentition in *Alligator mississippiensis*. Later development in the lower jaws of embryos, hatchlings and young juveniles. Journal of Zoology 212:191-222.

Westergaard B, Ferguson MWJ. 1990. Development of the dentition in *Alligator mississippiensis*: upper jaw dental and craniofacial development in embryos, hatchlings, and young juveniles, with a comparison to lower jaw development. The American Journal of Anatomy 187:393-421.

Wetzel RM. 1985. Taxonomy and distribution of armadillos, Dasypodidae. In: Montgomery GG, editor. The evolution and ecology of armadillos, sloths and vermilinguas. Washington, D.C.: Smithsonian Institution Press. p 23-46.

Wild R. 1993. A juvenile specimen of *Eudimorphodon ranzii* Zambelli (Reptilia, Pterosauria) from the Upper Triassic (Norian) of Bergamo. Rivista del Museo Civico di Scienze Naturali 'Enrico Caffi', Bergamo 16: 95-120.

Wilkinson M, Thorley J, Benton MJ. 1997. Uncertain turtle relationships. Nature 387:466.

Williams MS. 2003. Developmental anomalies of the scapula--the "omo"st forgotten bone. American Journal of Medical Genetics 120A:583-587.

Williston SW. 1911. American Permian Vertebrates. Chicago: University of Chicago Press.

Williston SW. 1925. The Osteology of the Reptiles. Cambridge: Harvard University Press. 304 p.

Wilson CW. 1914. Development and histology of the integument of the nine-banded armadillo (*Tatusia novemcincta*). Bulletin of the University of Texas, Scientific Series 36(308):1-18.

Witmer LM. 1995. Homology of facial structures in extant archosaurs (birds and crocodilians), with special reference to paranasal pneumaticity and nasal conchae. Journal of Morphology 225:269-327.

Witten PE, Hall BK. 2003. Seasonal changes in the lower jaw skeleton in male Atlantic salmon (*Salmo salar* L.): remodelling and regression of the kype after spawning. Journal of Anatomy 203:435-450.

Witten PE, Hansen A, Hall BK. 2001. Features of mono- and multinucleated bone resorbing cells of the zebrafish *Danio rerio* and their contributio to skeletal development, remodeling, and growth. Journal of Morphology 250:197-207.

Wyneken J. 2001. The Anatomy of Sea Turtles. US Department of Commerce NOAA Technical Memorandum NMFS-SEFSC-470:1-172.

Xu X, Wang X-L, Wu X-C. 1999. A dromaeosaurid dinosaur with a filamentous integument from Yixian Formation of China. Nature 401: 262-266.

Yates AM, Vasconcelos CC. 2005. Furcula-like clavicles in the prosauropod dinosaur *Massospondylus*. Journal of Vertebrate Paleontology 25: 466-468.

Zangerl R. 1945. Contributions to the osteology of the post-cranial skeleton of the Amphisbaenidae. American Midland Naturalist 33:764-780.

Zylberberg L, Castanet J, de Ricqles A. 1980. Structure of the dermal scales in Gymnophiona (Amphibia). Journal of Morphology 165:41-54.

Zylberberg L, Castanet J. 1985. New data on the structure and growth of the osteoderms in the reptile *Anguis fragilis* L. (Anguidae, Squamata). Journal of Morphology 186:327-342.

Zylberberg L, Geraudie J, Meunier F, Sire J-Y. 1992. Biomineralization in the integumental skeleton of the living lower vertebrates. In: Hall BK, editor. Bone, Volume 4: Bone Metabolism and Mineralization. Boca Raton, FL: CRC Press. p 171-224.

Zylberberg L, Wake MH. 1990. Structure of the scales of *Dermophis* and *Microcaecilia* (Amphibia: Gymnophiona) and a comparison to dermal ossifications of other vertebrates. Journal of Morphology 206:25-43.

APPENDIX 1. *ALLIGATOR MISSISSIPPIENSIS* SPECIMENS HISTOLOGICALLY PREPARED FOR THE CURRENT STUDY

Please note that additional materials from the collection of Prof. M. W. J. Ferguson (University of Manchester) were also consulted.

FS 16
Serially sectioned: head (1)

FS 17
Whole-mounted: complete embryo (2, Alizarin red; 2, Alizarin red and Alcian blue).
Serially sectioned: head (2); pectoral region (2); pelvic region (1).

FS 18
Whole-mounted: hemisectioned head (1, Alizarin red; 1, Alizarin red and Alcian blue); pectoral region (1); pelvic region (1).
Serially sectioned: head (2); pectoral region (1); pelvic region (1).

FS 19
Whole-mounted: hemisectioned head (2, Alizarin red; 2, Alizarin red and Alcian blue); pectoral region (1); pelvic region (1).
Serially sectioned: head (3); pectoral region (1); pelvic region (1).

FS 20
Whole-mounted: complete head (1, Alizarin red); pectoral region (1); pelvic region (1).
Serially sectioned: head (2); pectoral region (1); pelvic region (1).

FS 21
Whole-mounted: complete head (1, Alizarin red; 3, Alizarin red/Alcian blue); pectoral region (2); pelvic region (1).
Serially sectioned: head (3); pectoral region (1); pelvic region (1).

FS 22
Whole-mounted: complete embryo (1, Alizarin red; 1, Alizarin red/Alcian blue); complete head (1; Alizarin red); pectoral region (1); pelvic region (1).
Serially sectioned: head (1); pectoral region (1); pelvic region (1).

FS 23
Whole-mounted: complete head (1, Alizarin red); hemisectioned head (1, Alizarin red); pectoral region (1); pelvic region (2).
Serially sectioned: head (1); pectoral region (1); pelvic region (1).

Subadult, snout vent length (SVL) = 121 mm.
Whole-mounted: palpebral (1, Alizarin red).
Serially sectioned: palpebral (1); osteoderms from the nuchal shield.

Subadult, SVL = 175 mm.
Whole-mounted: palpebral (1, Alizarin red).
Serially sectioned: palpebral (1); osteoderms from the nuchal shield.

Subadult SVL = 195 mm.
Whole-mounted: palpebral (1, Alizarin red); complete gastralial system (1).
Serially sectioned: palpebral (1); osteoderms from the nuchal shield; gastralia (2).

Adult
Skulls: with maximum cranial lengths of 330 mm, 290 mm, 270 mm, and 120 mm
Serially sectioned: osteoderms (2); gastralia (2).